Defining the mechanism(s) of Hepatitis C virus (HCV) entry.

by

Anne-Katrin Schwarz

A thesis submitted to The University of Birmingham for the degree of doctor of philosophy.

College of Medical & Dental Sciences
Division of Immunity and Infection
The University of Birmingham

Supervisors: Professor Jane A McKeating and Dr Peter Balfe

May 2009

Abstract.

Hepatitis C virus (HCV) is a major human pathogen and the leading cause of cirrhosis and liver cancer worldwide. HCV entry is clathrin- and pH-dependent, and requires CD81, Scavenger receptor BI (SR-BI), and the tight junction (TJ) proteins Claudin-1 and Occludin.

Primary HCV strains cannot be efficiently cultured *in vitro*, making the evaluation of potential antiviral compounds in a biologically relevant context extremely difficult. Despite being suitable for high-throughput screening, most cell-based reporter assays rely on the secretion of serine alkaline phosphatase and thus do not allow the selection of HCV infected cells, or the screening of patient samples to identify cell culture infectious viral strains. We aimed to develop a cell-based reporter assay, which utilizes the viral NS3/4A protease to cleave and activate a fluorescent reporter protein constitutively expressed in Huh-7.5 hepatoma cells.

HCV tropism is restricted to the liver, where hepatocytes are polarized and form TJ, which are indispensable for normal liver functionality. We demonstrate that in confluent cells, SR-BI and Claudin-1 expression is increased and that HCV entry is enhanced when cellular contact is established. Furthermore, cell junction formation and SR-BI overexpression, respectively, accelerated virus entry, suggesting a key role for SR-BI in HCV internalization.

The mechanisms underlying HCV-associated hepatic injury are poorly understood, however, it is thought that HCV may disrupt TJ integrity, thus compromising hepatocyte polarity and function. We demonstrate that the HCV structural proteins modulate the expression and localization of TJ proteins, leading to their redistribution to cytoplasmic vesicles with possible consequences for TJ integrity *in vivo*.

Publications.

Schwarz A, Grove J, Hu K, Mee CJ, Balfe P, McKeating JA. **Hepatoma cell density promotes Claudin-I and Scavenger receptor BI expression and hepatitis C virus internalization**. J Virol 2009. *Manuscript accepted for publication.*

Schwarz A, Farquhar MJ, Mee CM, Pennant G, Harris HJ, Balfe P, McKeating JA. **Hepatitis C virus induces the relocalization of tight juntion proteins in hepatoma cells**. J Gen Virol 2009. *Manuscript submitted.*

Farquhar MJ, Hu K, Tomlinson M, Brimacombe C, Schwarz A, Mee CM, Harris HJ, Goodall M, Balfe P, McKeating JA. **Role of CD81 in HCV entry.** *Manuscript in preparation.*

Timpe JM, Stamataki Z, Jennings A, Hu K, Farquhar MJ, Harris HJ, Schwarz A, Desombere I, Roels GL, Balfe P, McKeating JA. **Hepatitis C virus cell-cell transmission in hepatoma cells in the presence of neutralizing antibodies.** Hepatology. 2008 Jan;47(1):17-24.

Grove J, Huby T, Stamataki Z, Vanwolleghem T, Meuleman P, Farquhar MJ, Schwarz A, Moreau M, Owen JS, Leroux-Roels G, Balfe P, McKeating JA. **Scavenger receptor BI and BII expression levels modulate hepatitis C virus infectivity** J Virol. 2007 Apr;81(7):3162-9.

Dedication.

I would like to dedicate this thesis to my mother, Christa Schwarz, my sisters, Bettina and Susanne, and a very special friend, Veronika Thiel.

Acknowledgements.

I would like to thank Professor Jane McKeating and Dr Peter Balfe for the opportunity to carry out a PhD and for their guidance, technical expertise and assistance throughout my project.
I would also like to thank the other members of the Birmingham HCV Research group for their technical assistance and support, and intellectually stimulating discussions, in no particular order: Joseph Grove, Claire Brimacombe, Michelle Farquhar, Helen Harris, Christopher Mee, Adam Jennings, Ke Hu, Zania Stamataki, Jennifer Timpe, Chris Davis and Garrick Wilson.
Thank you also to Professor David Adams and Dr David Mutimer for providing patient blood samples, and for their support and assistance throughout the early stages of my project.

This study would not have been possible without reagents kindly provided by the following people: Thierry Huby (INSERM, Paris), Jin Zhong, Dennis Burton and Frank Chisari (SCRIPPS, La Jolla), Takaji Wakita (National Institute of Infectious Diseases, Tokyo), Fedor Berditchevski (CRUK Cancer Research Insititute, Birmingham), John McLaughlan (MRC Institute for Virology, Glasgow), Margaret Goodall (University of Birmingham, UK), and Jin Zhang and Charles M. Rice (Rockefeller University, New York).

Table of contents

1 INTRODUCTION 1

1.1 A brief history of non A, non B post-transfusion hepatitis 1

1.2 The disease. 3
1.2.1 Epidemiology. 3
1.2.2 Immunobiology. 4
1.2.3 Immunopathogenesis. 11

1.3 Model systems for HCV study. 13
1.3.1 Primary cell culture and cell lines. 13
1.3.2 The replicon system. 15
1.3.3 HCV pseudoparticles (HCVpp) and cell-culture derived HCV (HCVcc). 17
1.3.4 Animal models. 19

1.4 The HCV Life Cycle. 22
1.4.1 HCV genome replication and polyprotein processing. 23
1.4.2 HCV Attachment And Entry. 27
1.4.3 HCV enters cells via clathrin-mediated endocytosis. 37
1.4.4 Assembly of the nucleocapsid and budding of virions. 41

1.5 Project objectives. 45

2 MATERIALS AND METHODS 47

2.1 Tissue culture. 47

2.2 Basic techniques. 48
2.2.1 Antibodies. 48
2.2.2 Preparation of human serum-derived IgG. 49
2.2.3 Flow cytometry. 50
2.2.4 Indirect immunofluorescence. 52
2.2.5 Western Blotting. 57

2.3 HCVpp and HCVpp based work. 60
2.3.1 Plasmids. 60
2.3.2 Preparation of HCV pseudoparticles (HCVpp). 61
2.3.3 Luciferase infection assay. 62
2.3.4 Preparation of cell culture proficient HCV (HCVcc). 63
2.3.5 HCVcc infection assay. 65
2.3.6 HCVcc internalization assay. 66
2.3.7 Treatment of cells with inhibitors. 67

2.4 Generation of TRIP viruses and transduction of cells to express receptors of interest. 69

2.5 Molecular cloning. 70
2.5.1 Restriction enzyme digest. 70
2.5.2 Ligation. 70
2.5.3 Transformation of competent cells. 71
2.5.4 PCR colony screening and plasmid DNA isolation. 71

2.6 Generation of the RCGFP(Δ5AB)MODC indicator cell line. 73

3 RESULTS 79

3.1 Developing an indicator cell line for HCV infection. 79
3.1.1 RCGFP(Δ5AB)MODC plasmid construction. 82
3.1.2 Proteolysis of the RCGFP(Δ5AB)MODC fusion protein in transiently transfected 293T and Huh-7.5 cell lines 85
3.1.3 Generation of RCGFP(Δ5AB)MODC Huh-7.5 cells - NS3/4A mediated cleavage of the fusion protein 91
3.1.4 Discussion 95

3.2 Cellular contact promotes HCV infection through the modulation of HCV entry receptor expression 103
3.2.1 Cellular contact modulates expression and localization of HCV entry receptors 105
3.2.2 Cellular contact promotes HCV infection at the entry level 108
3.2.3 Effect of cellular contact on HCV internalization kinetics 113
3.2.4 Statistical analysis of internalization assays. 126
Defining the 126
3.2.5 role of SR-BI and CLDN1 in HCV internalization. 126
3.2.6 Discussion 132

3.3 HCV induced alterations of tight junction protein expression and localization 140
3.3.1 HCV infection modulates expression and localization of the tight junction protein CLDN1. 140
3.3.2 JFH-1 infection modulates localization of OCLN and ZO-1 143
3.3.3 CLDN1 localizes to an unknown intracellular compartment in HCV infected cells 146
3.3.4 Relocalization of TJ proteins in Huh-7.5 cells is cytokine-independent and requires infection with HCV 149
3.3.5 HCV glycoproteins mediate CLDN1 and OCLN relocalization in infected cells 153
3.3.6 CLDN1 localizes to a longer-lived storage compartment in HCV infected cells 156
3.3.7 Endocytosis of intracellular forms of CLDN1 in HCV infected cells 160
3.3.8 Discussion 163

3.4 Concluding remarks. 173

4 BIBLIOGRAPHY. 176

List of Figures

Figure 1-1 Possible mechanisms of immune evasion by HCV. 6
Figure 1-2 Attenuation of IFN signalling by HCV. 9
Figure 1-3 The HCV life cycle. 22
Figure 1-4 The HCV genome and proteins. 24
Figure 1-5 HCV entry receptors. 27
Figure 1-6 Attachment, receptor binding and clathrin-mediated endocytosis of HCV. 40
Figure 1-7 Structure of the HCV virion. 41
Figure 2-1 Linear plot profile analysis. 55
Figure 2-2 BCA protein assay standard curve. 58
Figure 2-3 MTS cell proliferation assay standard curve. 68
Figure 2-4 Basic pZS-1 plasmid map (modified from Clontech, USA). 74
Figure 2-5 Restriction maps of the pZS-1 vector and Δ5B insert. 75
Figure 2-6 PstI/SalI restriction digest of the RCGFP(Δ5AB)MODC plasmid. 76
Figure 3-1 Schematic diagrams of the RCGFP(Δ5AB)MODC plasmid and NS3/4A cleavage sequence 84
Figure 3-2 ALLN treatment of 293T cells expressing the parental fusion protein. 86
Figure 3-3 Degradation of the RCGFP(Δ5AB)MODC fusion protein in 293T cells. 89
Figure 3-4 Proteloytic degradation of the RCGFP(Δ5AB)MODC fusion protein in transiently transfected Huh-7.5 cells. 90
Figure 3-5 Proteloytic degradation of the RCGFP(Δ5AB)MODC fusion protein in stable Huh-7.5 cell lines. 93
Figure 3-6 Analysis of NS3/4A mediated fusion protein cleavage. 94
Figure 3-7 NS3/4A mediated cleavage of the RCGFP(Δ5AB)MODC fusion protein. 96
Figure 3-8 Receptor expression is modulated in confluent Huh-7.5 cells. 107
Figure 3-9 Phase images of Huh-7.5 cells plated at low, standard and high density. 109
Figure 3-10 Cellular contact modulates HCVcc infectivity. 110
Figure 3-11 Cellular contact modulates HCV entry. 112
Figure 3-12 Proteinase K dependent HCV internalization assay. 114
Figure 3-13 HCV infection of adherent and non-adherent Huh-7.5 cells. 117
Figure 3-14 PK-mediated proteolysis of cell-bound infectious virus. 118
Figure 3-15 Time course of HCVcc sensitivity to proteolysis. 119
Figure 3-16 Neutralizing antibody (nAb) escape assay. 121
Figure 3-17 Neutralizing activity of anti-E2 nAb C1. 123
Figure 3-18 Time course of HCVcc sensitivity to antibody-mediated neutralization. 124
Figure 3-19 Modulation of HCVcc internalization kinetics with cell confluence. 125
Figure 3-20 CLDN1 and SR-BI overexpression in Huh-7.5 cells. 128
Figure 3-21 Localization of CLDN1 and SR-BI in transduced Huh-7.5 cells. 129
Figure 3-22 Effect of CLDN1 and SR-BI over-expression on the entry kinetics of JFH-1. 131
Figure 3-23 JFH-1 modulates CLDN1 expression and localization. 142
Figure 3-24 JFH-1 infection modulates CLDN1, occludin, and ZO-1 localization. 144
Figure 3-25 Co-localization of TJ proteins in HCV infected Huh-7.5 cells. 145
Figure 3-26 Localization of intracellular CLDN1 in HCV infected cells. 147
Figure 3-27 Co-localization of CLDN1 and HCV proteins. 148
Figure 3-28 Effect of cytokines on TJ protein distribution. 150
Figure 3-29 CLDN1 relocalization is associated with HCV infection. 152
Figure 3-30 HCV glycoproteins induce CLDN1 and OCLN redistribution. 155
Figure 3-31 Increased half-life of intracellular CLDN1 in HCV infected cells. 157
Figure 3-32 Effect of proteasome inhibition on CLDN1 protein level. 159
Figure 3-33 CLDN1 localization in HCV infected Huh-7.5 cells following inhibition of clathrin-mediated endocytosis. 162
Figure 3-34 Model of HCV entry. 174

List of Tables

Table 2-1 List of cell lines used. 47
Table 2-2 List of antibodies used. 48
Table 2-3 List of antibody concentrations used. 52
Table 2-4 List of plasmids used. 60
Table 2-5 List of inhibitors and growth factors used. 67
Table 3-1 Statistical analysis of HCVcc entry kinetics. 126
Table 3-2 CLDN1 and OCLN relocalization frequency in E1E2 expressing cells. 155

1 Introduction

1.1 A brief history of non A, non B post-transfusion hepatitis

Post-transfusion hepatitis (PTH) was first appreciated during and immediately after World War II, when the increasing number of blood and plasma transfusions led to a considerable increase in the number of hepatitis cases in the US. First evidence for the viral etiology of PTH was provided during the 1940s, when research groups in the United Kingdom and the US identified two immunologically distinct types of hepatitis, namely type A (infectious) and type B (serum). Several reports documented the faecal/oral transmission route of hepatitis type A, eliminating hepatitis A virus (HAV) as a causative agent of PTH (167, 260, 306, 316). Hepatitis type B, on the other hand, was demonstrably transmitted through blood and blood products (220, 222), and the discovery of the "Australia antigen", also referred to as HBV surface antigen (HBsAg), and its association with hepatitis B virus (HBV) confirmed the viral etiology of the disease (53, 221). In 1972, soon after the link between PTH and the Australia antigen was established (152), screening of blood from volunteer donors for HBsAg became a US federal regulation. As predicted by many researchers, exclusion of HBsAg-positive and commercial donors reduced the PTH rate by up to 97% (14). However, cases of hepatitis continued to occur even in recipients of HBsAg-negative blood transfusions, indicating that those individuals had contracted an infection associated with virus(es) other than HAV or HBV (13, 122, 330). Transfusion-associated Non-

A, non-B hepatitis (NANBH) was characterized by a shorter incubation period than HBV, and did not conform to the bimodal curve observed for HAV and HBV infection. Further evidence for an unknown infectious agent was provided by epidemiological studies reporting patients with recurring episodes of hepatitis post transfusion, something that was not observed in hepatitis type A and B infections (166, 238, 294, 340).

Despite extensive research in the 1970s and 1980s, the etiological agent(s) of NANBH remained elusive, mainly because no cell culture or animal model was available for the propagation of the unknown agent. The successful transmission of the NANBH agent into chimpanzees eventually made it possible to show that NANBH was caused by a small, enveloped virus (15, 123, 168, 381). However, due to the insufficient concentration of viral antigen in the chimpanzee serum, identification of the virus was delayed until Houghton and colleagues at Chiron, in collaboration with Daniel Bradley at the Center for Disease Control, tackled the problem with a blind immunoscreening approach. They extracted and reverse-transcribed nucleic acid from chimpanzee plasma containing the NANBH agent and used the resulting cDNA fragments to design a recombinant expression library in *E.coli*. By screening the expressed proteins against the serum of a chronically infected NANBH patient they were able to isolate and sequence a single immunoreactive clone designated 5-1-1 (81, 82). Based on the characteristics of the nucleotide sequence - the NANBH virus contains a 10,000 nucleotide positive-strand RNA genome consistent with members of the *Togaviridae* and

Flaviviridae families - the new virus was classified within a separate genus (*Hepacivirus*) of the *Flaviviridae* family and designated Hepatitis C Virus (HCV).

1.2 The disease.

1.2.1 Epidemiology.

To date about 170 million individuals worldwide are persistently infected with HCV (WHO, 2002). The prevalence of HCV infection varies in different parts of the world and is high in Northern Africa, South-East Asia and the Eastern Mediterranean, where up to 5% of the population are infected, compared to approximately 1.7% in Western Europe and North America (WHO, 2002; (17)). The clinical progression of the disease is usually slow and asymptomatic and in most cases it takes decades before severe liver damage occurs (5). Of the 70 to 80% of individuals who develop a chronic infection following exposure to HCV (10, 57, 60), approximately 30% develop liver cirrhosis, while end-stage liver failure and hepatocellular carcinoma are observed in 0.04 to 2.5% of chronically infected patients (10, 16, 71, 90). There is currently no vaccine (237) and antiviral therapies are only effective in about 50% of treated individuals (102, 169).

There are six major HCV genotypes which show approximately 30% divergence (366, 367). Despite sharing a basic virology, these genotypes differ in their geographical distribution and prevalence; genotypes 1,2 and 3 are distributed worldwide and are prevalent in Western Europe, Canada and

the USA (110, 197, 276, 382), while genotypes 4, 5 and 6 can be found in more distinct geographic areas (64, 72, 367).

The outcome of HCV infection is determined early, generally within six months of exposure to the virus, and seems to be partly associated with the HCV genotype (119). Individuals infected with HCV genotype 1 are more likely to develop chronic infection (270, 334) and hepatocellular carcinoma (101), whereas steatosis, an abnormal accumulation of lipids in the liver which is possibly associated with fibrosis, is most frequently observed in genotype 3 infection (342, 343). Also, genotype 1 shows greater treatment resistance than genotypes 2 and 3, with only 40-50% chronically infected individuals on combination therapy resolving a genotype 1 infection compared to 70-80% of those infected with genotype 2 and 3 (124, 426).

1.2.2 Immunobiology.

The main reservoir for HCV replication is hepatocytes in the liver, although several studies suggest that other cell types, such as peripheral blood mononuclear cells (PBMC) and dendritic cells may also be affected (21, 22, 226, 227, 236, 305, 312, 373). The frequency of HCV positive hepatocytes within an infected liver has proven difficult to determine (224, 228), however, viraemia is thought to be high with virus production rates in the range of $1x10^{12}$ RNA copies per day (231). Antibodies against HCV are usually detectable 6 to 8 weeks post infection (317) and can be detected in acutely and chronically infected individuals (251, 282). However, conflicting evidence

exists regarding the role of humoral immunity and B cells in viral clearance (111, 230, 251, 319, 372), particularly since antibody titers are usually high in chronic hepatitis C, suggesting limited neutralizing efficacy (111, 251, 282). Interestingly, sequence changes in the hypervariable-1 region (HVR1) of the HCV envelope glycoprotein E2 have been reported to occur around the same time as antibody seroconversion (56, 57, 119), suggesting that the virus might evade the immune response through escape mutations. Sequencing studies have revealed that clearance of the virus is associated with a reduction in viral diversity in the E1 and E2 coding regions, while a variety of viral quasispecies can be found in persistently infected individuals (119, 120).

Studies of infected individuals have shown that a strong and sustained $CD4^+$ T cell response is crucial to control acute HCV infection (56). RNA appears in the plasma a few days post infection and typically peaks about 8 to 10 weeks later, regardless of outcome (1, 38). Although viraemia is present early, T-cell responses are usually delayed and follow one of three basic patterns (1): in persistent infection, $CD4^+$ and $CD8^+$ T-cell responses are weak or undetectable (91, 284, 393) and fail to control viraemia. In some cases, the viral RNA level is transiently controlled, but viraemia rebounds as a result of a contracted $CD4^+$ T-cell response (91, 284, 393). In acute resolving infection, T-cell responses are vigorous and sustained and target multiple MHC class I-restricted epitopes in structural and non-structural HCV proteins (91, 233). It is not known whether the failure to develop a sustained antiviral response is the result of antigen overload during immunological priming, virus-induced defects

in antigen presentation, mutational escape of epitopes, deletion and functional anergy of T cells, or other causes (56). Overall, the outcome of HCV infection is most likely determined by the magnitude, diversity and quality of the adaptive immune response, while the primary failure to induce a T-cell response or T-cell exhaustion predict viral persistence (79, 333, 362).

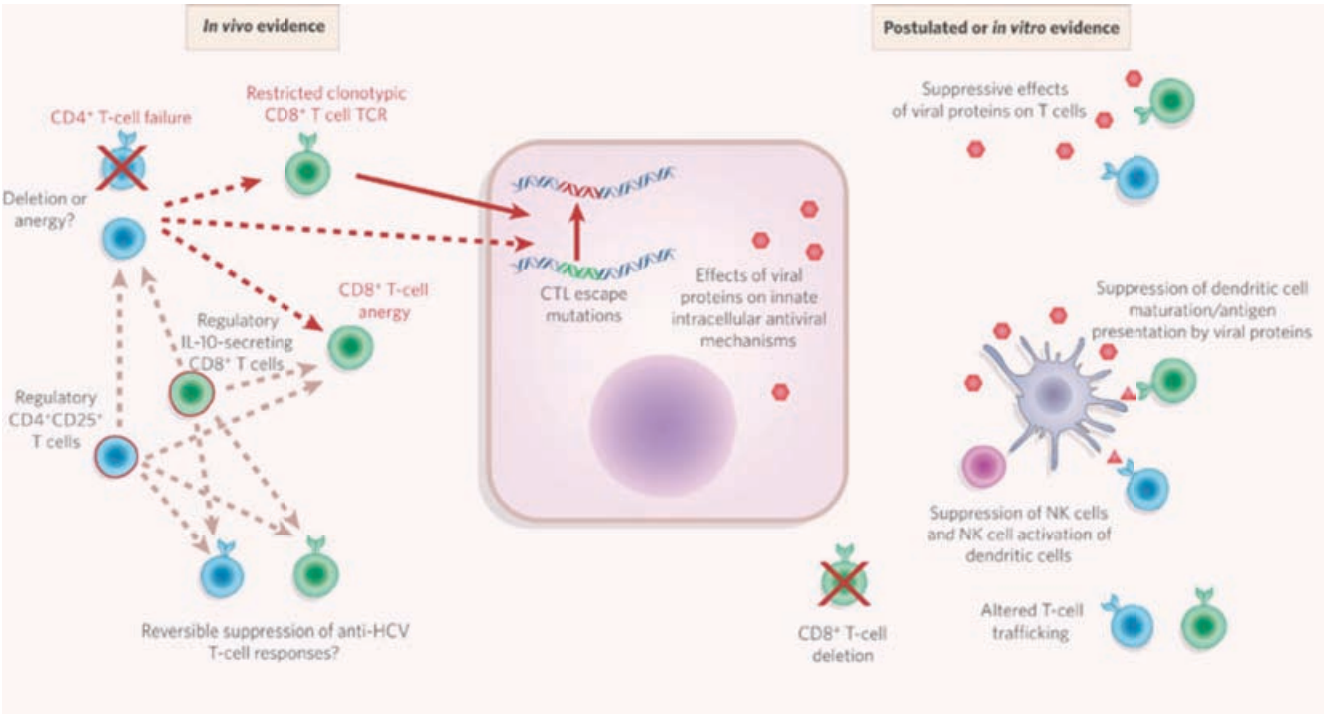

Figure 1-1 Possible mechanisms of immune evasion by HCV.

Red lines annotate mechanisms for which there is supporting *in vivo* evidence; dotted lines indicate mechanisms that are involved in viral persistence; triangles indicate inhibition of antigen presentation (image from (56)).

In addition to its ability to successfully evade host immune responses, HCV is also known for efficient allograft re-infection following liver transplantation. During the anhepatic phase of transplantation, HCV RNA levels typically decrease with a calculated elimination half-life of about 2 hours (144). This decrease in viral RNA concentration can be explained in part by the lack of

virion production by hepatocytes (135). After reperfusion of the graft, the viral load continues to decline rapidly and typically reaches its low about 24 hours later, presumably due to a massive entrance of HCV into the hepatocytes and uptake of the virus by the liver reticuloendothelial system (144). Viral kinetics then follows one of three basic patterns: RNA serum levels can increase rapidly, remain unchanged, or decrease progressively. From week 2 post transplantation, however, the viral RNA concentration in the serum increases exponentially in most patients, peaking by the fourth month after implantation (74). One year after transplantation, viral RNA levels usually exceed pretransplant levels by 10- to 20-fold (143).

To date the standard antiviral therapy for acute hepatitis C infection is treatment with pegylated interferon-α in combination with ribavirin, a guanosine analogue with antiviral activity (reviewed in (124)). In cell culture, virtually any cell type is able to produce type I IFN in response to viral exposure, however, *in vivo*, plasmacytoid dendritic cells (pDC) are seen as the "professional IFN α/β producing cells" (86, 194, 274). In addition to their direct antipathogenic activity, IFN-I has been shown to synergize with proinflammatory cytokines to activate innate effectors such as NK cells, macrophages, and dendritic cells (69) and may modulate antigen presentation and the adaptive immune response (232).

IFN-I production is induced when the innate mechanisms in infected cells and patrolling immune cells recognize pathogen-associated molecular patterns

(PAMPs), e.g. single-stranded and double-stranded viral RNA, and polyuridine signatures (reviewed in (207)). In hepatocytes, HCV dsRNA and proteins are engaged by retinoic-acid-inducible-gene-I (RIG-I) and Toll-like receptor (TLR)-3 (91, 119, 193). This engagement results in the phosphorylation and activation of Interferon-regulatory factor (IRF)-3 and the subsequent production and secretion of type I interferons IFN-α/β, both of which induce the transcription of various IFN-stimulated genes (ISG) through the JAK-STAT signalling pathway and establish a non-virus-specific antiviral state within the cell (39, 354).

HCV induces vigorous intra-hepatic IFN-I responses, however, these responses do not correlate with the outcome of infection (111, 139, 232, 378, 393). Intriguingly, HCV replicons are highly sensitive to IFNα *in vitro* (130), indicating that *in vivo* the virus disables IFN response pathways through multiple mechanisms (Figure 1-2): the core protein, for example, can suppress the JAK-STAT-pathway, while the viral protease NS3-4A functions as an antagonist of IRF-3 activation and IFN-β secretion by interfering with the TLR-3 and RIG-I signalling pathways (129, 242). In addition, the HCV proteins NS5A and E2 can inhibit RNA-regulated protein kinase (PKR), allowing the virus to evade in part the translational-suppressive actions of IFN-I (205). IFN-α therapy aims to substitute for the disrupted IFN production in infected hepatocytes, therein re-establishing ISG expression, promoting memory T-cell proliferation, and stimulating the activation of natural killer cells and dendritic cell maturation (124, 395).

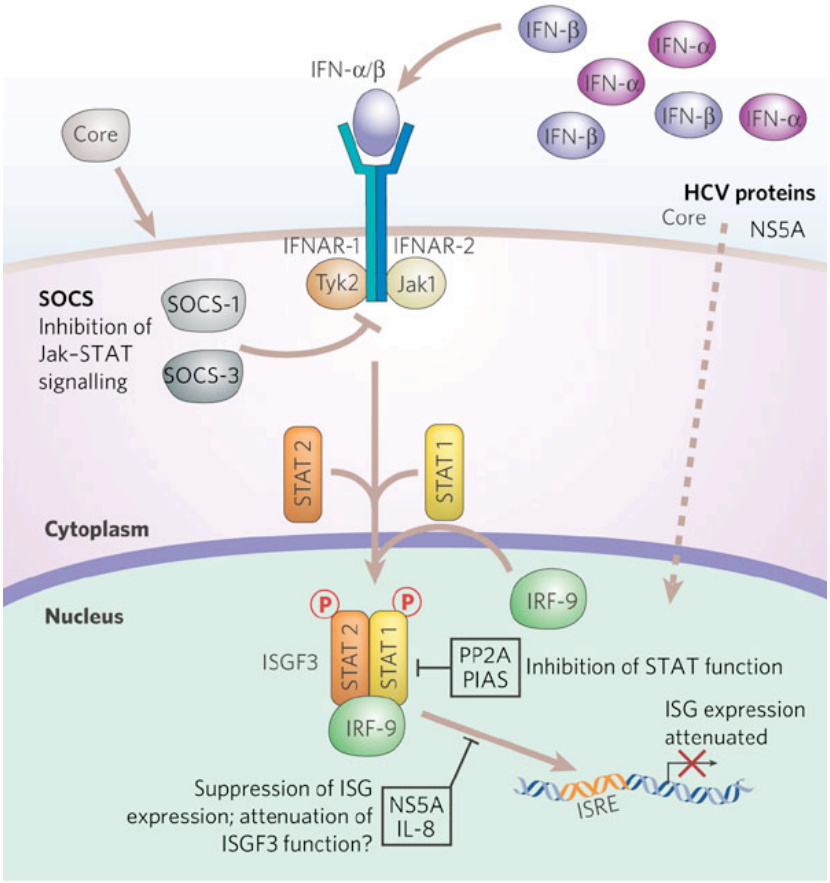

Figure 1-2 Attenuation of IFN signalling by HCV.

Receptor signalling by autocrine and paracrine IFN is subject to feedback inhibition by suppressor of cytokine signalling (SOCS) proteins. The HCV core protein induces expression of SOCS-3, which can suppress Jak–STAT signalling events and block the IFN-induced formation of ISGF3 (12). HCV protein expression in liver cells is associated with induction of the protein inhibitor of activated STAT (PIAS) expression and concomitant inhibition of STAT function in vivo. Patients with chronic HCV infection can exhibit high levels of serum IL-8 (328, 329), which interferes with IFN signalling events that catalyse ISGF3 assembly and function (image from (141)).

Interestingly, the resistance of different HCV genotypes to IFN therapy may in part be determined by the ability of E2 and NS5A to inhibit PKR. Indeed, E2 sequences of genotype 1, which is relatively resistant to IFN therapy, inhibit PKR more efficiently than E2 sequences of genotypes 2 and 3, which respond much better to IFN therapy (333, 388). Likewise, the outcome of IFN treatment of HCV-infected patients in a Japanese cohort correlated with the NS5A genotype (reviewed in (387)).

In order to prevent allograft rejection, patients are treated with immunosuppressive drugs after transplantation. The effect of most of these drugs on viral replication is unknown, although it has been reported that corticosteroid treatment enhances HCV RNA levels *in vivo* (143). Of the calcineurin inhibitors that are routinely used to reduce rejection after organ transplantation, only the effect of cyclosporin A (CSA) on HCV replication has been studied in more detail. CSA suppresses replication of HCV RNA in cultured human hepatoma cells carrying subgenomic (411) or full-length HCV replicons (189). Furthermore, CSA seems to inhibit HCV genome multiplication in cultured hepatocytes infected with plasma from HCV-infected individuals (411). Intriguingly, two other drugs, FK506 (tacrolimus) and rapamycin, which share pharmacological mechanisms that suppress T-cell activation with CSA, do not have any inhibitory effect on HCV RNA replication (300) supporting the hypothesis that the antiviral effect of CSA is not linked to its immunosuppressive activity (411). Instead, CSA might inhibit HCV

replication by binding to cyclophilin B, which has been shown to support replication by associating with the viral NS5B polymerase (412).

1.2.3 Immunopathogenesis.

The effective elimination of HCV infection requires the coordinated function of the innate and adaptive immune responses. However, evidence suggests that the activation of the immune response also plays a key role in the pathogenetic processes leading to progressive tissue damage (reviewed in (371)). Of note, hepatic injury usually coincides with the onset of an immune response during acute infection, but not with that of viral replication, which can occur in the absence of an inflammatory response (11, 60, 118). Also, it has been observed that immunosuppressive therapy may be accompanied by a transient amelioration of inflammatory activity and hepatocellular damage despite increased viraema (89) while termination of immunosuppressive therapy may result in inflammatory aggravation (116, 160). However, in the same study, HCV patients whose immune system was compromised due to hypogammaglobulinemia rapidly progressed to severe liver disease (89), suggesting that the host immune response may still be an important factor in the control of chronic infection.

HCV proteins including NS5A, core and NS3 have been reported to up-regulate TLRs (103, 261), resulting in the activation of transcription factors IRF3 and NF-κb and increased production of IFN-I (172). This in turn stimulates expression of ISGs and provides an amplification loop to further

promote IFN-I and ISG expression (129). In chimpanzees, acute resolving HCV infection is associated with a robust host response characterized by high level ISG expression in the liver (47). However, in chronic hepatitis C high ISG expression is apparently correlated with the extent of liver damage (301, 315), most likely because the up-regulation of TLRs and the stimulation of proinflammatory cytokines contribute to the pro-inflammatory environment. More importantly, the continued activation of cytokine secretion and HCV non-specific effector pathways in the absence of a functional cellular immune response may result in hepatocyte damage, fibrogenesis and malignant transformation (371).

Of note, IFN-inducible protein IP-10, the natural ligand of the CXCR3 chemokine receptor, is induced in hepatocytes surrounded by infiltrating lymphocytes (358) and may promote non-specific recruitment of CXCR3-expressing immune cells to sites of inflammation (339). In cytotoxic T-cells and NK cells, triggering of Fas or TNFR1 by Fas ligand or TNF secretion induces the activation of caspase 8 in susceptible target cells and, subsequently, apoptosis. HCV infection induces TNF production in hepatocytes, although elevated serum TNF levels are mostly observed in the acute phase of hepatitis C (154, 397). However, it is interesting to speculate that in HCV infection, intrahepatic T-cells expressing Fas ligand may interact with Fas-positive hepatocytes to induce cell death, since high Fas serum levels seem to correlate with the severity of hepatic injury in chronic hepatitis C (176, 180, 311). Furthermore, the amount of infiltrating cytotoxic ($CD8^+$) T-

cells reportedly correlates with hepatocellular apoptosis (321), unlike the level of transaminases, which are released into the serum following hepatocellular injury.

In addition to stimulating IFN-I production, NF-κb is involved in the regulation of chemokines, thus activating the recruitment of NK and NKT cells, which exert cytolytic activity and inhibit viral replication by secreting inflammatory cytokines. NK cells play a crucial role in the antiviral host response, however, in chronic HCV infection they secrete abundant levels of interleukin-10 and TGFβ (304), both of which stimulate the proliferation and extracellular matrix deposition of hepatic stellate cells (HSCs) (325). In normal liver, HSCs are nonparenchymal, quiescent cells whose main functions are to store vitamin A and to maintain the normal basement membrane-type matrix. However, in response to liver injury, HSCs switch to an activated state in which they become highly proliferative and synthesize "fibrotic" matrix rich in type I collagen (131, 132).

1.3 Model systems for HCV study.

1.3.1 Primary cell culture and cell lines.

For more than two decades the major limitation for HCV research was the lack of a cell culture system that allowed efficient propagation of the virus. Until HCV was identified in 1989, insight into the elusive NANBH agent was provided almost exclusively by serological and epidemiological studies, since immortalized cell lines seemed to be unsusceptible to HCV infection, while

systems based on the cultivation of primary cells isolated from the tissues of chronically infected patients and infection of primary hepatocytes with HCV, respectively, were hampered by the low level of HCV replication. Moreover, experiments were difficult to reproduce since the infectivity of the sera generally did not correlate with the HCV RNA titre. HCV-specific antibodies present in the sera of most chronically infected patients also impaired the productivity of infection, as did the quality of the hepatocyte preparation. To add to the difficulties, the low viral replication rate demanded the use of a highly sensitive detection method. Flaviviruses, like other positive strand RNA viruses, replicate via a negative strand RNA intermediate and it was assumed that HCV was no exception. Thus, *in vitro* studies used strand-specific reverse transcriptase polymerase chain reaction (RT-PCR) to detect the negative-sense molecule, which was believed to be indicative of viral replication (347). Although it was now possible to detect very low levels of HCV RNA, the new method was fraught with problems, including the potential for contamination and lack of strand-specificity of the reaction due to self-priming of the RNA, false priming of the incorrect strand, and random priming by cellular nucleic acids (162, 225, 384). Since these problems were difficult to overcome, additional criteria were introduced to verify replication in HCV-infected cells. These included sequence analysis to demonstrate genomic variability, successful transmission from infected to naïve cells, “curing” infected cells with interferon a, and detection of viral antigens.

Despite the technical difficulties implied with the primary cell culture system, Iacovacci et al. (185, 186) and Lanford et al. (225) were able to propagate serum-derived HCV in primary human and chimpanzee hepatocytes, respectively. Both studies reported a significant increase of HCV positive stranded RNA within the first four days of infection, while the negative stranded RNA signal became first detectable on day four and increased markedly thereafter. Lanford and colleagues furthermore noted that primary liver cells isolated from baboons were not susceptible to infection supporting the idea that HCV has a narrow host range. Interestingly, a positive stranded RNA signal was detectable in these cells up to 11 days post inoculation despite their apparent non-permissiveness, demonstrating that caution must be exercised when differentiating between newly synthesized RNA and the original inoculum.

1.3.2 The replicon system.

Although primary cell culture provided some insight into the basic principles of HCV infection, the heterogeneity of the inoculum, the low RNA replication rate, and the inability to manipulate the genome made it difficult to analyze the viral life cycle in any detail. In a first attempt to overcome these obstacles, Lohmann et al. created a neomycin-selectable HCV minigenome (replicon) based on the *Con1* consensus genome cloned from liver-derived viral RNA (254). Originally, a full-length genome was used to transfect various cell lines and primary human hepatocytes. However, the full-length RNA failed to replicate for unknown reasons prompting Lohmann et al. to generate a

number of bicistronic constructs, which comprised of the 5'-HCV internal ribosome entry site (IRES), a neomycin phosphotransferase gene, the genotype 1b non-structural genes NS2 or NS3 to NS5B under the control of an Encephalomyocarditis virus (EMCV) IRES, and the HCV 3'-nontranslated region (NTR).

Subsequently, Blight et al. generated similar neomycin-selectable replicons based on a *HCV-H* genotype 1a infectious clone described by Kolykhalov and colleagues (50, 213). Unlike their full-length counterparts the new subgenomic replicons replicated to a high level, a fact that was attributed to cell-culture adaptive mutations in the NS3, NS5A and NS5B region (50, 219, 253). Based on these findings, several groups successfully generated full-length replicons with single amino acid substitutions in the genes encoding the non-structural viral proteins (51, 187, 203, 322). As expected these cell culture-adaptive mutations markedly enhanced RNA levels as well as the frequency of cells supporting replication. However, Huh-7 cells harbouring full-length replicons of the prototypic viral strains *Con1* and *HCV-H* still failed to produce infectious particles although the *Con1* strain was infectious *in vivo (63)*, indicating that the structural proteins were assembly competent. Furthermore, the number of HCV RNA replication-competent cells within the total population remained low even for adapted replicons, suggesting that the cellular background was a major determinant of replication efficiency.

To enhance permissiveness of the Huh-7 cell line, Blight et al. transfected Huh-7 cells with subgenomic replicons with either the wildtype amino acid sequence, a serine-to-ileucin substitution (S2204I) in the NS5A region, or a 47-amino acid NS5A deletion (5AD47) (52). Cells supporting viral replication were selected and cured of HCV RNA by prolonged treatment with interferon (IFN) a. The resulting clonal cell lines were then tested for their ability to support HCV replication following re-transfection with subgenomic and full-length replicons. One clone in particular, designated Huh-7.5, showed an up to 33-fold increase in the frequency of cells able to support HCV replication, as well as a significantly enhanced replication capacity. A key feature of the host antiviral defense is the production of IFNα and IFNβ and subsequent expression of IFN-stimulated genes in response to viral double stranded RNA or GU-rich single stranded RNA (354). In most cells, these specific *pathogen-associated molecular patterns* (PAMPs) are recognized by Toll-like receptors (TLRs) (310). However, in cultured hepatocytes PAMPs are recognized by a cellular helicase, RIG-I, which triggers activation of the IFN-regulatory transcription factor-3 (IRF3), IFN production, and expression of the IFN-stimulated genes. In Huh-7.5 cells, however, a mutation in RIG-I abolishes PAMP signalling to IRF3, thus inhibiting the cellular antiviral response and conferring increased permissiveness for HCV RNA replication (380).

1.3.3 HCV pseudoparticles (HCVpp) and cell-culture derived HCV (HCVcc).

The replicon system provides a valuable tool to study HCV replication. However, it does not allow studies of virus attachment and entry as mediated

by glycoprotein-receptor interactions. First attempts to generate HCV-like particles in insect cells using Baculoviruses that contained the cDNA of the HCV E1/E2 structural proteins (37) were only moderately successful. Recombinant Vesicular stomatitis virus (VSV) that expressed genes encoding the HCV structural proteins fused to domains of the VSV envelope proteins also failed to infect permissive cell lines (65), although the HCV glycoproteins were efficiently incorporated into the carrier-virus-envelope. Several groups finally developed infectious HCV pseudoparticles (HCVpp) by expressing the E1/E2 structural proteins in 293T cells together with a packaging construct encoding the HIV genome minus the *env* gene, and the *gag* and *pol* genes of murine leukaemia virus (MLV) or VSV (30, 106, 183). Co-expression of these constructs led to the efficient assembly of infectious replication-deficient HCV pseudoparticles, which allowed in depth studies of virus binding, attachment, and internalization, and helped to identify novel HCV receptors.

Finally, Wakita and colleagues cloned a genotype 2a replicon (JFH-1) from a Japanese patient with fulminant hepatitis, which replicated efficiently in liver-specific and non-liver specific cell lines without the need for adaptive mutations and supported the secretion of infectious viral particles in cell culture (244, 408). Subsequently, another research group produced infectious HCV genotype 1a (Hutchinson strain; H77-S) (419), a strain that is most prevalent in the U.S. and many other countries (424). Using these cell culture-derived infectious particles (HCVcc) it is now possible to study the HCV life cycle from entry to release. Recently, Lindenbach et al. constructed a chimeric

JFH-1 genome containing the core to NS2 region of HCV strain J6 (244), which not only produced infectious particles *in vitro*, it also replicated efficiently in chimpanzees and uPA-SCID mice (245), allowing for the first time the dissection of the HCV life cycle *in vitro* as well as *in vivo*.

1.3.4 Animal models.

For more than a decade, the chimpanzee was the only animal model available to study HCV infection. Like humans, chimpanzees have detectable HCV RNA within a few days of infection with viral titers usually reaching 10^5–10^7 RNA genome copies/ml, and a rise in viraemia is usually followed by an increase in serum aminotransferase (ALT) levels (reviewed in (94)). Furthermore, the majority of infected animals display necroinflammatory changes in liver biopsies and 40-60% of infected animals progress toward chronic viral persistence (33, 48). The chimpanzee model was used to characterize the infectious agent of NANBH (15, 123, 381), and to clone the HCV genome for the first time (81). Finally, the chimpanzee model was instrumental in the establishment of HCV infectious molecular clones (213, 416).

One major advantage of the chimpanzee model is the ability to monitor the progression of hepatitis C from beginning to end. This is of particular interest since HCV infection in humans is usually asymptomatic, making it difficult to study the acute phase of infection. In chimpanzees, however, liver biopsy samples can be obtained before the exposure and at intervals post-

inoculation, allowing the analysis of events starting immediately after HCV infection, such as changes in gene regulation and cellular immune responses to viral antigens (94). Furthermore, studies in the chimpanzee model have shed light on different aspects of the cellular immune responses and their role in viral clearance and persistence, respectively (91, 302, 363, 392), and the role of memory immune responses in HCV re-infection (34, 48, 331, 413).

The ideal model for studying HCV would be one that adequately represents most aspects of human HCV infection and disease, is affordable, easily available, and reproducible. During the past decade, several groups have developed transgenic mouse models to examine the effects of the HCV core and the envelope glycoproteins on hepatocytes. However, studies using these transgenic mice yielded conflicting results (292, 293, 314, 342), putting into question the suitability of this *in vivo* model. Recently, however, several groups have reported the creation of chimeric (xenograft) mice harbouring human hepatocytes (99, 279, 281). These mice are immunodeficient and suffer from severe, chronic liver disease caused by overexpression of the noxious protein urokinase. Overproduction of urokinase not only causes hepatocyte death, it also causes individual hepatocytes to delete portions of the urokinase transgene and to acquire a replicative advantage over surrounding cells. As a result, the liver is rapidly repopulated with largely nontransgenic cells, a survival advantage that is extended to hepatocytes transplanted from mouse, rat, and human (279). Chimeric mice, such as the SCID/uPA mouse, have been successfully infected with HCV derived from

human serum and have been shown to support viral replication at clinically relevant titers (281), allowing investigators for the first time to study HCV infection in a small animal model.

Indeed, the new *in vivo* model system has proven useful in the evaluation of novel anti HCV therapies. uPA/SCID mice were used to test a gene therapy approach to treat HCV by delivering a modified form of the BH3-interacting death agonist (BID), a member of the Bcl-2 family of pro-apoptotic proteins which is crucial for death receptor-mediated apoptosis (182). More recently, the xenograft mouse model was employed to study the neutralizing efficacy of human monoclonal antibodies (mAbs) against genetically diverse HCV isolates (230). Here, Law et al. were able to demonstrate that human mAbs from the serum of HCV infected patients protected against heterologous viral infection, suggesting that a prophylactic vaccine against HCV may be achievable. Meuleman et al. in turn demonstrated that CD81 is required for HCV infection *in vivo* and that prophylactic treatment with anti-CD81 antibodies protects uPA/SCID mice from a subsequent infection with HCV strains of various genotypes (280).

1.4 The HCV Life Cycle.

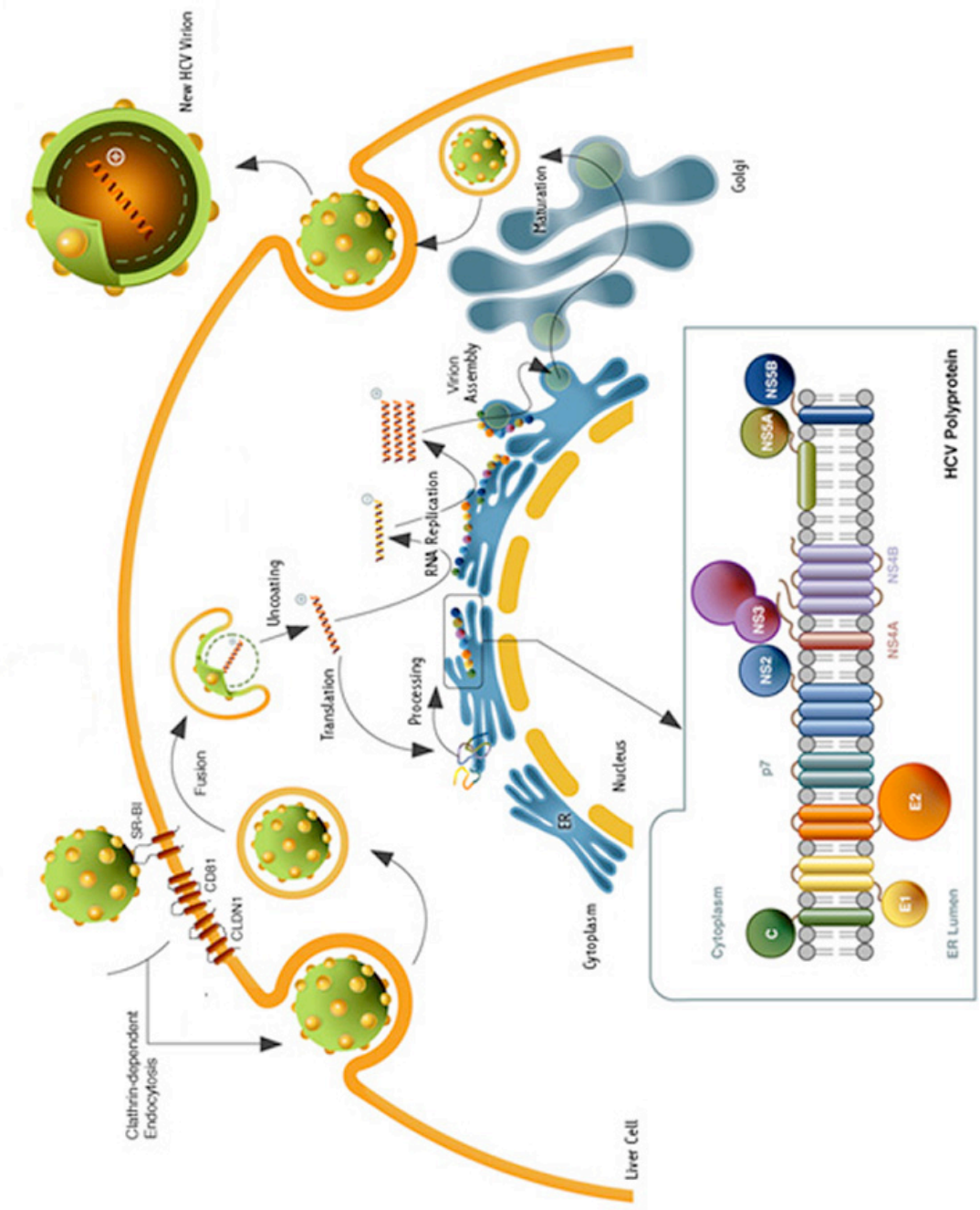

Figure 1-3 The HCV life cycle.

(modified from Tibotech Pharmaceuticals, Belgium)

1.4.1 HCV genome replication and polyprotein processing.

The genome of HCV is well characterized as a single-stranded 9.6 kb RNA molecule comprising a single open reading frame (ORF) that encodes a 3000 amino acid polyprotein precursor flanked by two nontranslated regions (NTRs). As the HCV genome lacks a 5' cap, translation of the genome depends on an internal ribosome entry site (IRES) which is located within the highly conserved 5'NTR and directly binds 40S ribosomal subunits to induce translation of the precursor protein (246). The polyprotein precursor is co- and posttranslationally processed by viral and host proteases into a variety of structural and non-structural proteins. The amino terminal one-third of the polyprotein harbours the core protein and the envelope glycoproteins E1 and E2, followed by a small integral membrane protein, p7, a metalloprotease that might function as an ion-channel (158). The carboxy-terminal two-thirds of the precursor protein encode the non-structural proteins, which are involved in the coordination of the virus life cycle.

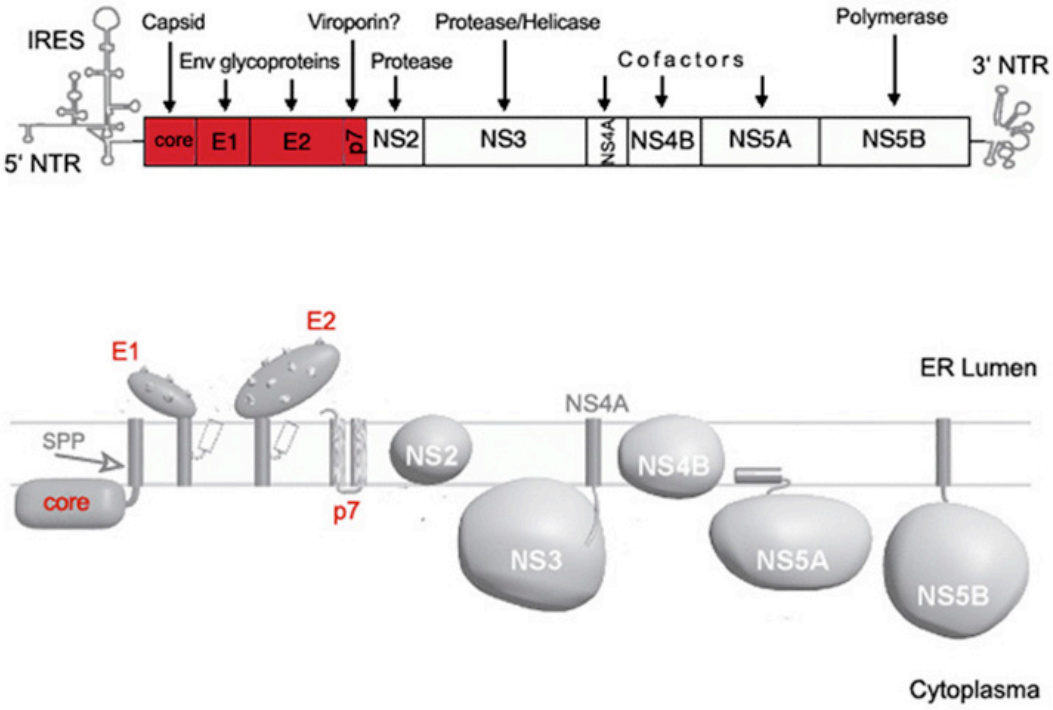

Figure 1-4 The HCV genome and proteins.

Translation depends on an internal ribosome entry site (IRES) within the 5' non-translated region (NTR). The polyprotein precursor is posttranslationally processed by host and viral proteases and the HCV structural (red) and non-structural proteins are localized within the ER membrane. (image modified from (78)).

Following cleavage of the structural proteins by host proteases, two viral enzymes further process the polyprotein. The NS2-3 proteinase cleaves at the NS2/3 junction (157, 175), whereas the NS3-4A serine protease cleaves at all downstream sites with a temporal sequence that is thought to be crucial for replication (100). In addition to its protease function, NS3 serves as a RNA helicase, unwinding double-stranded RNA in a 3' to 5' direction. Recently, it was also shown that NS3-4A cleaves the mitochondrial antiviral signalling (MAVS) protein, which interacts with a receptor for intracellular viral dsRNA (RIG-I) and induces the IFN response. Cleavage of the MAVS protein results in its dislocation from the mitochondria and perturbance of its activity, helping HCV to evade innate immunity (243).

HCV replication proceeds via synthesis of a complementary minus-strand RNA using the viral genome as a template. This minus-strand RNA then serves as a template to generate multiple nascent HCV genomes. The key enzyme responsible for both steps is NS5B (289), which is localized to the ER lumen, where it is anchored to the membrane via an insertion sequence (350) that may serve as a docking site for transmembrane protein-protein interactions. NS5B is able to initiate synthesis of the minus- and plus-strand RNA in a primer-dependent way as well as *de novo*, although *in vitro* the enzyme seems to prefer the primer-dependent variant (9, 126, 201). Interestingly, NS5B binds to a wide variety of RNA and DNA templates and so far it is unclear how template specificity is achieved, although it has been shown that recombinant NS5B can recognize HCV RNA through a conserved stem-loop structure made up from sequences of the 3' coding region and the

3'NTR of the polyprotein (77). Interestingly, protease treatment of permeabilized cells destroys most non-structural proteins without compromising the activity of NS5B, suggesting that only a small fraction of NS proteins is actively engaged in replication (286).

Not much is known about the function of the serine phosphoprotein NS5A, except that it exists in a hypo- and a hyperphosphorylated form (199, 332, 390) and that it modulates HCV RNA replication by interacting with NS5B and various cellular regulatory factors (149, 402), (361). Indeed, adaptive mutations in NS5A domains I and II enhance the ability of the virus to replicate *in vitro* (50, 219, 252). NS5A domain III is not involved in RNA replication, however, Tellinghuisen et al. recently demonstrated that a single serine residue deletion in domain III inhibits phosphorylation of the casein kinase II consensus motif in this region of NS5A (389), disrupting the production of infectious virus at an early stage of particle assembly. Furthermore, it has been suggested that NS5A might play a role in the development of IFN resistance, due to the protein's ability to inactivate double-stranded RNA dependent kinase (PKR), thus modulating the IFN-stimulated antiviral response (140). Finally, NS5A can function as a transcriptional trans-activator. The exact nature of this mechanism is unclear but it has been proposed that the protein, which is localized to the ER, activates cellular transcription factors by inducing oxidative stress in the host cell (153). In this way NS5A might also contribute to the liver disease pathogenesis associated with HCV infection.

1.4.2 HCV Attachment And Entry.

The first step in the viral life cycle is the binding of the virus to the host cell via interaction of the viral glycoproteins with one or more cell surface receptors. In some cases these receptors serve as mere attachment factors, however, they may also be involved in the internalization of bound virus particles via one of two major entry routes, namely fusion of the viral envelope with the plasma membrane or uptake via endocytic-like pathways (reviewed in (267, 369)).

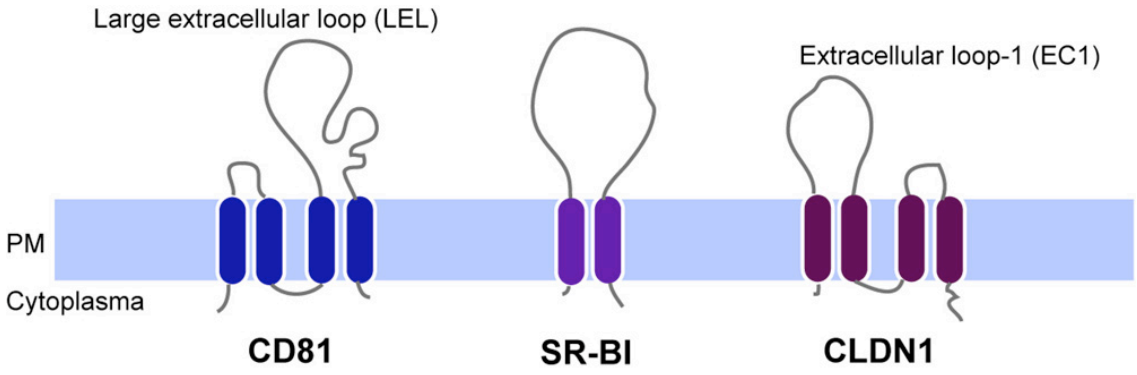

Figure 1-5 HCV entry receptors.

The receptor activity of CD81 and Claudin-1 (CLDN1) depends on critical residues within the LEL and EC1 domains, respectively.

Tetraspanin CD81

CD81 is a 26-kDa surface protein composed of four hydrophobic transmembrane domains and two hydrophilic extracellular domains (EC1 and EC2) (239). Like other members of the tetraspanin superfamily, CD81 is expressed in a range of organisms, including mouse and chimpanzee, and on most human tissues apart from red blood cells and platelets (113). The cytoplasmic and transmembrane domains as well as small extracellular loop of CD81 are highly conserved between species, while the large extracellular domain varies considerably both in length and sequence, thus contributing to species-specific interactions. Cross-linking experiments have shown that human CD81 mediates a number of signal transduction events involved in the regulation cell proliferation, morphology, differentiation, adhesion, and motility (241).

Soluble truncated versions of HCV glycoprotein E2 bind with high affinity to human lymphoma and hepatocarcinoma cell lines. By screening a cDNA expression library from a subclone of the human T-cell lymphoma cell line Molt-4 with recombinant E2, Pileri et al. identified CD81 as the E2-binding partner (324). Binding of E2 to CD81 was mapped to the large (major) extracellular loop of the tetraspanin and it was furthermore demonstrated that the E2-CD81 interaction is species-specific; only fusion proteins containing the large extracellular loop (LEL) of the human protein bound E2 in immunoblots, while no interaction with mouse protein was observed (324). Using alanine scanning mutagenesis positions L162, I182, N184 and F186

within the LEL were subsequently shown to be involved in the CD81-E2 interaction (98, 107, 128).(174).

Further evidence for the important role of CD81 in HCV entry was provided by studies demonstrating that the soluble form of CD81 LEL and monoclonal anti-CD81 mAbs inhibit HCVpp and HCVcc infection of human hepatoma cells and primary human hepatocytes (32, 183, 244, 427). Furthermore, CD81 knockdown hepatoma cells are no longer susceptible to HCVpp and HCVcc infection (8, 427), while ectopic expression of CD81 confers HCVpp and HCVcc permissiveness to otherwise non-permissive HepG2 and HH29 hepatoma cells (93, 183, 229, 427). Furthermore, HCVpp bearing glycoproteins from various genotypes varied in their ability to infect HepG2 expressing CD81, suggesting genotype specific differences in CD81-E2 interactions (229, 273). However, infection with all genotypes could be blocked by CD81 and SR-BI specific antibodies in a dose-dependent manner (156). Together these data suggest that susceptibility to HCV is CD81-dependent. However, CD81 alone is not sufficient to mediate glycoprotein-dependent HCV cell entry since ectopic expression of CD81 fails to confer permissiveness to non-hepatic cell lines (30, 183) and retroviral particles displaying functional E1E2 glycoprotein complexes fail to infect some human cell lines although CD81 expression levels are comparable to those of HCV-permissive cells (427). Also, the capacity of CD81 to internalize is poor compared to receptors like SR-BI (320), and the abundant expression of CD81 is unlikely to explain the hepatotropism of HCV. However, the level of

CD81 surface expression seems to determine the efficiency of HCV infection in human hepatoma cells and it has furthermore been reported that a minimal threshold of CD81 expression is necessary to render these cells HCV permissive (215). Recently, the importance of CD81 for *in vivo* HCV infection was confirmed by Meuleman et al. who showed that prophylactic treatment with anti-CD81 antibodies completely protected human liver-uPA-SCID mice from a subsequent challenge with HCV consensus strains of different genotypes (280).

Tetraspanins build 'tetraspanin webs' through interaction with each other and other protein partners (240, 344). Within these multi-molecular complexes tetraspanins form primary associations with a limited number of so-called tetraspanin partners. CD81 specifically interacts with two novel immunoglobulin proteins, EWI-F (FPRP, CD315) and EWI-2 (PGRL, CD316) (75, 76, 84, 376, 377), which are thought to link the tetraspanin web to the actin cytoskeleton by interacting with the Ezrin-Radixin-Moesin (ERM) protein Ezrin (345). Very recently, it has been demonstrated that ectopic expression of a cleavage product of EWI-2, designated EWI-2wint (without its N-terminus), markedly reduces HCVpp and HCVcc infection in human hepatoma cells, most likely by blocking the E2-CD81 interaction (337). Interestingly, EWI-2wint is not present in primary hepatocytes indicating that permissiveness of a cell line to HCV infection might not only depend on the presence of specific entry factors but also on the absence of specific inhibitor(s).

Scavenger-Receptor Type B Class I (SR-BI)

Human SR-BI (CLA-I) is a 82 kDa glycoprotein consisting of a cytoplasmic C-terminal and N-terminal domain and two membrane-spanning domains which are separated by a large extracellular loop (ECL) (336). SR-BI is highly expressed in tissues with crucial roles in cholesterol metabolism, i.e. adrenal glands, ovaries and hepatic tissues, and is responsible for the selective uptake of various lipids including native, oxidized, and acetylated low density lipoprotein (LDL) (4), high density lipoprotein (HDL) (3), and very low density lipoprotein (VLDL) (67). In its role as a lipoprotein receptor, SR-BI mediates the bidirectional exchange of lipids at the cell membrane via a three step-process. Binding of cholesteryl ester (CE)-rich HDL and LDL leads to formation of a productive ligand-receptor complex (374) , which then facilitates incorporation of CE molecules into the plasma membrane (338), as well as the efflux of cholesterol to lipoproteins and other acceptors (195, 196).

Soluble E2 (sE2) binds to CD81-negative human HepG2 hepatoma cells via SR-BI (349), and this interaction has been shown to be specific (26, 349) although attempts to demonstrate a direct interaction between SR-BI and the E1E2 heterodimer have been unsuccessful, probably due to the SR-BI binding sites not being accessible to E2 in the context of the E1E2 heterodimer (reviewed in (87)). However, SR-BI has been shown to interact with HCVpp via the hypervariable region-1 (HVR-1) of the E2 glycoprotein (32) and that this region is essential for the HDL-mediated enhancement of HCVpp infectivity (407). The exact role of SR-BI in HCV entry is poorly understood.

However, recent evidence suggests that both CD81 and SR-BI are required for productive HCV entry, and that SR-BI might form a receptor complex with CD81 and/or other cell surface molecules to facilitate uptake of virus particles. While $CD81^-/SR\text{-}BI^+$ HepG2 cells are not susceptible to HCVpp infection despite their E2-binding capacity, ectopic expression of CD81 restores permissiveness in these cells (30, 427). Further evidence for the importance of SR-BI has been provided by the findings that pre-incubation of $CD81^+/SR\text{-}BI^+$ HepG2 and Huh-7 cells with anti-SR-BI antiserum reduces HCVpp infectivity up to 80% depending on the HCVpp genotype (32), while high levels of SR-BI significantly increase the susceptibility of Huh 7.5 cells to HCV infection (159). Finally, ectopic expression of SR-BI in rat hepatoma cells, where endogenous SR-BI expression levels are undetectable, confers permissiveness to HCVpp and HCVcc infection (105), confirming that SR-BI is indispensable for HCV infection.

In human plasma, circulating HCV particles can be complexed with HDL, LDL, or VLDL (20, 263, 309, 394) and it seems plausible that SR-BI might mediate viral entry through indirect interaction with HCV-associated lipoproteins. Indeed, native HDL has been shown to markedly increase HCVpp infectivity (31, 407), not only when added pre binding but also when added to pseudoparticles prebound to target cells. In addition, it has been observed that lipid transfer inhibitors strongly reduce the enhancing effect of HDL on HCVpp infectivity (407). Together, these findings indicate that HDL might

facilitate viral entry by affecting the lipid transfer activity of SR-BI, rather than by serving as a carrier for virus particles.

Claudin-1 (CLDN1)

The 21 kDa CLDN1 protein belongs to a family of highly conserved transmembrane proteins involved in tight junction (TJ) formation (291). Like occludins, another group of TJ proteins, claudins consist of short cytoplasmic amino and carboxy-termini, four membrane spanning domains, and a large (EL1) and small (EL2) extracellular loop. Claudins are expressed in most tissues including the liver, where they interact with each other to form intercellular TJ strands (reviewed in (155). In addition, most claudins carry a PDZ-binding motif on their C-terminus through which they directly interact with the tight junction-associated *zonula occludens* (ZO) proteins -1, -2, and -3 (190). Blocking this interaction results in the formation of aberrant TJ strands along the lateral cell membrane (271), suggesting that the interaction with ZO-1 and/or additional factors is essential for the correct incorporation of claudins into tight junctions. Furthermore, it has been shown that claudins are crucial for the barrier function of tight junctions, as mutations in claudin-16 and claudin-4 (paracellin-1) impair the paracellular permeability to calcium, magnesium and sodium, respectively (181, 368), and claudin-1 knockout mice die from dehydration within one day of birth due to defects in their epidermal barrier function (137).

CD81 and SR-BI are essential for HCV entry but do not confer susceptibility to HCV to non-hepatic cells (32, 183, 427), indicating that additional hepatocyte-specific factor(s) are required for productive infection. In a recent study it has been demonstrated that non-permissive 293T cells, human embryonic kidney cells that express CD81 and SR-BI, but not CLDN1, become susceptible to HCV infection as a result of CLDN1 expression (114), identifying CLDN1 as a crucial HCV entry factor. When a Flag epitope is inserted in the large extracellular loop of CLDN1, an anti-Flag antibody inhibits HCVpp infection in a dose-dependent manner (114), suggesting a direct interaction between the tight junction protein and HCV. On the other hand, the expression level of CLDN1 does not modulate HCVpp or HCVcc infectivity, which hints at an indirect interaction. Evans and colleagues therefore propose that virus-receptor interactions prior to CLDN1 engagement might trigger conformational changes in the TJ protein that are required for HCV binding, similar to HIV binding to the CCR-5 co-receptor, which requires prior interaction with CD4 (415). Even more recently, CLDNs 6 and 9, which are expressed in the liver and on peripheral blood mononuclear cells (PBMCs), were identified as additional co-receptors for HCV (428) based on the observation that 293T cells expressing CLDN6 or 9 become HCVpp permissive, while the expression of other claudins does not confer susceptibility to infection. Interestingly however, not every $CD81^{+}$/$SR\text{-}BI^{+}$ non-permissive human cell lines becomes susceptible to HCV infection, even when ectopically expressing CLDN1 (114), suggesting that productive viral infection requires at least one more human-specific viral entry factor.

Indeed, another TJ protein, occludin (OCLN), was recently identified as a crucial factor for HCV entry (326). Ectopic expression of OCLN rendered non-permissive murine and human cell lines susceptible to HCVpp infection, whereas OCLN silencing in permissive cells impaired HCV entry. However, OCLN alone was not sufficient to confer permissiveness to unsusceptible cells, indicating that all four HCV entry factors have to act in concert to allow efficient infection.

Other putative HCV attachment and entry factors.

In binding studies using soluble E2 (sE2) it has been observed that the HCV envelope glycoprotein interacts with a number of different cellular factors including the C-type lectins L-SIGN and DC-SIGN (145, 258, 327), the low density lipoprotein (LDL) receptor (LDLr) (6, 288), and glycosaminoglycans (GAGs) (27, 423). GAGs are proteoglycans that have been posttranslationally modified by glycosyltransferases in the Golgi apparatus. where polysaccharides are added to the protein (proteoglycan) core (142).

GAGs are thought to capture HCV on the cell surface and transfer bound particles to a second – and more specific – receptor. This initial attachment is probably mediated by interaction of E2 with heparan sulfates, which are a highly sulfated form of GAGs and commonly found in the plasma membrane, where they serve as a ubiquitous target for viral attachment (28, 44). However, conflicting evidence exists regarding the role of GAGs in HCV entry.

Soluble E2 reportedly interacts with heparin, a structural homologue of heparan sulfate (27, 423). Also, heparinase, an enzyme able to degrade heparan sulfates at the cell surface, inhibits HCV attachment to target cells (148, 216). Furthermore, the hypervariable region (HVR1) of E2 has been shown to interact with heparan sulfates, however this interaction does not result in the binding of HCVpp (35). In line with this observation, E2 does not bind to heparin in the context of HCVpp, possibly because the heparin-binding domain is not accessible on the mature form of the glycoprotein (66). Instead, the association of the E2 glycoprotein with heparan sulfates might occur via electrostatic interactions involving basic residues probably including the E2 HVR1 (27, 28).

The LDL receptor was proposed as a HCV entry factor because of the association of the virus with LDL and VLDL, and indeed Agnello et al. demonstrated that LDLr-mediated endocytosis of serum-derived HCV is inhibited by anti-LDLr-antibodies (6). In the same study, HCV endocytosis was inhibited in competition assays with LDL and VLDL, indicating that the LDLr is involved in the internalization of HCV in hepatoma (HepG2) and B cell lines. Furthermore, the LDLr has been shown to mediate endocytosis of serum-derived HCV in primary hepatocytes (287). Intringuingly, these results could not be reproduced with HCVpp (30), suggesting that to enter cells via the LDLr, HCV particles might need to associate with LDL or VLDL.

The intercellular adhesion molecule 3-grabbing nonintegrins DC-SIGN and L-SIGN have been proposed as HCV candidate receptors as sE2 binds to both receptors with high affinity (258). Furthermore, DC and L SIGN bind HCV virus like particles (HCV VLPs), HCVpp and serum-derived HCV and this interaction can be inhibited using exogenous mannose ligands and receptor specific antibodies (29),(145, 257, 258).

Since DC-SIGN and L-SIGN are expressed on dendritic cells and liver/lymph node sinusoidal endothelial cells, respectively, but not on hepatocytes, it is likely that these lectins contribute to the persistence of infection and/or the dissemination of HCV to target organs by capturing and transmitting virus particles to susceptible cells (92, 257).

1.4.3 HCV enters cells via clathrin-mediated endocytosis.

Following attachment to the cell surface, virus particles are internalized, which requires fusion of the viral envelope with the cellular membrane. In the case of viruses like human immunodeficiency virus (HIV) and herpes simplex virus (HSV), this event takes place at the cell surface at neutral pH, while for classical flaviviruses fusion occurs in an endosomal compartment at low pH (161, 170). Recent studies based on HCVpp (183) and HCVcc (401) have demonstrated the pH-dependency of HCV entry. Furthermore, it is now known that HCV enters cells via the clathrin-mediated endocytic pathway (49, 278). Clathrin and associated proteins assemble at the cell membrane to form a so-called coated pit in a process that is driven by dynamin (reviewed in

(295). Maturation of the clathrin-coated pits into early endosomes is characterized by shedding of the protein coat and acidification. Once HCV has entered the target cell, the low pH of the coated pit triggers conformational changes of the envelope glycoprotein and fusion with the endosomal membrane leading to release of the viral genome into the cytoplasm.

The fusion of viral and host membranes is mediated by two major classes of viral fusion proteins, class I and II (reviewed in (210)). The HCV envelope proteins are thought to resemble the folding pattern of class II fusion proteins (318), which change conformation in response to a cellular trigger such as low pH, leading to the exposure of the fusion peptide (209, 268). As discussed, HCV entry requires acid pH and indeed, compounds that prevent acidification of the endosomes inhibit HCVpp infection (49, 88, 183, 278). Interestingly, exposure of cell-bound virus to low pH does not affect HCV infectivity (49, 401), suggesting that HCV glycoproteins require an additional trigger, such as receptor interaction, to become sensitive to low pH.

HCVpp entry is significantly reduced in Huh-7 cells expressing a dominant-negative Rab5 GTPase mutant, which interferes with cargo delivery to early endosomes, but not in cells expressing a Rab7 GTPase mutant, which interferes with transport to late endosomes, indicating that HCV entry requires delivery of the virus to early but not to late endosomes (278). Furthermore, Meertens et al. observed a 20-min lag between HCVpp internalization and

fusion, while for other viruses, like semliki forest virus or vesicular stomatitis virus, both of which fuse in early endosomes, these events were closely related (278). These findings suggest that additional post-internalization events, for instance interactions with cellular protein factors and/or enzymatic modifications within the endosome, may be required for productive HCV entry.

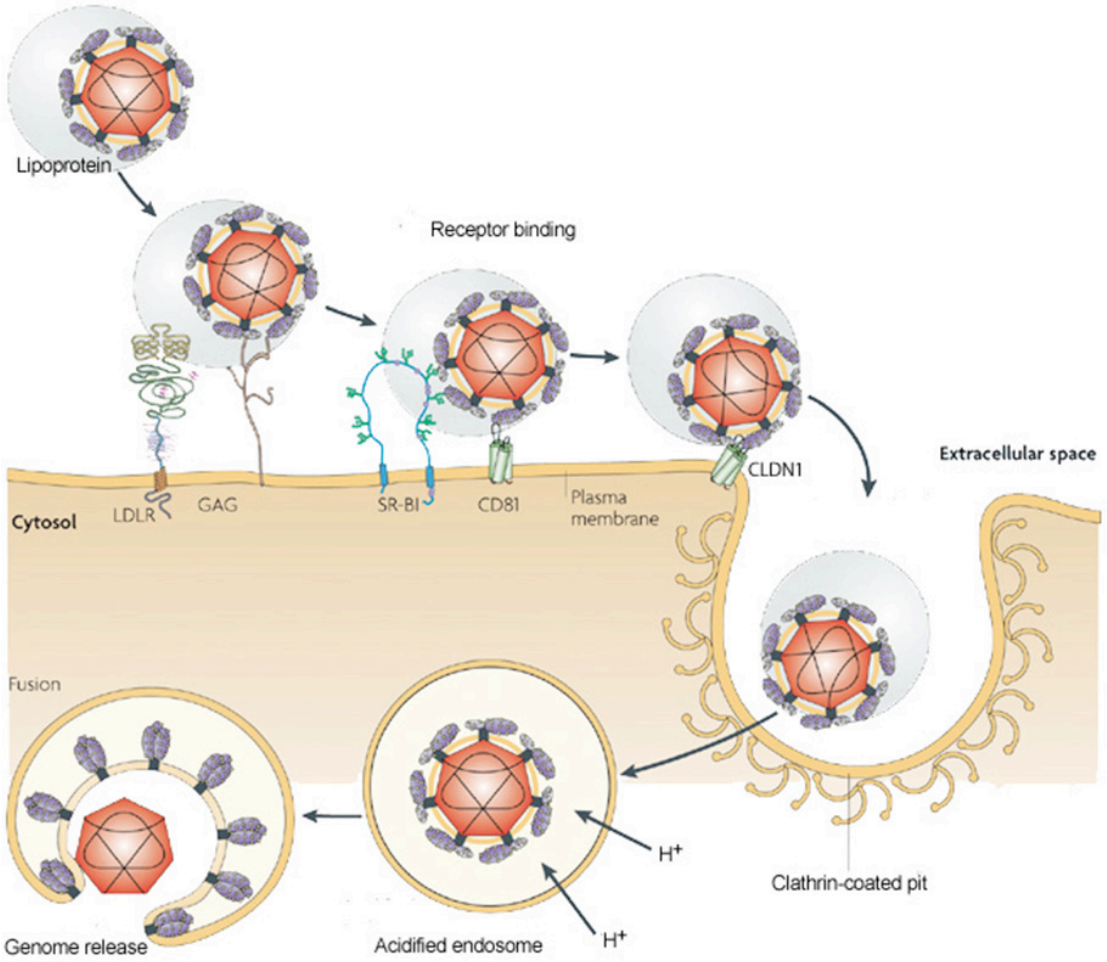

Figure 1-6 Attachment, receptor binding and clathrin-mediated endocytosis of HCV.

Circulating HCV particles can be associated with low- and very-low-density lipoproteins. Virus attachment and entry possibly involve the low density lipoprotein receptor (LDLR), glycosaminoglycans (GAG), SR-BI, CD81 and CLDN1. The latter functions at a late stage of cell entry, possibly in conjunction with occludin (326) at tight junctions of polarized hepatocytes. Following internalization via clathrin-mediated endocytosis, acidification of the endosome induces HCV glycoprotein membrane fusion, and uncoating and genome release into the cytoplasma via an unknown mechanism (image source: (290)).

1.4.4 Assembly of the nucleocapsid and budding of virions.

Each HCV particle consists of a nucleocapsid, which is composed of the core protein, and a lipid bilayer envelope studded with E1E2 heterodimers. How the viral particles are assembled remains largely unknown, but it is assumed that following translation, the polyprotein is targeted to the ER membrane by its C-terminal tail and subsequently processed at the core/E1, E1/E2, and E2/p7 junctions to generate the mature forms of E1 and E2.

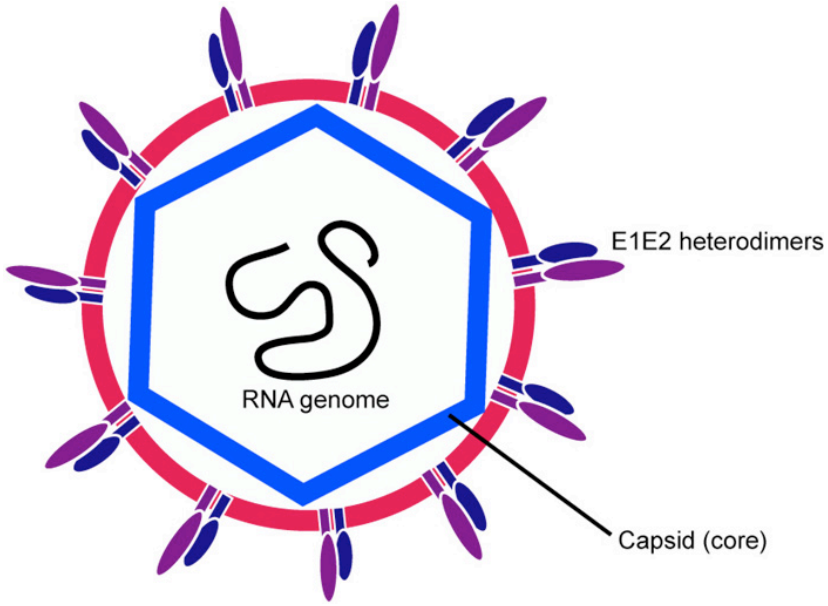

Figure 1-7 Structure of the HCV virion.

The envelope glycoproteins are anchored to the ER membrane by their C-terminal hydrophobic domains, while their N-terminal ectodomains translocate to the ER lumen where they are extensively glycosylated and acquire disulfide bonds (58). E2 then interacts with E1 to form a non-covalent heterodimeric complex, which is believed to represent the building block for the viral envelope (30, 108, 109). Core is cleaved by a host signal-peptide peptidase to generate a 23 kDa precursor form of the protein (p23) (248). p23 remains anchored to the cytoplasmic side of the ER membrane via its C-terminal hydrophobic tail (157) and undergoes further processing to produce the 21 kDa mature core protein (p21) (248, 275, 418), which is a pre-requisite for the assembly of the viral envelope (7). Furthermore, p21 associates with lipid droplets (275), and is probably involved in the biogenesis of these structures (23), suggesting a role for core protein in steatosis, the retention of lipids in the liver (reviewed in (150).

Once core protein processing is completed, several positively charged amino acid residues at the N-terminus of the mature protein are thought to interact with defined structures within the 3' and 5' NTR of the HCV RNA (96, 117). This interaction probably facilitates the oligomerisation of the core protein and initiates the virus packaging reaction (264). In addition, core may repress translation from the IRES, thereby inducing a switch from translation/replication to assembly (359).

E1 and E2, which are actively retained in the ER (109, 112) are likely to interact with the core protein via their C-terminal membrane anchors, as none of the envelope proteins contains a long cytoplasmic tail that could serve as a recognition sequence for core to initiate the assembly process (255). Retention of the envelope glycoproteins suggests that the viral nucleocapsids bud through the ER membrane to acquire their lipid bilayer envelopes. In this case, the completed virions may be released from the cell via the secretory pathway, a theory that is supported by the observation that N-linked glycans can be found on the surface of purified virus particles, suggesting virus transit through the Golgi apparatus (25).

The mechanisms underlying HCV particle assembly and release are still largely unknown. However, it becomes increasingly clear that HCV utilizes the hepatic VLDL assembly pathway to produce infectious lipo-viral-particles (LVP). Intriguingly, secreted infectious HCV particles are of lower buoyant density than intracellular HCV particles, suggesting that low density is gained during egress (147). Indeed, inhibition of VLDL assembly using MTP inhibitors and silencing of apolipoproteins prevented release of particles (73, 146, 299). Furthermore, treatment with Brefeldin A, which blocks protein export from the endoplasmic reticulum (ER) and causes disruption of the Golgi complex therein inhibiting the secretory pathway, led to an intracellular accumulation of virus (184). Together, these findings support the important role of the VLDL assembly machinery in HCV particle assembly and release.

The association between the HCV structural proteins and host apoproteins is possibly mediated by lipid droplets (LD), which are intracellular organelles responsible for lipid storage. Indeed, virus particles are often found in close proximity to LDs, indicating that some steps of virus assembly may take place around these structures (285). Viral core protein reportedly translocates to LDs and recruits nonstructural viral proteins and replication complexes to LD-associated membranes (54, 55, 355). Furthermore, core directs the redistribution of droplets along the microtubule network to membranes bearing genome replication complexes (54). Thus, it is currently believed that assembly occurs at these juxtapositions, where viral RNA and proteins frequently accumulate (184, 259, 285, 386).

1.5 Project objectives.

This study is divided into two main sections.

The aim of the study described in chapter 3.1 was to generate an indicator Huh-7.5 cell line suitable for the screening of patient-derived HCV strains and the isolation of HCV permissive cells. Most cell-based reporter assays are based on cells expressing (sub)genomic replicons in which cleavage of a fusion protein by the viral serine protease NS3/4A results in secretion of serine alkaline phosphatase (SEAP) into the culture medium (235, 313). We constructed a reporter plasmid, which encodes for a fusion protein consisting of a GFP protein linked to a proteasome targeting signal through a recognition site for NS3/4A protease. In cells constitutively expressing the fusion protein, NS3/4A-mediated cleavage liberates GFP from its proteasome-targeting signal and results in the accumulation of green fluorescence in the cytoplasm, allowing the identification and selection of HCV infected cells.

The recent identification of CLDN1 and Occludin as crucial HCV entry factors (114, 326) highlights the importance of studying the role of tight junctions (TJ) in HCV infection. We facilitated the HCVcc system to investigate (i) the role of cell junctions in the regulation of viral entry co-receptor expression and distribution, and (ii) possible effects on viral entry.

Chronic hepatitis C infection can lead to progressive liver damage including fibrosis and cirrhosis. The mechanisms underlying HCV-associated hepatic

injury are poorly understood, however, it becomes increasingly clear that TJ integrity is compromised in HCV infected liver. In chapter 3.3 we focussed on the HCV-mediated modulation of TJ protein expression and localization and the mechanism(s) underlying these processes.

2 Materials and Methods

2.1 Tissue culture.

Cells were maintained in T75 tissue culture flasks (Becton Dickinson, NJ, USA) in Dulbecco's modified Eagle's Medium (DMEM) supplemented with 10% foetal bovine serum (FBS) (Gibco, CA, USA), 1% non-essential amino acids (Gibco), 1% L-Glutamine (Gibco), and 50 units/ml penicillin and 50 μg/ml streptomycin (P/S) (Gibco). Cells were maintained at 37°C and 5% CO_2 throughout.

Cell lines		
Name	**Species/Tissue**	**Source**
Huh-7	Human hepatoma	Dr. Y-J. Tan, Institute of Molecular and Cell Biology, Singapore
Huh-7.5	Human hepatoma	Dr. C.M. Rice, Rockefeller University, NY
Huh-7.5/CLDN1	Human hepatoma	In house; see entry on lentivirus transduction
Huh-7.5/SR-BI	Human hepatoma	In house; see entry on lentivirus transduction
293T	Human embryonic kidney	American Type Culture Collection
Hep-G2	Human hepatocellular carcinoma	American Type Culture Collection
Hep-G2/CD81	Human hepatocellular carcinoma	In house

Table 2-1 List of cell lines used.

2.2 Basic techniques.

2.2.1 Antibodies.

Primary antibodies					
Antibody name	**Antigen**	**Type**	**Specificity**	**Species**	**Source**
Anti-CLDN1 (1C5-9D)	Human CLDN1	Purified IgG	Monoclonal	Mouse	Abnova, Taiwan
Anti-CLDN1 (JAY.8)	Human CLDN1	Purified IgG	Polyclonal	Rabbit	Invitrogen, CA
Anti-Occludin (Z-T22)	Human Occludin	Purified IgG	Polyclonal	Rabbit	Invitrogen, CA
Anti-ZO-1 (ZR-1)	Human ZO-1	Purified IgG	Polyclonal	Rabbit	Invitrogen, CA
Anti-Cla1	Human SR-BI	Purified IgG	Polyclonal	Mouse	BD Transduction Laboratories, NJ, USA
Anti-SR-BI (R25)	Human SR-BI	Animal Sera	Polyclonal	Rabbit	Dr. T. Huby, INSERM, Paris
M38	Human CD81	Hybridoma SN	Monoclonal	Mouse	Dr. F. Berditchevski, CRUK Cancer Insitute, Birmingham, UK
2s131	Human CD81	Hybridoma SN	Monoclonal	Mouse	In house; K. Hu and M. Goodall
9E10	HCV NS5A	Hybridoma SN	Monoclonal	Mouse	Dr. C. M. Rice, Rockefeller University, NY
C1	HCV E2	Purified IgG	Monoclonal	Human	Dr. D. Burton, The Scripps Institute, La Jolla, CA
JM122	HCV core	Hybridoma SN	Monoclonal	Human	Dr. J. McLaughlan, MRC Institute for Virology, UK
IgG P1-6	HCV	Patient sera	Polyclonal	Human	In house; see entry on patient IgG isolation
EEA1	Human EEA-1	Purified IgG	Polyclonal	Mouse	BD Transduction Laboratories, NJ, USA
CD63	Human CD63	Hybridoma SN	Monoclonal	Mouse	Dr. F. Berditchevski, CRUK Cancer Insitute, Birmingham, UK
Lamp1 (clone 25)	Human LAMP-1	Purified IgG	Monoclonal	Mouse	BD Transduction Laboratories, NJ, USA
ERGIC53 (G1/93)	Human ERGIC53/M60	Purified IgG	Monoclonal	Mouse	Alexis Biochemicals, Nottingham, UK
GM130 (clone 35)	Human GM130	Purified IgG	Monoclonal	Mouse	BD Transduction Laboratories, NJ, USA
VG67e	Human VEGF	Purified IgG	Monoclonal	Mouse	Santa Cruz Inc., CA
Anti-β-actin (AC-15)	Human β-actin	Purified IgG	Monoclonal	Mouse	Sigma-Aldrich, MO
Secondary antibodies					
Anti-mouse Alexa Fluor	Mouse IgG (H+L)	Purified IgG	Polyclonal	Goat	Molecular Probes, Invitrogen, CA
Anti-mouse Alexa Fluor	Mouse IgG (H+L)	Purified IgG	Polyclonal	Goat	Molecular Probes, Invitrogen, CA
Anti-mouse Alexa Fluor	Mouse IgG (H+L)	Purified IgG	Polyclonal	Goat	Molecular Probes, Invitrogen, CA
Anti-rabbit Alexa Fluor 4	Rabbit IgG (H+L)	Purified IgG	Polyclonal	Goat	Molecular Probes, Invitrogen, CA
Anti-rabbit Alexa Fluor 5	Rabbit IgG (H+L)	Purified IgG	Polyclonal	Goat	Molecular Probes, Invitrogen, CA
TRITC goat anti-mouse	Mouse IgG (H+L)	Purified IgG	Polyclonal	Goat	Invitrogen, CA
TRITC goat anti-human	Human IgG (H+L)	Purified IgG	Polyclonal	Goat	Invitrogen, CA
Anti-mouse HRP	Mouse IgG	Purified IgG	Polyclonal	Sheep	Amersham Biosciences, PA

Table 2-2 List of antibodies used.

2.2.2 Preparation of human serum-derived IgG.

Isolation of IgG .

Blood samples from patients infected with HCV were kindly provided by Dr. David Mutimer and Dr. David Adams of the Queen Elizabeth Hospital Liver Unit.

Vacutainers containing 3-5ml blood and a clotting activator were centrifuged at 3000 rpm, brake 4, for 10 mins at 4°C in a 5804R centrifuge (Eppendorf, Germany) in sealed buckets. Using a disposable Pasteur pipette, the serum was carefully collected, transferred to Falcon tubes, and stored in a secure biological hazard container at -80°C.

Prior to isolation of IgG, serum was heat inactivated by incubation at 60°C for 1.5 hrs. A 5ml column containing 2.5ml of Fast Flow protein G conjugated sepharose beads (GE Healthcare, UK) was prepared and connected to a peristaltic pump (Pharmacia, Sweden).

Following a wash with 10ml phosphate buffered saline (PBS) (Gibco), 10ml serum was passed through the column, followed by another PBS wash.

IgG was eluted with 10ml 0.1M glycine (Sigma-Aldrich, MO, USA) at pH 2.7, thereafter, the acidic eluate was immediately neutralized with 650μl 1M TRIS (Sigma-Aldrich) at pH 9.0.

The eluate was dialysed against PBS over night at 4°C and the IgG concentration determined using a UV spectrophotometer (Amersham, UK).

IgG neutralization assay.

To test the neutralizing efficiency of serum-derived IgG, Huh-7.5 cells were seeded at $1.5x10^4$ cells/well in 48-well microplates.

HCVcc were diluted in DMEM + 3% FBS + P/S containing the appropriate concentration of IgG (ranging from 10 to 50 μg/ml) and inoculated with the cells for 1 hr at 37°C. Thereafter, the HCV-IgG mix was removed, the cells washed with excess PBS and the infection allowed to proceed for 48 hrs.

Viral infectivity was determined by enumerating NS5A positive foci and expressed as mean foci forming units (FFU). The percentage neutralization was calculated by comparison of the level of infection after inhibitory treatment to that of untreated (no serum) cells. Serum from a HCV negative patient was used as a control.

2.2.3 Flow cytometry.

Flow cytometry is a technique used for counting, examining and sorting of cells suspended in a stream of fluid. When a beam of single wavelength laser light is directed onto this stream of fluid, suspended particles passing through the beam scatter the light and attached fluorescent dyes are excited into emitting light at a higher wavelength than the light source. The combination of scattered and fluorescent light is picked up by detectors, which are set up in line with the laser beam (Forward Scatter; FSC) or perpendicular to it (Side Scatter; SSC). Fluctuations in brightness at each detector provide information about the physical and chemical structure of each individual particle; FSC correlates with the cell volume and SSC depends on the inner complexity of

the particle such as the type of cytoplasmic granules or the membrane roughness (reviewed in (375)).

To retrieve them from cell culture dishes (Corning, NY, USA) cells of interest were treated with trypsin (Gibco) for 3-5 min at 37°C, resuspended in 10% DMEM and counted using a haemocytometer.

Thereafter, cells were pelleted in a 5804R centrifuge (Eppendorf, Germany) at 1200 rpm for 3 min and diluted to $2x10^6$ cells/ml in PBS + 0.5% bovine serum albumin (BSA) (Sigma-Aldrich).

If cells required fixation prior to staining, they were treated for 5 min with 1% paraformaldehyde (PFA) on ice (TAAB, UK), followed by a PBS wash and resuspension in PBS + 0.5% BSA. If permeabilization was necessary, fixed cells were resuspended in PBS + 0.5% BSA + 0.01% saponin (Sigma-Aldrich) and all subsequent steps carried out in this buffer. To block non-specific binding, cells were incubated for 20 min on ice. If using saponin, this also served as a permeabilization step.

Antibody staining was performed in 96 well U bottomed microplates (Corning, NY, USA) with $2x10^5$ cells/well (for antibody concentrations see). Briefly, 100 µl of cell suspension was transferred to each well, the cells pelleted by centrifugation at 1200 rpm for 3 min and resuspended in 70-100 µl of primary antibody diluted in PBS + 0.5% BSA (+0.01% saponin). Species matched IgGs were used as controls throughout.

After 45 min incubation with the primary antibody, cells were washed twice with excess PBS and resuspended in 70-100 μl of fluorescently conjugated secondary antibody diluted as above.

Cells were incubated for 45 min in the dark to prevent photobleaching, and washed twice with PBS as above. In the case of live staining the cells were fixed prior to analysis. Staining intensities were measured using a Facscalibur flow cytometer (Becton Dickinson), the data captured with Cell Quest (Becton Dickinson) and analyzed using FlowJo software (Tree Star, OR, USA).

2.2.4 Indirect immunofluorescence.

Primary antibodies		
Antibody	**Application**	**Dilution**
9E10	IF, FC	1/200
9E10	WB	1/400
Rabbit Anti-CLDN1	IF	1/500
Anti-CLDN1 (Abnova)	IF, WB	1/1000
	FC	1/500
Rabbit Anti-Occludin	IF	1/500
Rabbit Anti-ZO-1	IF	1/500
Anti-ClaI	IF	1/400
	WB	1/250
Anti-SRBI (R25)	FC	1/100
M38	IF, FC	1/20
Anti-CD81 1.3.3.22	WB	1/200
2s.131	IF	1/5
C1	IF	1/4000
ERGIC53	IF	1/2000
GM130	IF	1/250
EEA1	IF	1/250
Lamp1	IF	1/250
beta-Actin	WB	1/5000
Secondary antibodies		
Alexa Fluor 488	IF, FC	1/1000
Alexa Fluor 594, 633	IF, FC	1/500
TRITC IgG	IF	1/250
Anti-mouse HRP	WB	1/2500

Table 2-3 List of antibody concentrations used.

IF, indirect immunofluorescence; FC, flow cytometry; WB, Western blotting.

Fluorescence microscopy.

(Epi)fluorescence microscopy is based on the following principle: a component of interest in the specimen is specifically labelled with fluorophores and illuminated with light of a specific wavelength. The absorbed light excites the fluorphores, causing them to emit longer wavelengths of light (i.e. of a different colour than the absorbed light). To make the emitted fluorescence visible, the illumination light is separated from the much weaker emitted light by using an emission filter (341).

Cells were seeded in 48- well cell culture microplates at $1.5x10^4$ cells/well and stained 72 to 96 hrs post seeding (unless stated otherwise).

To fix specimens, cells were washed twice with excess PBS and treated for 5 min with ice cold methanol (Fisher Scientific, UK) or, in the case of CD81 staining, by 20 min treatment with 2% EM-grade formaldehyde (TAAB Laboratories, UK) diluted with serum-free DMEM. Subsequently, cells were washed twice with PBS and blocked for 20 min with PBS + 1% BSA.

Primary antibody staining was achieved by incubation for 45 min at RT with antibody diluted in PBS + 1% BSA. In the case of SR-BI staining, cells were incubated with the primary antibody over night at 4°C to ensure sufficient binding.

To wash the cells, diluted antibody was removed by careful aspiration, followed by the addition of excess PBS; the process was then repeated.

Secondary antibody staining was achieved by incubation for 45 min at RT in the dark with fluorescently conjugated secondary antibody diluted in the appropriate buffer.

Cells were washed twice as above and the staining visualized using a fluorescent microscope (Nikon TE2000, Japan). Images were taken using a digital camera (Hammatsu, Japan).

Laser scanning confocal microscopy (LSCM).

Cells were seeded in 24-well culture microplates on 13μm borosilicate cover slips. Prior to seeding, cover slips were sterilized by dipping in pure ethanol and washed once with PBS, after which they were pre-treated with 1 mg/ml collagen IV (Sigma) diluted with PBS for 1 hr at RT followed by a PBS wash.

Staining was performed as described for fluorescence microscopy. In addition, nuclei were counterstained by incubation with 10 μg/ml DAPI (Sigma) for 1 min at RT in the dark followed by a PBS wash. Cover slips were mounted onto glass slides using ProLong Antifade mounting reagent (Invitrogen, CA, USA) and mounted slides stored at -20°C.

LSCM was performed on a Zeiss Meta Head Confocal Microscope utilizing a 63x 1.2NA objective. Background fluorescence of samples was corrected based on control samples stained with species-matched IgG and secondary antibody only, respectively.

Linear plot profile analysis (LPPA).

LPPA was used to measure HCV receptor expression levels at the plasma membrane and in the cytoplasma of sub-confluent and confluent cells, the hypothesis being that the amount of fluorescently labelled receptor molecules correlates with fluorescence intensity *viz*. brightness.

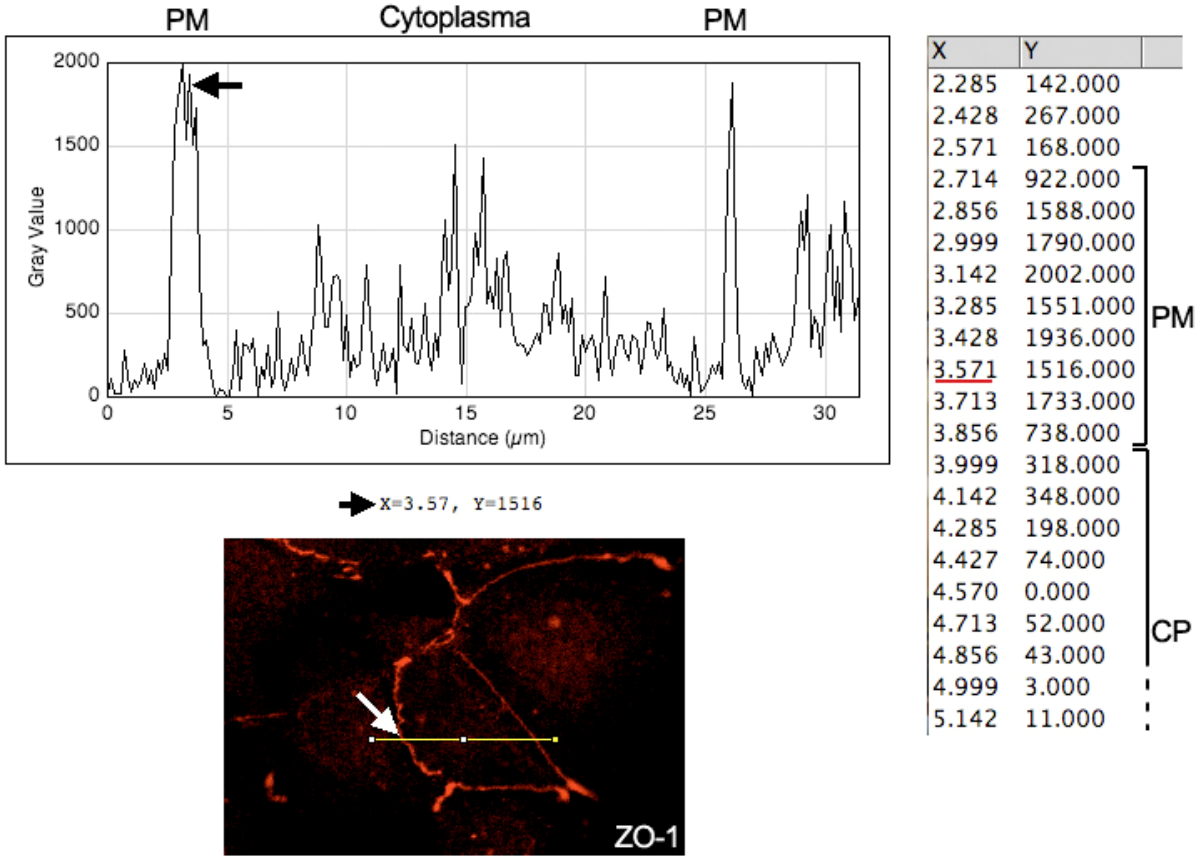

Figure 2-1 Linear plot profile analysis.

A 1 pixel wide line was drawn across a single cell and grey values (brightness) recorded along the line. Peaks represent the plasma membrane (PM) in contrast to the space between cells and the cytoplasma (CP).

5-10 images were acquired per receptor and cell seeding density. LPPA in ImageJ (v1.83) (2) was used to analyze receptor expression.

A linear plot profile involves using a line histogram of 1 pixel thickness to display fluorescence intensity in a graphical format. To achieve this, a line was drawn horizontally across the cell of interest, making sure that it crossed the plasma membrane at each side (Figure 2-1). The linear plot profile generated a histogram with two obvious peaks, representing the grey value (brightness) of the plasma membrane in contrast to the empty space between cells (background) and the intracellular space (cytoplasma).

On the histogram, the x-value indicates the distance (in μm) from the start of the line and the y-value indicates the brightness of the pixel. The histogram plot was converted to a list of x/y values; per cell, 5 values were recorded per peak and 10 random values for the area in between peaks. Data was expressed as arbitrary fluorescence units (AFU) i.e. mean grey value. Statistical analysis and comparison of plasma membrane and cytoplasmic receptor expression levels was performed using a paired t test.

LSCM of HCVcc infected cells.

For the analysis of receptor distribution in HCV infected cells, naïve Huh-7.5 cells were seeded at $0.5x10^6$ cells per T25 tissue culture flask. 24 hrs post seeding, the culture media was replaced with 3.5ml of HCVcc virus diluted in DMEM + 3%FBS + P/S or culture media only (negative control).

Cells were inoculated with HCVcc virus for 18-20 hrs, after which they were trypsinized and re-seeded onto collagen treated borosilicate cover slips at $1.5x10^5$ cells/well in DMEM + 3% FBS + P/S.

72 hrs post infection, cells were methanol fixed and stained for indirect immunofluorescence as described previously.

To determine the level of infection, $5x10^4$ cells/well were seeded in a 48-well tissue culture plate and stained for NS5A at 72 hrs post infection.

2.2.5 Western Blotting.

Proteins were routinely dissolved in suitable buffers and stored at -20°C.

Lysates were prepared by seeding $2x10^6$ Huh-7.5 cells in 10 cm Petri dishes in DMEM + 10% FBS + P/S. 24-26 hrs after seeding the culture media was removed and the cell monolayer rinsed with PBS at RT. All subsequent steps were carried out on ice using fresh, ice-cold buffers to prevent protein degradation.

5 ml of ice cold PBS were added per Petri dish and adherent cells removed using the barrel end of a small syringe. The cell suspension was transferred to Universals and pelleted by centrifugation at 1200 rpm for 5 min at 4°C.

The cell pellet was resuspended in 1 ml ice cold RIPA buffer (PBS + 1% Triton X-100 + 0.5% Sodium Deoxycholate + 0.1% SDS; 1x Complete Mini Protease Inhibitor Cocktail Tablet + 1x Complete PhosStop Phosphatase Inhibitor Cocktail Tablet (Roche)) and incubated on ice for 30 min.

The lysate was centrifuged at 15 000 rpm in a Biofuge primo R centrifuge (Heraeus) for 15 min at 4°C to separate nuclei and unsolubilized cell membranes from protein, after which the supernatant was collected and frozen at -20°C.

Protein was quantified using the BCA Protein Assay kit (Thermo Scientific, IL, USA) according to the manufacturer's instructions. Briefly, 10 μl of each sample or BSA standard were mixed with 200 μl of BCA Working Reagent in a 96-well microtiter plate in triplicates and incubated at 37°C for 30 min. Thereafter, the plate was allowed to cool to RT and the absorbance at 590 nm measured using an ELISA plate reader.

To determine the protein concentration of each sample, a standard curve was prepared by plotting the average Blank-corrected 490 nm measurement for each BSA standard versus its concentration in μg/ml.

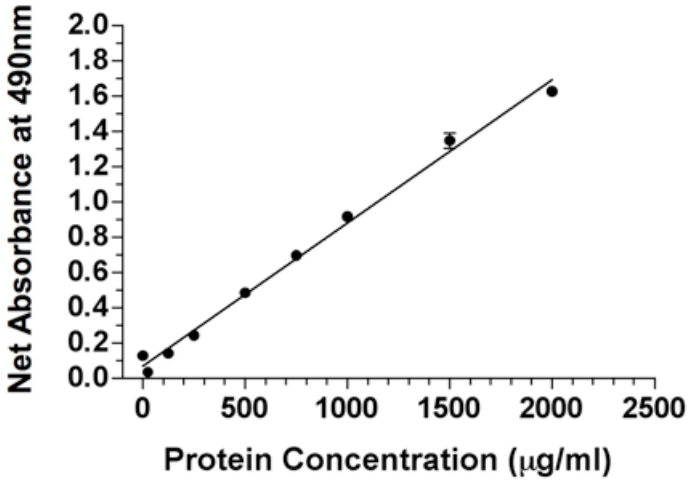

Figure 2-2 BCA protein assay standard curve.

BSA protein standards were diluted in RIPA buffer and incubated with BCA working reagent for 20 min at 37°C, thereafter absorbance at 490nm was measured using an ELISA plate reader.

SDS Polyacrylmide Gel Electrophoresis (SDS-PAGE).

Proteins were separated on 12% slab polyacrylamide (PAA) gels. To prepare samples, defined amounts of protein were mixed with 3x Laemmli loading dye (H_2O + 30% v/v Glycerol + 6% w/v SDS + 0.02% v/v Bromophenol Blue + 0.2M Tris-HCl; pH 6.8) with or without 10% 2-mercaptoethanol and the total volume adjusted to 25 μl with H_2O. Samples were heat-denatured at 95°C for 5 minutes and allowed to cool to RT prior to loading.

Proteins were separated by electrophoresis using the Mini Protean 3 System (Bio-Rad Laboratories, CA, USA) according to the manufacturer's instructions. Briefly, 20 μl of protein sample were loaded per lane and gels run at 200 volts for 30-45 min.

Proteins were transferred onto PVDF membranes (Millipore, MA, USA) using a Mini Trans-Blot Electrophoretic Transfer Cell System (Bio-Rad) according to the manufacturer's recommendations. Briefly, PVDF membranes were cut to the appropriate size and pre-treated with methanol for 1-2 min, rinsed with ultra pure water, and incubated in transfer buffer (25mM Trizma base + 0.2M Glycine + 200 ml MeOH + 0.5 ml 10% SDS) at RT for 5-20 min. Gels were equilibrated in transfer buffer for 5 min to prevent shrinking and incomplete transfer. Transfer was carried out at 350 mA for 60 min at RT.

Immunoprobing and chemiluminescent detection of proteins.

All subsequent steps were carried out in 50 ml Falcon tubes with gentle agitation on a tube roller (Barloworld Scientific, UK) at RT. To block unspecific binding of antibodies, membranes were incubated in 2.5 ml of TBST (10mM

Trizma base + 0.1M Sodium Chloride + 10% v/v Tween 20) + 5% dry milk for 30 min at RT.

After which the blocking buffer was removed and the membranes were incubated with primary antibodies (for concentrations see) diluted in 2 ml TBST + 5% dry milk for 60 min followed by three 5 min washes with excess TBST. Incubation with HRP-conjugated secondary antibodies (diluted 1/2500 in TBST) was carried out as described above.

Chemiluminescent detection of HRP-conjugated antibodies was performed using the ECL Western Blotting Detection System (Amersham, UK) according to the manufacturer's instructions. Briefly, membranes were immersed in ECL detection reagent for 1 min, wrapped in Saran foil, and exposed to CL-XPosure Blue X-Ray Film (Thermo Scientific) for 1-5 min.

2.3 HCVpp and HCVpp based work.

2.3.1 Plasmids.

Plasmids	
Name	**Source**
HCVcc JFH-1	Dr. T. Wakita, National Institute of Infectious Diseases, Tokyo
HCVcc J6/JFH	Dr. C. M. Rice, The Rockefeller University, New York
JFH-1 SGR	Dr. T. Wakita, National Institute of Infectious Diseases, Tokyo
TRIP SR-BI	In house
TRIP CLDN1	In house
TRIP CD9	In house
HIV gag-pol 8.2	Aaron Diamond AIDS Research Center
VSV-G	Aaron Diamond AIDS Research Center
CSGW GFP	Aaron Diamond AIDS Research Center
NL4.3.Luc.R$^-$E$^-$	Aaron Diamond AIDS Research Center
JFH E1E2	Dr. J. Zhang, The Rockefeller University, New York
H77 E1E2	Dr. J. Zhang, The Rockefeller University, New York
MLV.env	Aaron Diamond AIDS Research Center

Table 2-4 List of plasmids used.

2.3.2 Preparation of HCV pseudoparticles (HCVpp).

The HCVpp system used in this study is similar to that described by Hsu et al. and Pohlmann et al. (183, 327). HCVpp are based around a replication deficient HIV *gag-pol* core but carry the HCV E1E2 glycoproteins. Infection is detected by an eGFP or Luciferase (Luc) reporter gene packaged into the HCVpp. As the particles do not encode any HCV structural proteins and are incapable of further rounds of replication they only mimic the entry process of HCV.

HCVpp were synthesized in a similar manner to TRIP particles (see section 2.4). 24 hrs prior to transfection, 293T cells were seeded in 6-well cell culture microplates coated with 0.1 mg/ml poly-L-lysine hydro bromide (Sigma, CA, USA) at $6x10^5$ cells/well in P/S free DMEM + 10% FBS. Media was replaced with P/S free DMEM + 3% FBS 1 hr prior to addition of DNA.

Cells were transfected using the Fugene (Roche, Switzerland) kit according to the manufacturer's instructions. Briefly, 6 μl Fugene mixed with 100 μl Optimem (Gibco) were added to a mix of plasmids encoding HCV E1E2 (800-1000 ng), HIV gag-pol (250 ng) and an eGFP (250 ng) or Luc reporter gene (800 ng). The Fugene- DNA mix was incubated 20 min at RT and then added to the cells. Transfection was performed for 6 hrs at 37°C, thereafter, the culture media was refreshed.

Culture media containing HCVpp was harvested 48 hrs post transfection and infection of target cells performed immediately.

2.3.3 Luciferase infection assay.

Target cells were seeded at $1.5x10^4$ cells/well in 48-well cell culture microplates and inoculated for up to 8 hrs with HCVpp containing culture media diluted 1:2 in DMEM + 3% FBS + P/S. Thereafter, the media was refreshed.

Infection was assessed after 72 hrs with a luminometer (Luc reporter) using a Luciferase Assay System (Promega) according to the manufacturer's instructions.

Renilla luciferase assay.

1x lysis buffer and luciferase reagent were prepared according to the manufacturer's instructions and stored at -20°C.

To prepare the cell lysates, culture media was removed and cells once washed with excess PBS. Thereafter, 50 μl of lysis buffer were added to each well and the mix incubated for 10 min at RT.

20 μl of lysate was then transferred to a white polystyrene 96-well assay plate (Corning, NY, USA). Following priming of the reagent injector with 1-2 ml of Renilla luciferase agent, 100 μ of luciferase reagent were dispensed per well and luminescence recorded over 10 seconds with a 2 second delay using a Centro LB960 luminometer Berthold Technlogies, UK).

Firefly luciferase assay.

1x lysis buffer was prepared and stored as described above. Luciferase assay reagent was prepared by adding 10 ml of luciferase assay buffer to a vial of

lyophilized luciferase assay substrate. Working aliquots were stored at -80°C for up to one month.

Cell lysates were prepared as described above. 20 μl of lysates were transferred to white polystyrene 96-well assay plates, mixed with 40 μl of luciferase assay reagent and luminescence measured immediately.

2.3.4 Preparation of cell culture proficient HCV (HCVcc).

Currently, all HCVcc viruses are constructed around the non-structural proteins of HCV strain JFH-1, a unique isolate capable of producing particles in certain hepatoma cell lines (244, 408, 429). The HCVcc viruses used in this study are JFH-1 wildtype and a chimeric J6/JFH virus, which encodes core, E1, E2, p7 and NS2 of strain J6 HCV (244, 408, 429). In each case, virus was produced by transcription of RNA from a plasmid encoding the HCV genome, introduction of RNA plasmids into Huh-7.5 cells by electroporation, and subsequent harvest of secreted HCVcc particles.

RNA synthesis.

RNA transcripts of the HCV genome were produced using the T7 RNA polymerase kit (Ambion, TX, USA) according to the manufacturer's instructions. Briefly, 5 μg of plasmid containing a cDNA clone of the HCV genome were linearized by *XbaI* digest (Promega).

1 μg of linearized plasmid was used as a template for RNA transcription, the reaction mixture was incubated at 37°C for 3-4 hrs, after which the RNA was

purified using the RNeasy MinElute kit (Qiagen, NL) according to the manufacturer's instructions.

RNA quality was assessed by gel electrophoresis on a 1% agarose gel (Bioline, UK). Typical yields, as measured by UV spectrophotometry (Amersham), were 250-1000 ng/μl.

Electroporation (EP).

Huh-7.5 cells at 60-80% confluence were trypsinized, resuspended in DMEM and counted using a haemocytometer.

To prepare, cells were washed with excess ice cold PBS and pelleted by centrifugation at 1250 rpm for 5 min at 1°C. This process was repeated and the cells were resuspended in ice cold PBS at $1.5x10^7$ cells/ml and placed on ice.

To electroporate, 400 μl of cell suspension was mixed with 3 μg of genomic RNA and transferred to a 0.2 cm EP cuvette (Sigma-Aldrich). EPs were carried out at 780 volts in an Electro Square Porator (Harvard Apparatur, MA, USA).

Following the EP the cells were allowed to stand for 5 min at RT prior to being transferred into 10 ml of pre-warmed DMEM + 10% FBS + P/S. 8 ml of the cell suspension were seeded in a T75 tissue culture flask (Corning), and the remainder put into 2 wells of a 24-well tissue culture plate to allow the monitoring of HCV protein expression.

At 48 hrs post EP; the efficiency of viral replication was quantified by detection of the HCV non-structural protein NS5A. Indirect immunofluorescence was carried out following the protocol detailed in section 2.2.

HCVcc particles were harvested between 4 and 14 days post EP; after which the cells were discarded. To harvest, cells were cultured in a minimal volume of DMEM + 3% FBS + P/S (usually 7 ml per T75 tissue culture flask) and media containing secreted virions collected every 8-14 hrs. Harvested virus was clarified by centrifugation at 3000 rpm for 5 min and frozen at -80°C until use.

2.3.5 HCVcc infection assay.

All HCVcc infectivity data presented in this thesis was obtained using the following protocol (unless stated otherwise):

Naïve Huh-7.5 cells were seeded at the appropriate density (usually $1.5x10^4$ cells/well) in 48-well cell culture microplates 24 hrs prior to infection. To infect, the media was replaced with 150 μl of HCVcc virus diluted in DMEM + 3% FBS + P/S.

Cells were inoculated for 1-8 hrs at 37°C, washed with PBS, and 150 μl of DMEM + 3% FBS + P/S added per well. Infections were allowed to proceed for 48 to 72 hrs, as stated in the figure legends.

Infected cells were methanol fixed and NS5A positive cells or foci enumerated using indirect immunofluorescence.

2.3.6 HCVcc internalization assay.

Proteinase K-dependent HCVcc internalization assay.

$2x10^6$ Huh-7.5 cells were seeded in T75 tissue culture flasks and incubated at 37°C over night. The following day, the cells were trypsinized and counted.

$2x10^5$ Huh-7.5 cells were pelleted at 1200 rpm for 3 min, resuspended in 1 ml DMEM + 3%FBS and transferred to Eppendorf tubes.

To infect, cells were pelleted as described above and resuspended in HCVcc diluted with ice cold hepes-buffered DMEM + 3%FBS. Cells were incubated for one hour on ice, thereafter unbound virus was removed by washing cells once with cold PBS.

HCVcc entry was initiated by incubating the cells at 37°C. After different time periods, the cells were pelleted and resuspended in ice cold hepes buffered DMEM + 3% FBS containing 50 μg/ml proteinase K (Sigma) to remove non-internalized particles, and incubated on ice for 1 hr.

Post treatment the cells were washed twice with ice cold hepes-buffered DMEM + 10% FBS to inactivate proteinase activity, counted, and re-seeded at equal densities in duplicates in 24-well tissue culture plates.

Viral infectivity was determined 48 hrs post infection by counting NS5A positive foci. Data was expressed as percentage HCVcc entry; this was calculated by comparison of the level of infection in proteinase treated cells to that in untreated cells at each time point.

Neutralizing antibody-dependent HCVcc internalization assay.

Huh-7.5 cells were plated at $1.5x10^4$ cells/well in 48-well plates and the following day infected with virus diluted in hepes-buffered DMEM + 3% FBS for 1 hr on ice.

Thereafter, unbound virus was removed by washing cells once with cold PBS and entry initiated by elevating the temperature to 37°C.

To neutralize non-internalized particles, 10 μg/ml of mouse-anti-E2 mAb (C1) or 50 μg/ml of patient-derived polyclonal IgGs were diluted in DMEM + 3% FBS and added directly to the cells.

Viral infectivity was determined at 48 hrs post infection as described above. The data was expressed as percentage HCVcc entry; this was calculated by comparison of the level of infection at every given time point to the level of infection after 2 hr (100% loss of inhibition).

2.3.7 Treatment of cells with inhibitors.

Inhibitors and growth factors			
Name	**Effect**	**Opt. Conc.**	**Source**
Calpain Inhibitor-I (ALLN)	Proteasome inhibitor	36 μM	Sigma-Aldrich
Cycloheximide (CHX)	Inhibitor of protein biosynthesis	20 mg/ml	Sigma-Aldrich
Chlorpromazine	Inhibits clathrin-mediated endocytosis	15 μM	Sigma-Aldrich
Tumor necrosis factor-α (TNFα)	Growth factor	1 ng/ml	Sigma-Aldrich
Interferon-γ (IFNγ)	Proinflammatory cytokine	100 U/ml	Sigma-Aldrich

Table 2-5 List of inhibitors and growth factors used.

Inhibitors were reconstituted in ultrapure water or DMSO and stored at 4°C or -20°C according to the manufacturer's guidelines.

The cytotoxicity of all compounds was tested using the CellTiter One Solution Cell Proliferation (MTS) Assay (Promega). Briefly, cells of interest were seeded at $1.5x10^4$ cells/well of a 48-well cell culture microplate in DMEM + 10% FBS + P/S and incubated over night. The following day, cells were washed once with excess PBS and 200 μl of the MTS (tetrazolium compound) working solution added per well.

Cells were incubated at 37°C for 1 hr, thereafter 100 μl of the supernatant was transferred to a 96-well ELISA plate and absorbance at 490nm measured using an ELISA plate reader. To determine the cell survival rate, a standard curve was prepared by seeding cells at increasing densities ranging from 0.3 to $6x10^4$ cells/well and plotting the average Blank-corrected 490 nm measurement for each density against the cell number.

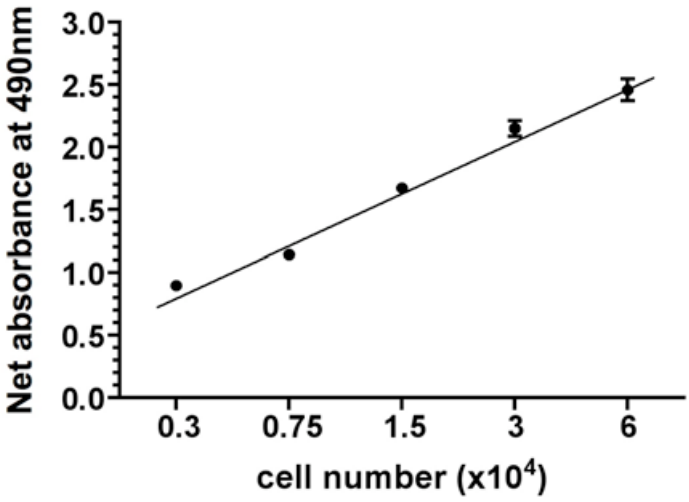

Figure 2-3 MTS cell proliferation assay standard curve.

Inhibitors were diluted in DMEM + 3% FBS + P/S and incubated with the cells as stated in the respective figure legends.

2.4 Generation of TRIP viruses and transduction of cells to express receptors of interest.

The TRIP system (425) is based on a retrovirus gene expression vector and produces virus vector particles, formed around a replication deficient HIV gag-pol core, that bear the envelope glycoprotein of vesicular stomatitis virus (VSVG). TRIP virus particles can package a gene of interest as an RNA transcript, subsequent transduction of a cell line with the TRIP system results in reverse transcription of the target gene and insertion into the host genome. In this study, transduced cells were not under selection, however, they maintained exogenous gene expression for around 2-3 weeks, after which they were discarded.

TRIP particles were produced by Fugene transfection of 293T cells with plasmids encoding the constituent elements as described in section 2.3.2. 293T cells were seeded in 6-well culture microplates coated with 0.1 mg/ml poly-L-lysine hydro bromide (Sigma, CA, USA) at $6x10^5$ cells/well in DMEM + 3% FBS.

The following day, 400ng VSVG, 600ng HIV gag-pol and 600ng of target gene plasmid DNA were introduced into the cells by a 6 hr transfection, after which the culture media was changed to DMEM + 3% FBS + P/S.

Culture media containing assembled TRIP particles was harvested at 48 hrs post transfection and passed through a 0.2 μM filter to remove contaminating 293T cells. Harvested supernatants were pooled and target cells infected immediately.

Target cells were seeded at $4x10^5$ cells/well in 6 well culture microplates 24 hrs prior to transduction. To transduce, cells were incubated over night with TRIP culture media diluted 1:1 in DMEM + 3% FBS + P/S, after which the media was replaced with DMEM + 10% FBS + P/S.

Transduction efficiency was assessed after 24-48 hrs by monitoring expression of the TRIP eGFP control and flow cytometric detection of target gene(s).

2.5 Molecular cloning.

In order to construct plasmids carrying the gene of interest, the following basic procedures were used:

2.5.1 Restriction enzyme digest.

1 to 2 μg of DNA were digested using 5 or 10 units of the respective restriction enzyme in a total volume of 20 μl. Digests were performed for 60 min at 37°C using the buffers recommended by the manufacturer.

2.5.2 Ligation.

Following restriction digest, DNA samples were run on 1% agarose gels at 50 volts and purified using the Qiagen MinElute kit (Qiagen) according to the manufacturer's instructions.

The ligation reaction was carried out in a total volume of 10 μl, including 5 μl of 2x ligation buffer (Promega) and 10 units of T4 DNA ligase (Promega). 50 ng of vector DNA was used per ligation reaction, the molar ratio of vector:

insert was 1:10. The ligation reaction was allowed to proceed for 30 min at RT.

2.5.3 Transformation of competent cells.

Competent cells were thawed on ice for about 5 minutes and kept on ice during the whole procedure. For each transformation reaction 50 μl of competent One Shot *E. coli* T1 Phage-resistant cells (Invitrogen) and 5 μl of the ligation reaction (10 pg - 100 ng DNA) were carefully mixed and incubated on ice for 30 min. Subsequently, DNA uptake was enabled by heat shocking the cells at 42°C for 45 sec in a water bath. Following 1 min incubation on ice, 150 μl of pre-warmed T-Broth medium (23g TB + 2 ml Glycine +/- 5g agarose in sterile H_2O) were added to the cell suspension, which was then spread on TB agar plates containing 100 μg/ml ampicillin and 20 μg/ml kanamycin for selection of cells carrying the plasmid of interest.

2.5.4 PCR colony screening and plasmid DNA isolation.

50μl 10x PCR buffer (w/o $MgCl_2$) , 30μl 25mM $MgCl_2$, 15μl 10mM dNTPs, 15μl of each 10μM primer and 1 unit/100μl Taq polymerase were adjusted to a final volume of 500 μl with sterile water.

For colony screening, single colonies were picked with sterile toothpicks and transferred to a 96-well PCR plate by dipping into wells containing 25 μl of PCR reaction. After which the toothpicks were inoculated over night in 2 ml of

liquid TB medium supplemented with 100 μg/ml ampicillin and 20 μg/ml kanamycin at 37°C with agitation for subsequent preparation of plasmid DNA.

PCR was performed following the program detailed below:

5 min	95°C
15 sec	94°C ⎫
15 sec	50°C ⎬ 30 cycles
90 sec	72°C ⎭
∞	4°C

Plasmid DNA was isolated with the Fast plasmid MINI prep system (Eppendorf) according to the manufacturer's instructions. Briefly, 1.5 ml of the bacterial culture was pelleted by 1 minute centrifugation at 13000 rpm. The supernatant was discarded, 400 μl ice-cold Complete Lysis Solution were added and the suspension mixed thoroughly by constant vortexing at full speed for 30 seconds. The lysate was incubated at RT for 3 min and transferred to a Spin Column Assembly by decanting. The Spin Column Assembly was centrifuged for 60 sec at 13000 rpm. 400 μl of Wash buffer were added and the column centrifuged again for 60 sec at maximum speed. The filtrate was discarded and the column centrifuged at maximum speed for 1 min. Subsequently, the Spin Column was transferred to a Collection Tube, 50 μl of Elution buffer were added and the assembly centrifuged at 13000 rpm for 1 minute. The eluted DNA was used immediately or stored at –20°C.

2.6 Generation of the RCGFP(Δ5AB)MODC indicator cell line.

Our cloning strategy used an existing plasmid, the pZSProSensor-1 (Clontech, CA, USA). This eukaryotic vector encodes a high efficiency proteolytic targeting signal (mouse ornithine decarboxylase; MODC) fused to the 3' end of the gene for *Zoanthus sp.* Green Fluorescent Protein (ZsGreen; RCGFP) and can be used to monitor proteasome activity in living cells. When the proteasome is active, RCGFP will not accumulate, however, when proteasome activity is inhibited, the fusion protein will accumulate in cells, resulting in an increase in green fluorescence under 496 nm light. By inserting the gentoype 1a NS5A/5B sequence (Δ5AB) between the RCGFP and the MODC gene, we aimed to generate a reporter protein that will be cleaved by the viral NS3/4A protease, allowing the detection and isolation of HCV infected cells. This work was carried out in collaboration with Dr. Peter Balfe.

The Δ5AB insert was generated by annealing two redundant oligonucleotides (Invitrogen) that contained substitutions (W) for adenine (A) and thymidine (T) in the region encoding the NS3/4A protease recognition site (cytosine-cytosine-serine; CCS):

Δ5AB+ GGG AAG CAG ATA CTG AGG ACG TCG TCT GCW GCW GCA TGA GCT ACG GAT CCG CGC
Δ5AB– GCG GAT CCG TAG CTC ATG CWG CWG CAG ACG ACG TCC TCA GTA TCT GCT TCC CGC

Sense and antisense strand oligonucleotides were mixed 1:1 and annealed at 94°C for 1 min with controlled cool-down.

The pZS-1 vector (1 μg) was linearized by digestion with *SacII* and gel purified using the Qiagen Elution kit (Qiagen, NL) according to the manufacturer's instructions and the Δ5AB insert ligated into the vector.

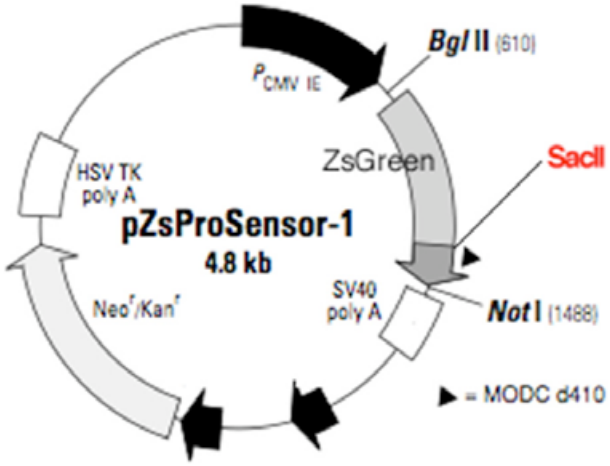

Figure 2-4 Basic pZS-1 plasmid map (modified from Clontech, USA).

Transformation of *E.coli* with RCGP(Δ5AB)MODC plasmids was carried out as described in section 2.5.3.

Colonies were screened for the Δ5AB insert by PCR using the following insert flanking primers (Invitrogen):

forward	5' TTCATCCAGCACAAGCTGAC
reverse	5' CCATGGCTCTGGATCTGTTT
	(the sequence shown is the reverse complement)

Δ5AB positive colonies were cultured over night in TB medium and plasmid DNA isolated using the Qiagen Fast Plasmid MINI kit as described previously. In addition to generating the NS3/4A recognition site, replacement of the amino acid substitutions with A or T will result in formation of *PstI* and/or *PvuII* restriction sites. (see diagram below).

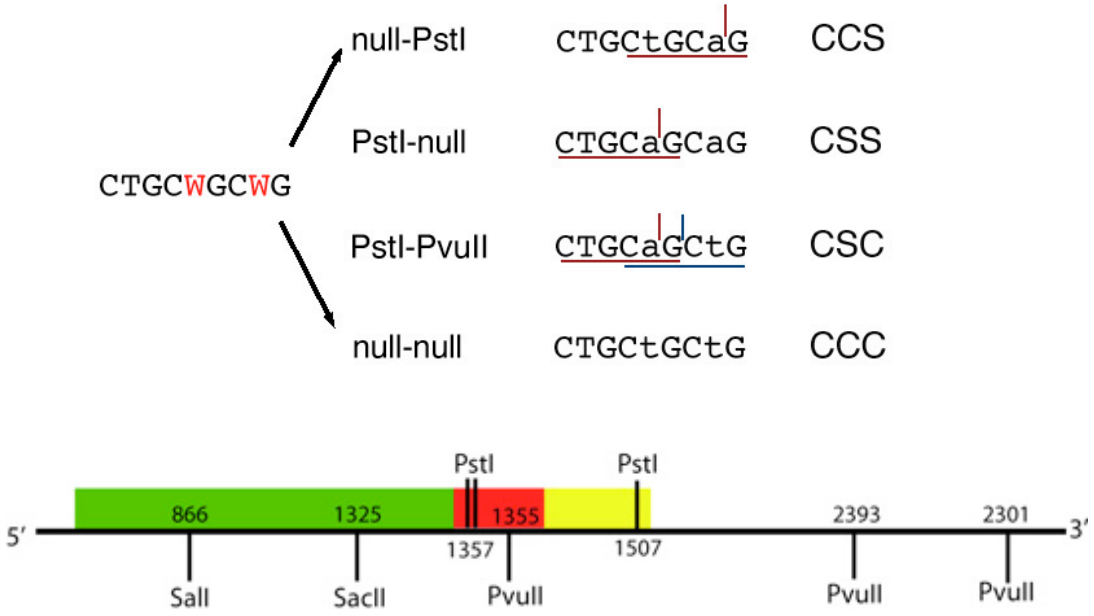

Figure 2-5 Restriction maps of the pZS-1 vector and Δ5B insert.

Amino acid substitutions generate *PstI* and/or *PvuII* restriction sites in the Δ5AB sequence, which are characteristic for the respective NS3/4A cleavage motifs. Below: Restriction map of the pZS1 vector encoding the Δ5AB (red), RCGFP (green) and MODC (yellow) sequences.

To determine whether the Δ5AB sequence was encoding a functional (CCS) or non-functional fusion protein, plasmids were test digested with *PvuII* and *Pst/SalI,* respectively. Since the wildtype pZS1 vector contains a *PstI* and two *PvuII* restriction sites and the Δ5AB insert may contain a *PvuII* and /or a *PstI* restriction site depending on the A/T substitutions, *PvuII* digestion results in 3

bands (608, 1037, 3225 bp) for plasmids encoding the CSC protease target site and 2 bands for all other versions of the insert. Likewise, *PstI/SalI* double digestion results in 3 bands (148, 492, 4229 bp) for plasmids encoding the CCS, CSS, or CSC target sites, and 2 bands (580, 4229 bp) for the wildtype vector and plasmids encoding the CCC sequence. A representative test digest is shown in Figure .

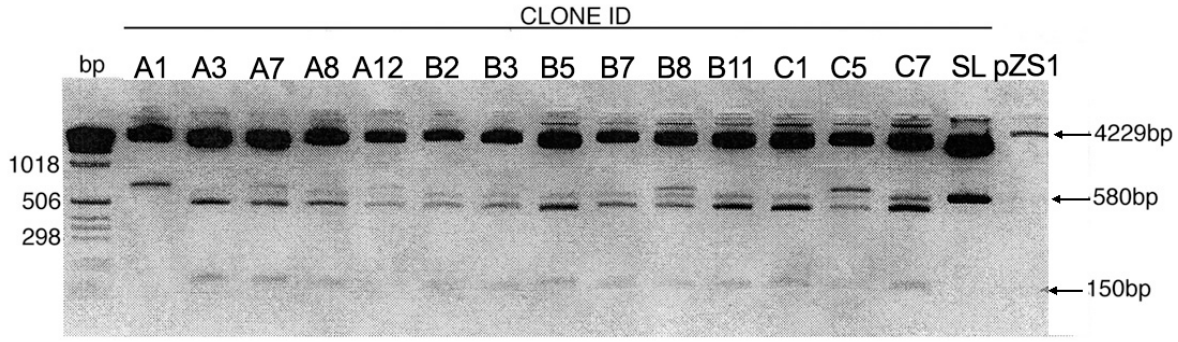

Figure 2-6 *PstI/SalI* restriction digest of the RCGFP(Δ5AB)MODC plasmid.

Digestion of plasmids encoding serine-containing NS3/4A cleavage motifs results in 3 bands at ~150, 490 and 4229bp (clones A3-C7), whereas the triple cysteine motif (clone A1) and the self-ligated wildtype vector (SL) yield 2 bands at 580 and 4229bp. Additional bands are due to partial digestion. Samples were run on a 3% agarose gel.

Selected clones were sequenced using the insert flanking primers described above to determine orientation of the insert and to confirm the sequence of the protease target site.

For transient transfection, 293T cells were seeded at $3x10^5$ cells/well in poly-L-lysine coated 12-well tissue culture plates in P/S free culture media, which was replaced with pre-warmed Optimem prior to transfection.

Transfections were carried out using the Calcium Phosphate Profection (Promega, WI, USA) kit according to the manufacturer's instructions. Briefly, 2 μg of plasmid DNA was diluted with nanopure water to a final volume of 37,7μl and 5,3μl of 2M calcium phosphate added, followed by 43μl of 2x HBS. The mix was incubated at RT for 30 min, after which the transfection mixture was added to the cells. Transfections were carried out for 5 hrs at 37°C, thereafter the media was replaced with DMEM + 3% FBS + P/S. Expression efficiency was typically monitored 24 hrs post transfection.

Transient transfection of Huh-7.5 cells was carried out using the Lipofectamine 2000 (Invitrogen, CA, USA) kit according to the manufacturer's instructions. Briefly, Huh-7.5 cells were seeded at $6x10^5$ cells/well in 6-well culture plates in P/S free media.

Per transfection reaction, 6 μl of Lipofectamie reagent were mixed with 250 μl serum-reduced medium (Optimem) and combined with 4 μg DNA diluted with 250 μl Optimem. The mix was incubated at 37°C for 30 min and added to the cells. Transfections were carried out at 37°C over night, thereafter the media was replenished with DMEM + 10%FBS + P/S. Expression efficiency was typically monitored 24 hrs post transfection.

To generate stable cell lines, cells were passaged 1:10 into fresh culture DMEM + 10% FBS 24 hrs post transfection. The following day, the media was changed to DMEM + 10% FBS + 1 mg/ml G418 (Sigma-Aldrich) and refreshed on a regular basis to remove dead cells. Stable cell lines were maintained in G418 containing culture media and expression of the RCGFP reporter gene monitored by fluorescent microscopy.

3 Results

3.1 Developing an indicator cell line for HCV infection.

Since primary HCV strains cannot be efficiently cultured *in vitro*, the evaluation of potential antiviral compounds in a biologically relevant context has so far proven extremely difficult. However, with the recent development of the replicon system it is now possible to design cell-based assays for the analysis of potential HCV inhibitors. These cell-based assays complement enzymatic assays, because they can determine whether potential inhibitors are able to penetrate the cell and act in an appropriate cellular environment. In theory, every step in the viral replication cycle can be considered as potential drug targets. However, as many fundamental aspects of HCV replication are still unknown, efforts to develop new antiviral agents have focused on the NS3/4A serine protease and the NS5B RNA-dependent RNA polymerase, both of which have been shown to be essential for viral replication. Early cell-based assays to study HCV protease activity relied on the cleavage of peptidic substrates by purified viral enzymes (177, 370). To enable efficient screening of inhibitors, cell-free assays were engineered that relied on chromatographic (383), colorimetric (HPLC) (379) or fluorescence (385) detection methods. However, while these assays allowed high-throughput screening, they were also laborious, inefficient or sensitive to interferences, and did not allow one to assess the ability of compounds to penetrate the cell membrane. The most recent generation of cell-based reporter assays with the

potential to identify inhibitors of NS3/4A protease is based on the co-expression of HCV protease and a cleavable reporter substrate, such as serine alkaline phosphatase (SEAP), which is linked to a secretion signal (80, 235, 313). As secretion of the reporter substrate into the culture medium depends on cleavage by NS3/4A, efficient inhibition is reflected by a decrease in the reporter substrate concentration (42, 234, 235).

Despite being fast, sensitive and suitable for high-throughput screening, the aforementioned cell-based reporter assays do not allow the identification and selection of HCV infected cells or the screening of patient samples to identify cell culture infectious viral strains. Therefore, we aimed to develop a cell-based reporter assay, which utilizes the viral NS3/4A protease to cleave and activate a fluorescent reporter protein constitutively expressed in HCV permissive Huh-7.5 hepatoma cells.

The HCV genome consists of a single open reading frame encoding a 3000 amino acid polyprotein precursor, which is co- and post-translationally processed into the structural and non-structural viral proteins. Following cleavage of the structural proteins by host proteases, the viral proteinase NS2/3 cleaves at the NS2/3 junction, whereas the NS3/4A serine protease cleaves further downstream at the NS3/4A, NS4A/4B, NS4B/5A and NS5A/5B junctions with a temporal sequence that is thought to be crucial for replication (reviewed in (100). We used the transcleavage ability of NS3/4A on the NS5A/5B domain of genotype 1a to generate a GFP-fusion protein which will

be liberated in cells expressing the HCV genome and can be monitored by fluorescence microscopy, flow cytometry or in a 96-well plate reader equipped with FITC filter sets.

It has been demonstrated that processing at the NS4B/5A and NS5A/5B sites is affected by amino acid substitutions at the conserved acidic (P6) and cysteine (P1) positions. In fact, NS5A/5B processing is completely abolished when a Cys→Gly, Arg, Asn or Asp substitution is introduced at P1 (24, 214), making this cleavage site an ideal target for a cell-based reporter assay.

3.1.1 RCGFP(Δ5AB)MODC plasmid construction.

As a backbone for the reporter plasmid we used a Proteasome Sensor Vector (pZS-1; Clontech), which is designed to express a proteasome-sensitive fusion protein composed of a *Zoanthus sp.* derived green fluorescent protein (Reef Coral Green Fluorescent Protein; RCGFP) and a mouse ornithine decarboxylase degradation domain (MODC) (Figure 3-1). An NS3-4A-specific cleavage site (Δ*5AB*; EADTEDVVCCSMSY), which corresponds to the amino acid sequence spanning the NS5A and NS5B junction, was inserted in frame between the RCGFP reporter gene and the MODC, thereby creating the RCGFP(**Δ**5AB)MODC fusion protein. In cells expressing the viral proteins the NS3/4A protease should cleave at its designated site thus liberating the RCGFP reporter protein from the MODC proteasome-targeting signal and leading to an accumulation of green fluorescence in the cytoplasm, which can be detected and quantified by microscopy, flow cytometry, or in a 96-well plate reader with FITC filter sets. In uninfected cells, the fusion protein is constitutively targeted to the proteasomes and degraded once it is translated.

The sequence for NS3/4A cleavage, Δ5AB, was based on the NS5A/5B domain of genotype 1a and constructed by annealing two redundant oligonucleotides (Figure 3-1), which contained substitutions (W) for adenine (A) and thymidine (T) in the nucleotide region coding for the recognition site (cytosine-serine-cytosine; CCS) of the viral enzyme. In addition to the S→C substitution, random replacement of the redundant nucleotides generated *PstI* and/or *PvuII* restriction site(s), which allowed subsequent discrimination of the

four possible NS3/4A target sequences (CCS, CSS, CCC, CSC). Furthermore, the blunt-end insertion of the Δ5AB oligonucleotide between the RCGFP and MODC genes via a single *SacII* restriction site resulted in random sense- or anti-sense orientation of the insert. Consequently, translation of the RCGFP(Δ5AB)MODC sequence yielded eight different versions of the fusion protein: six proteins containing a non-functional cleavage site (CCC, CSC, CSS) in sense or antisense orientation, one containing a functional cleavage site (CCS) in antisense orientation, and one encoding the functional fusion protein.

Transformation of the ligation reaction into *E. coli* yielded a total of 218 clones that were screened for the Δ5AB insert by PCR (for primer sequences see Materials and Methods). Δ5AB positive plasmids were test digested with *PstI* and *PvuII* to identify clones carrying one or both restriction sites (Fig. 1/1). Of the 92 clones carrying the Δ5AB sequence, 19 were *PstI* positive i.e. contained either a functional (CCS; null-*PstI*) or non-functional (CSS; *PstI*-null) cleavage site, 37 were *PstI/PvuII* positive i.e. carried a non-functional CSC cleavage site, and 36 were *PstI/PvuII* negative i.e. contained a non-functional CCC cleavage site. Eighteen of these clones were sequenced to confirm the results of the test digest and to determine orientation of the Δ5AB insert.

A

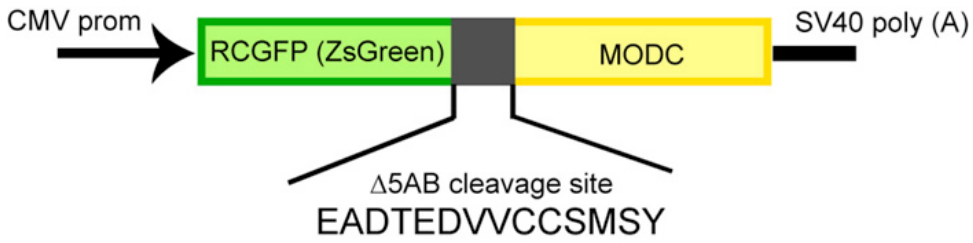

B

NS3-4A target sequence:

```
Δ5AB+ GGG AAG CAG ATA CTG AGG ACG TCG TCT GCW GCW GCA TGA GCT ACG GAT CCG CGC
Δ5AB- GCG GAT CCG TAG CTC ATG CWG CWG CAG ACG ACG TCC TCA GTA TCT GCT TCC CGC
```

C

```
                                          PvuII
      SacII                                PstI PstI       BamHI
       |                                     |    |          |
5′ GCCCCCGCGGGAAGCAGATACTGAGGACGTCGTCTGCT/AGC T/AGCATGAGCTACGGATCCGCGCTCACGGCCA 3′

   F        E  A  D  T  E  D  V  V  C  C  S  M  S  Y  R  S    null-PstI
   NF       E  A  D  T  E  D  V  V  C  S  S  M  S  Y  R  S    PstI-null
   NF       E  A  D  T  E  D  V  V  C  S  C  M  S  Y  R  S    PstI-PvuII
   NF       E  A  D  T  E  D  V  V  C  C  C  M  S  Y  R  S    null-null
```

Figure 3-1 Schematic diagrams of the RCGFP(Δ5AB)MODC plasmid and NS3/4A cleavage sequence

A. The NS3/4A cleavage sequence was inserted between the RCGFP reporter gene and the MODC proteasome targeting sequence on the pZS-ProSensor-1 vector (Clontech) via a single *SacII* restriction site. **B.** Redundant oligonucleotides were used to generate four different versions of the NS3/4A cleavage site. **C.** Random replacement of the redundant nucleotides (W) with adenine or thymidine generates three non-functional (NF) and one functional (F) protease cleavage site. In addition, the S→C substitution generates a *PstI* and/or *PvuII* restriction site, allowing discrimination of the different fusion protein versions by restriction digest.

3.1.2 Proteolysis of the RCGFP(Δ5AB)MODC fusion protein in transiently transfected 293T and Huh-7.5 cell lines

To assess functional expression of the fusion protein, 293T cells, which showed higher transfection efficiency than Huh-7.5 cells, were transiently transfected with the different reporter plasmids and subsequently treated with the proteasome inhibitor ALLN (N-acetyl-leucyl-leucyl-norleucinal; Calpain Inhibitor-I) to induce accumulation of green fluorescence. To optimize ALLN concentration and treatment time, 293T cells were transfected with the parental pZS1 vector and treated with 10 or 50 μg/ml ALLN for 2, 4 and 6 hrs. Treated cells were fixed and mean fluorescence intensity (MFI) and the percentage of fluorescent cells determined by flow cytometry (Figure 3-2). We found that the effect of ALLN on RCGFP protein accumulation was increased with prolonged treatment time, whereas a higher inhibitor concentration did not increase fluorescence intensity or the percentage of green cells. To avoid cytotoxic effects, transfected 293T cells were treated with 10 μg/ml ALLN for 6 hrs in all subsequent experiments.

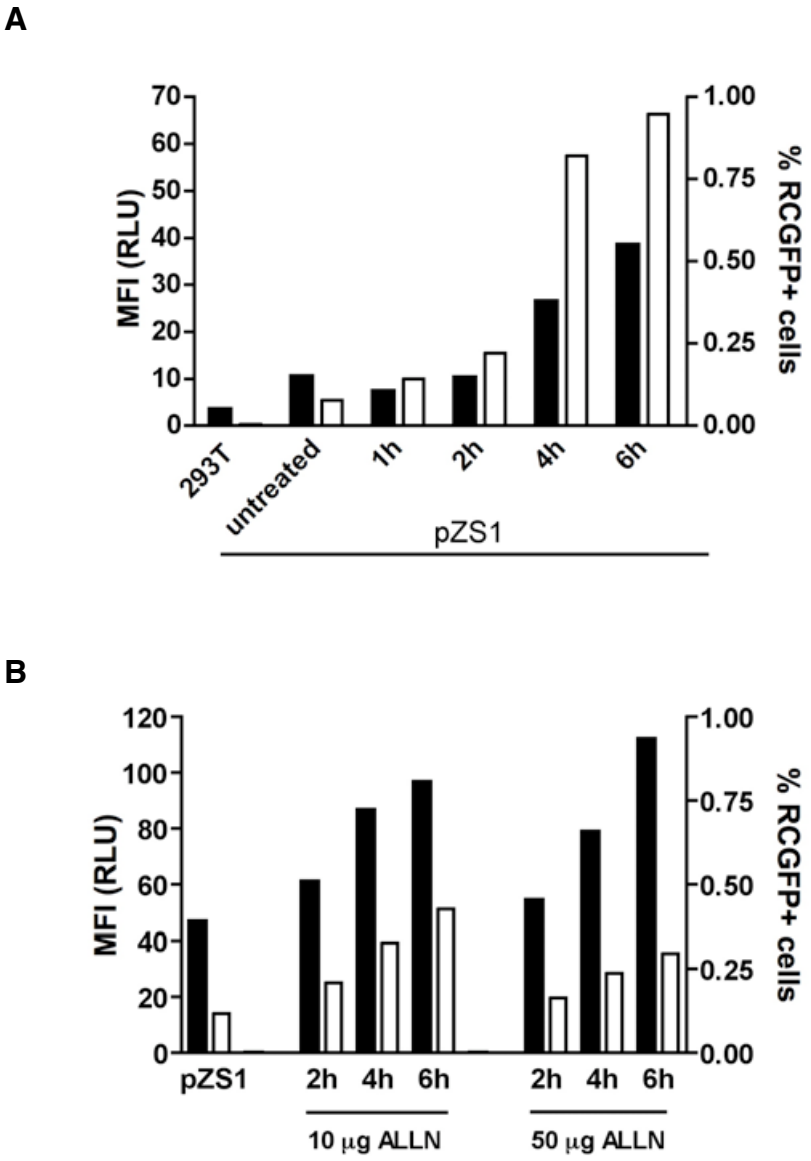

Figure 3-2 ALLN treatment of 293T cells expressing the parental fusion protein.

293T cells were transiently transfected to express the parental pZS1 vector. **A**. 24 hrs post transfection, cells were treated with 10 μg/ml ALLN for 1-6 hrs and mean fluorescence (MFI; black bars) and the percentage RCGFP positive cells (white bars) determined by flow cytometry. **B**. cells were treated with 10 or 50 μg/ml ALLN for 2, 4 or 6 hrs, untreated cells (pZS1) were used as a control. MFI and % RCGFP + cells were monitored by flow cytometry. Both experiments were performed in duplicate; data from representative experiments is shown.

293T cells expressing functional and non-functional RCGFP(Δ5AB)MODC fusion proteins were treated with ALLN for 6 hrs and fluorescence in the presence and absence of the inhibitor was monitored by flow cytometry. Relatively high mean fluorescence was detected in most of the ALLN-untreated cell lines and in control cells transfected with the parental pZS-1 vector (Figure 3-3). Transfection with lower amounts of plasmid DNA reduced protein expression levels slightly, however, green fluorescence was still detectable in ALLN-untreated cells. Overall, fluorescence levels were on average 2-fold increased following proteasome inhibition, indicating that in the absence of ALLN the fusion protein was still efficiently degraded.

Since the effect of ALLN on fusion protein degradation was only modest, it was difficult to select plasmids based on their susceptibility to proteasome inhibition. Instead, we chose one plasmid with amino acid substitutions in Δ5AB (clone U1) and one plasmid carrying a functional NS3/4A cleavage sequence (clone U9). Both clones responded comparably well to ALLN-mediated proteasome inhibition, demonstrating 5-fold (U1) and 6-fold (U9) increased fluorescence levels, respectively, following proteasome inhibition. In addition, we chose one plasmid (clone A3) as a negative control, which did not respond to ALLN treatment but which contained a triple cysteine cleavage site that we believed to be definitely non-functional. All three plasmids were transiently transfected into Huh-7.5 cells and functional expression of the fusion protein assessed 24 hrs post transfection by treating the cells with ALLN for 2, 4, 6 and 12 hrs. Fluorescence was monitored by fluorescent

microscopy throughout to assure maximum inhibition. Following treatment with ALLN for 12 hrs cells were fixed and their fluorescence determined by flow cytometry. In the presence of ALLN the percentage of fluorescent cells (Figure 3-4), as well as the mean fluorescence intensity (MFI) were increased up to 10-fold compared to untreated cells, confirming efficient degradation of the fusion protein in Huh-7.5 cells in the absence of the proteasome inhibitor.

Clone ID	*NS3-4A* recognition site	*Δ5AB* orientation	Mean Fluorescence Intensity (RLU) untreated	+10ug/ml ALLN
pZS-1	n.a.	n.a.	47,7	86,7
C1	CCS	antisense	67,7	15,3
U1	CCS	antisense	24,1	121
U9	CCS	sense	44	291
A8	CSC	sense	248	442
A12	CSC	sense	29,9	46,4
B2	CSC	sense	104	154
B3	CSC	sense	56,1	71,7
B11	CSC	sense	100	140
C7	CSC	sense	290	362
B7	CSS	sense	141	202
B8	CSS	sense	105	121
B5	CSS	antisense	23,1	86,9
A7	CSS	antisense	29,4	72,9
A1	CCC	antisense	10,9	28,7
A3	CCC	sense	709	694

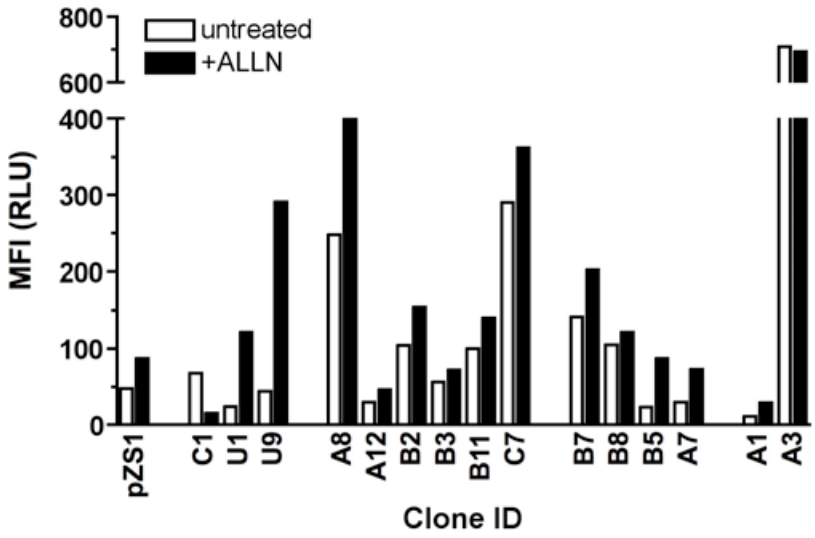

Figure 3-3 Degradation of the RCGFP(Δ5AB)MODC fusion protein in 293T cells.

Cells were transiently transfected to express functional and non-functional versions of the fusion protein and 24 hrs post transfection treated with the proteasome inhibitor ALLN for 6 hrs. Following treatment, cells were fixed with paraformaldehyde and fluorescence (MFI) analyzed by flow cytometry. Shaded boxes represent clones that were used in subsequent experiments. (n.a.= not applicable).

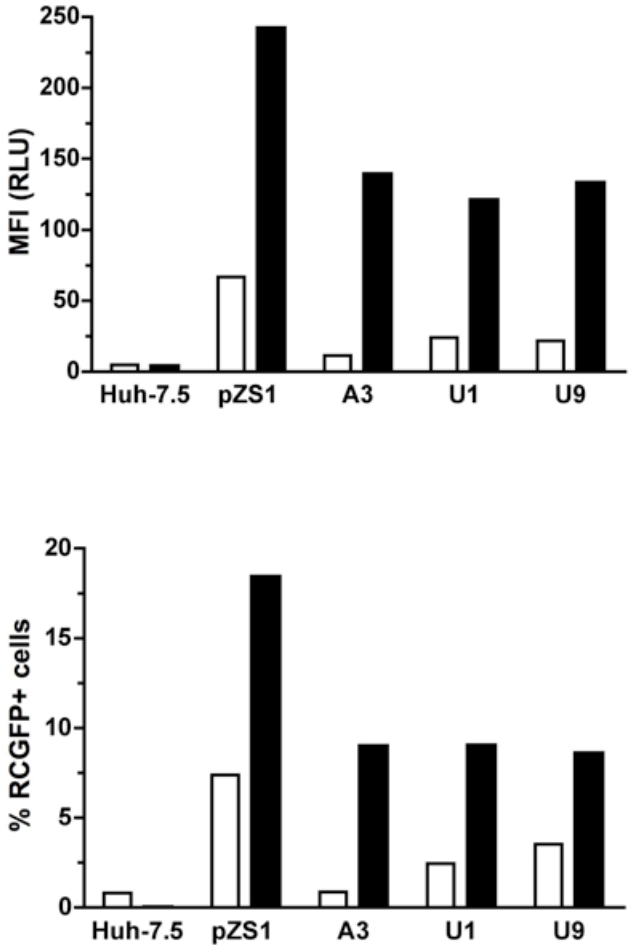

Figure 3-4 Proteloytic degradation of the RCGFP(Δ5AB)MODC fusion protein in transiently transfected Huh-7.5 cells.

Cells were transiently transfected to express fusion proteins containing a functional (U9) or non-functional (A3, U1) NS3/4A cleavage motif. 24 hrs post transfection, cells were treated with the proteasome inhibitor ALLN (black bars) for 12 hrs. Untreated cells (white bars) were used as controls. Following treatment, cells were fixed and the mean fluorescence intensity (MFI) and percentage RCGFP positive cells monitored by flow cytometry. The experiment was performed in triplicate; data from a representative experiment is shown.

3.1.3 Generation of RCGFP(Δ5AB)MODC Huh-7.5 cells - NS3/4A mediated cleavage of the fusion protein

To generate stable cell lines, Huh-7.5 cells were transfected with plasmids derived from clones U1 and U9 or the parental pZS-1 vector, and put under G418 selection at 48 hrs post transfection. Clone A3, which contained an antisense oriented CCC cleavage site was omitted because of possible negative effects of the triple cysteine sequence on correct protein folding. As before, functional expression of the fusion protein was determined by treating the stable cell lines with ALLN and analyzing fluorescence by flow cytometry. Mean fluorescence levels in all transfected untreated cell lines were comparable to parental Huh-7.5 cells, indicating that the fusion protein was efficiently degraded by the proteasome. Following proteasome inhibition, the number of RCGFP positive cells increased 35% (Figure 3-5).

In order to determine the efficiency of NS3/4A mediated cleavage of the Δ5AB fusion protein the stable cell lines were infected with high titer J6/JFH and the number of NS5A-RCGFP double positive cells determined by flow cytometry at 48 hrs post infection. Unexpectedly, although up to 80% of cells were NS5A positive J6/JFH infection did not induce accumulation of green fluorescence in infected cells (Figure 3-6), indicating that NS3/4A mediated cleavage of the fusion protein was inefficient or absent. The lack of cleavage can be explained by the discrepancy in NS3/4A and target sequence localization, since the fusion protein is randomly distributed within the cytoplasm, while the viral protease is targeted to the endoplasmic reticulum (ER). By inserting an ER-

targeting signal or an ER-resident protein such as PERK upstream of the RCGFP gene this problem could be solved, although it is not clear whether targeting of the fusion protein to the ER would interfere with subsequent targeting to the proteasomes.

In summary, although the RCGFP(Δ5AB)MODC reporter constructs were shown to function as expected, their failure to respond to the presence of NS3/4A in infected cells was disappointing. We therefore decided to suspend further development of this system in order to focus on the work described elsewhere in this thesis. Future work on this approach to detecting infection, including the modifications suggested above, should allow us to increase the probability of success.

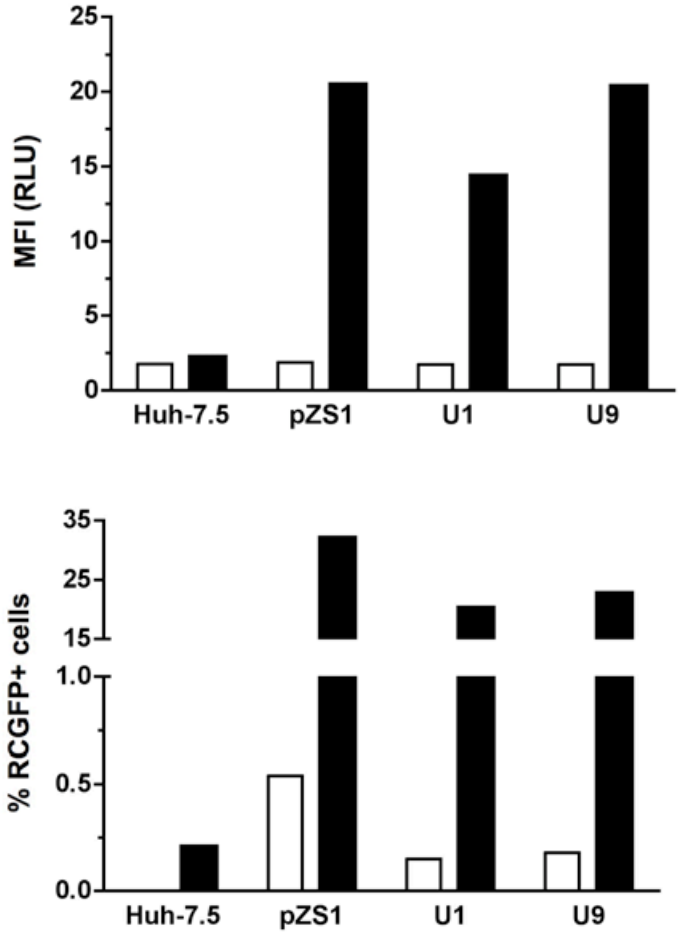

Figure 3-5 Proteloytic degradation of the RCGFP(Δ5AB)MODC fusion protein in stable Huh-7.5 cell lines.

Cells were transfected to express fusion proteins containing a functional (U9) or non-functional (A3, U1) NS3/4A cleavage motif and maintained in G418-containing media. Cells were treated with 10 μg/ml ALLN for 12 hrs (black bars), untreated cells were used as controls (white bars). Mean fluorescence intensity (MFI) and percentage RCGFP positive cells were monitored by flow cytometry. Data from a representative experiment is shown.

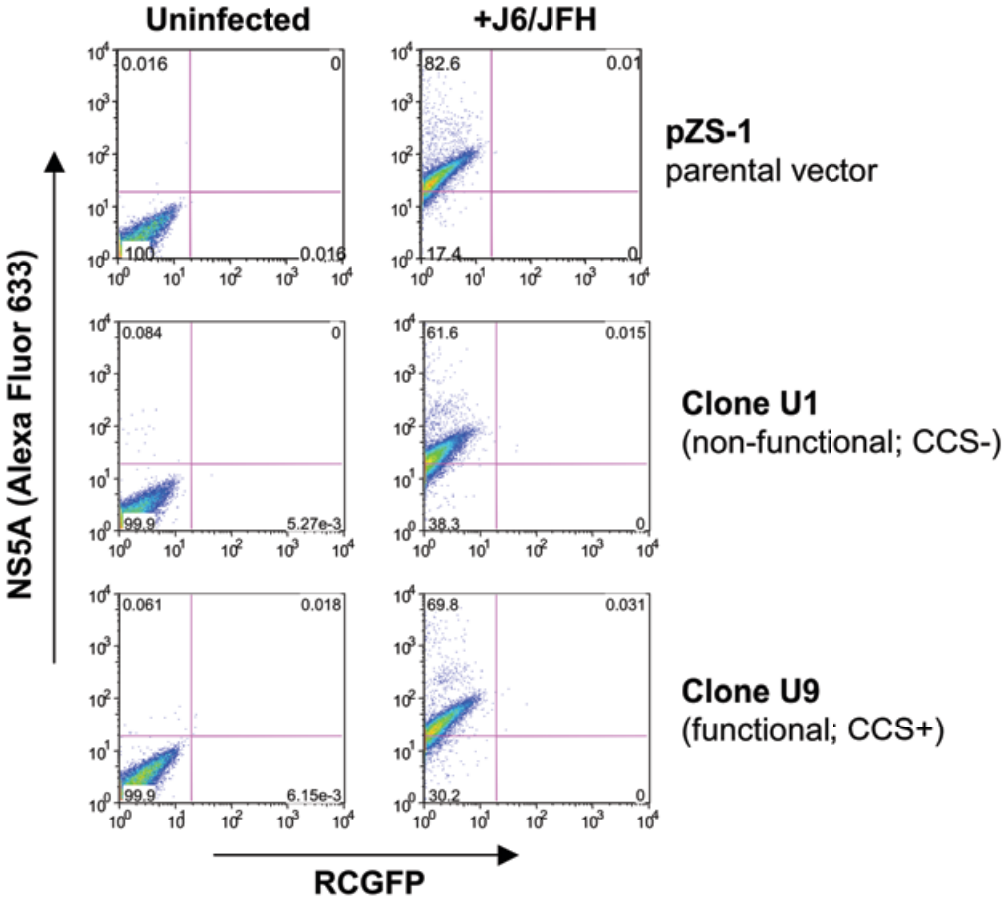

Figure 3-6 Analysis of NS3/4A mediated fusion protein cleavage.

Stable cell lines were infected with J6/JFH in the absence of G418. 72 hrs post infection, cells were fixed and stained with an NS5A-specific antibody (9E10; 1/200 dilution), bound antibody was detected using the Alexa Fluor 633 (1/1000 dilution). Fluorescence was monitored by flow cytometry.

3.1.4 Discussion

In this study, we aimed to develop a live cell assay for the identification and selection of HCV infected cells based on the ability of the viral NS3/4A serine protease to cleave in *trans* the non-structural proteins NS4A to NS5B. Our system is based on the Proteasome Sensor Vector (pZS-1) (85), which was designed for studies of proteasome function in mammalian cells and encodes the *Zoanthus sp.* GFP gene (Reef Coral Green Fluorescent Protein; RCGFP) coupled to a mouse ornithine decarboxylase (MODC) proteasome degradation domain. By inserting the NS5A/5B cleavage domain of genotype 1a (Δ5AB) between the RCGFP reporter gene and the MODC domain we modified the RCGFP-MODC fusion protein to become a substrate for NS3/4A (Fig. 1). In the presence of viral protease the constitutively expressed reporter protein is liberated from the proteasome targeting signal and green fluorescence accumulates in the cytoplasm. Based on this one component system we aimed to produce a novel 'indicator' cell line, Huh-7.5-RCGFP(Δ5AB), that would allow quantification of HCV infectivity by flow cytometry, real-time studies of viral replication, and the isolation of infected cells.

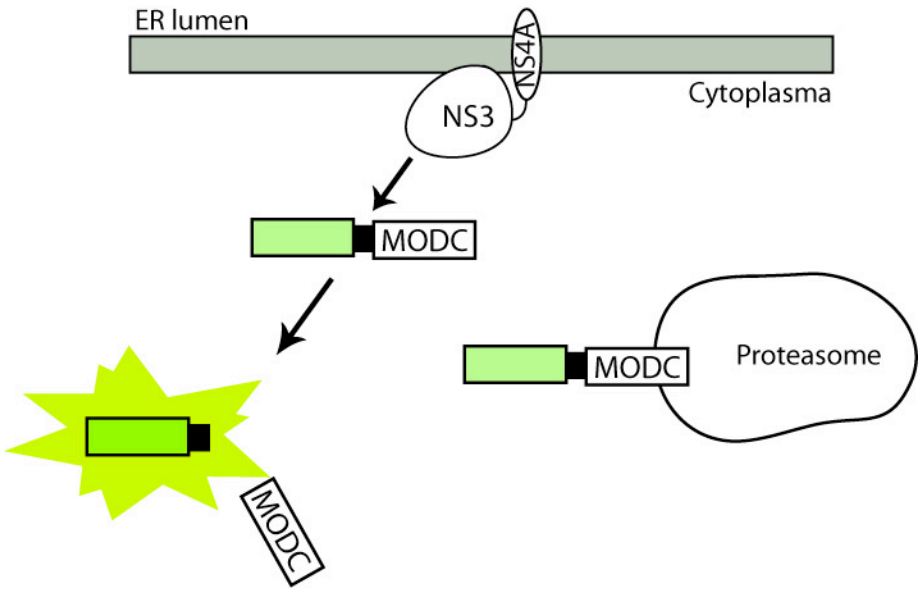

Figure 3-7 NS3/4A mediated cleavage of the RCGFP(Δ5AB)MODC fusion protein.

In HCV infected cells, NS3/4A cleaves in *trans* at the Δ5B recognition site and liberates the GFP reporter protein from the MODC proteasome targeting signal, resulting in the intracellular accumulation of green fluorescence.

In the absence of NS3/4A protease, the RCGFP(Δ5AB)MODC fusion protein is constitutively degraded by the proteasome and only accumulates in the cytoplasm when proteasome activity is altered, for instance by treating cells with an inhibitor of proteasome-dependent proteolysis such as ALLN. We measured relatively high green fluorescence in transiently transfected 293T cells in the absence of ALLN (Figure 3-3), which we assume was due to incomplete degradation of the fusion protein. One reason for this might be that the Δ5AB domain affects correct folding of the fusion protein, thus interfering with proteasome targeting. The mean fluorescence intensity (MFI) of 293T cells expressing RCGFP(Δ5AB)MODC constructs varied significantly between

clones and was in some cases up to 7-fold increased compared to the parental vector (Figure 3-3), which may suggest that fusion protein folding is hampered in these cells. However, considering that accumulation of RCGFP was also observed in 293T cells expressing the parental fusion protein, it is likely that proteasome 'overload' due to each cell containing multiple plasmids is responsible for the incomplete degradation. Notably, the activity of lysosomal as well as proteasomal proteolytic pathways depends on the growth conditions of cells and it has been reported that proteasome activity is markedly reduced at cell confluence, especially in cells already deprived of amino acids (133, 134). These findings may offer an additional explanation for the inefficient protein degradation in transiently transfected 293T cells. In our experience, transfection is most efficient when cells are in the growth phase i.e. approximately 50-70% confluent. Which means that the cells – considering a 24-28 hour doubling time - had reached confluence by the time fluorescence was monitored.

In transiently transfected 293T cells, proteasome inhibition with ALLN markedly increased the cytoplasmic accumulation of RCGFP, as reflected by increases in the fluorescence intensity and the percentage of RCGFP-positive cells within the population (Figure 3-3), suggesting that the fusion protein was functional. Based on the results from the proteasome-inhibition assay, we selected several clones containing functional and non-functional NS3/4A cleavage sites for transient transfection into Huh-7.5 cells. Interestingly, we measured up to 5-fold higher mean fluorescence in ALLN-untreated Huh-7.5

cells expressing the parental pZS-1 vector than in cells carrying a RCGFP(Δ5AB)MODC construct (Figure 3-4). Likewise, the percentage of RCGFP-positive cells within the population was up to 5-fold increased in pZS-1 expressing Huh-7.5 cells. These findings probably suggest that insertion of the Δ5AB domain alters transfection efficiency in Huh-7.5 cells. It is known that constructs of large size, such as bacterial artificial chromosome (BAC) and P1-derived artificial chromosome (PAC) DNA, substantially reduce transfection efficiency. However, the size-effect of a 54 bp DNA fragment on transfection efficiency is debatable. Alternatively, insertion of the Δ5AB domain downstream of the reporter gene might affect the ability of the CMV promoter to drive RCGFP expression. Indeed, Yin and colleagues have reported previously that inserting DNA fragments ranging from a couple of hundred to a couple of thousand base pairs downstream of a luciferase reporter gene significantly reduced relative luciferase activity in transient transfection assays through modulation of promoter activity (420).

Overall, we observed low initial fluorescence in transiently transfected Huh-7.5 cells expressing the RCGFP(Δ5AB)MODC constructs. Following proteasome inhibition, the mean fluorescence intensity increased approximately 4-fold in the clones containing non-functional NS3/4A cleavage sites and approximately 12-fold in the clone containing the functional domain, confirming efficient degradation of the fusion protein. Stable transfection of these plasmids into Huh-7.5 cells yielded similar results, with pZS-1 and all

RCGFP(Δ5AB)MODC clones showing low initial fluorescence and markedly increased fluorescence following proteasome inhibition (Figure 3-5).

To test the ability of NS3/4A protease to cleave the RCGFP(Δ5AB)MODC fusion protein, we infected the stable cell lines with high-titer HCVcc J6/JFH and monitored green fluorescence by flow cytometry at 72h post infection. Interestingly, we did not detect any RCGFP accumulation in NS5A-positive cells (Figure 3-6), suggesting that NS3/4A had failed to cleave at its designated site. Possible explanations for this observation include (i) insufficient NS3/4A expression, (ii) inability of the J6/JFH (genotype 2a) protease to recognize the genotype 1a Δ5AB domain, (iii) failure to provoke cleavage due to localization of viral protease and fusion protein to different cellular compartments.

In a recent study, Breiman et al. reported that in HCV infected Huh-7 cells efficient cleavage and activation of a PERK(Δ5AB)GalVP16 chimeric protein positively correlated with high expression of the viral proteins (59), while chimera activation was low in HCV-infected hepatocytes, which are known for poor infection and low replication rates (68). However, it is worth noting that in the same study it was demonstrated that in Huh-7 cells cleavage at the NS5A/5B domain occurs even when NS3/4A is expressed at the low level typical for normal infection conditions (i.e. low infectivity and/or inefficient genome replication). In our experiments, infection with high-titer J6/JFH (MOI of >0.3) yielded 60-80% NS5A positive cells and a more detailed analysis of

the mean fluorescence intensity by flow cytometry revealed that a great proportion of infected cells expressed NS5A at a high level (Figure 3-6). Since the polyprotein precursor is cleaved in *trans* by the NS3/4A protease, NS5A expression is most likely indicative of the expression of other viral proteins. Therefore, we conclude that NS3/4A levels were sufficient to efficiently cleave the fusion protein and induce the intracellular accumulation of detectable amounts of RCGFP.

The Δ5AB transcleavage motif used in our study was derived from the genome sequence of HCV gentoype 1a strain H77. In theory, NS3/4A protease activity could be strain specific resulting in failure of the genotype 2a (J6/JFH) protease to recognize and cleave a NS5A/5B motif derived from a different strain. However, the active site residues of the NS3 protease are strictly conserved between genotypes with the exception of positions 123 (canonic arginine) and 168 (aspartic acid), which in genotype 3a have been replaced with threonine and glutamine, respectively (46). More importantly, NS3/4A proteases of different HCV genotypes including 1a, 1b, 2a and 3a showed comparable activity on genotype 1a polyprotein substrates and the genotype 1a NS5A/5B transcleavage motif (46, 159).

In the absence of the NS4A cofactor the NS3 serine protease is diffusely distributed in the cytoplasm and nucleus. However, when co-expressed with NS4A, NS3 is directed to the endoplasmic reticulum (ER) (414), which is the principal site for the biosynthesis of HCV proteins. The RCGFP(Δ5AB)MODC

fusion protein, on the other hand, either resides in the cytoplasm or is targeted to the proteasome for degradation. Given that NS3/4A failed to cleave the chimera despite high expression of the viral proteins, it is likely that the protease and its substrate have to be in close proximity i.e. in the same cellular compartment to provoke cleavage. Linking the chimera to an ER-targeting signal would solve this problem, however, we assume that targeting to the ER would interfere with proteasomal degradation.

Two different strategies could be employed to circumvent this problem: (i) a one component system in which cleavage at the transcleavage motif of the chimera releases a tagged membrane-bound protein, (ii) a two component system in which cleavage at the Δ5AB domain leads to the release of a transcription factor and subsequent activation of a reporter protein. Both strategies would allow targeting of the chimera to the ER through fusion with an ER resident protein, such as PERK, and the detection of HCV infection in live cells. We propose a one component system in which the fluorescently tagged extracellular domain of a membrane-anchored protein such as CD8α is fused with an ER-retention signal (*ERS*), generating a *ERS*(Δ5AB)CD8α chimera. Upon cleavage by NS3/4A, CD8α would be transported to the cell membrane and cytoplasmic fluorescence would be markedly reduced, allowing the identification of HCV positive cells. A similar approach in which the localization of CD8α is dependent on NS3/4A protease activity has been reported previously (313). However, while the aforementioned assay requires fixation or cell lysis and staining with an anti-CD8α antibody to quantify HCV

infection and NS3/4A activity, our system could be used to isolate and propagate cells capable of supporting HCV replication.

While our study was in progress, Breiman et al. reported the development of a two component system for the NS3/4A dependent identification and selection of HCV infected cells (59). This NS3/4A transactivation system is based on processing of a PERK(Δ5AB)Gal4VP16 chimera by viral protease, which releases the Gal4VP16 transcription factor and amplifies expression of a GFP reporter gene, allowing simple and effective monitoring of HCV expression in different cell lines and the clonal selection of cells permissive to HCV infection.

3.2 Cellular contact promotes HCV infection through the modulation of HCV entry receptor expression

Cell junctions are membrane specializations that can be visualized as dense structures by electron microscopy and are characterized by a close apposition of the membranes of neighbouring cells and a cytoplasmic plaque (121, 211). Cell junctions are composed of different cell adhesion molecules (CAMs) and proteins such as occludins, claudins, and junctional adhesion molecules (JAMs), and can be divided into three groups depending on their function (reviewed in (406): anchoring junctions, communicating (gap) junctions, and tight junctions (TJ). Through serving as a barrier to the intra-membrane diffusion of components, TJ play an important role in maintaining cell polarity, which is characterized by the asymmetric distribution of macromolecules within the cell and the organization into functionally distinct apical and basolateral domains (reviewed in (360).

Conflicting evidence exists as to whether human hepatoma cells form functional tight junctions (TJ). Benedicto et al. recently reported increased transepithelial resistance (TER) and reduced permeability to soluble dextran in confluent Huh-7 cells (40), while in our experience Huh cells from different sources failed to polarize ((277), unpublished observations). However, regardless of polarization status, the TJ proteins claudin-1 (CLDN1), occludin (OCLN) and Zonula occludens-1 (ZO-1), are enriched at cellular junctions in confluent cells and form a polygonal web resembling the TJ protein

distribution pattern characteristic for polarized MDCK and Caco-2 cell lines (95, 136).

The importance of CLDN1 in the viral entry process is indisputable. However, it is unknown whether CLDN1 expression levels define productive HCV entry. Evans and colleagues suggest that the protein acts at the post-binding stage, where it may facilitate fusion between the virion and the cell membrane (114), but whether high CLDN1 levels promote this process is unclear. In contrast, high CD81 and SR-BI surface expression levels have been shown to enhance HCV infectivity (159, 215). In our experience, cell density is an important determinant of HCV infectivity *in vitro* and a certain degree of cellular contact is required for productive infection. Given that CLDN1 and other TJ proteins are enriched at sites of cellular contact, it seems likely that the expression of other surface receptor molecules may be modulated in a similar manner, thus promoting HCV entry.

Recently, it has been demonstrated that HCV can transmit in cell culture by the release and infection of cell-free particles and through direct dissemination between cells (396). The latter route is enhanced at cell confluence and appears to be CLDN1-dependent since ectopic expression of CLDN1 in 293T cells allowed cell-cell transmission of HCV infectivity. Indeed, a recent study proposes a correlation between the TJ-like distribution of CLDN1 and the cellular tropism of HCV (249, 417), suggesting that the protein may have to be

localized to the plasma membrane to render non-permissive cell lines susceptible to HCV infection.

3.2.1 Cellular contact modulates expression and localization of HCV entry receptors

To study the effect of cellular contact on HCV entry receptor expression and localization, Huh-7.5 cells were plated on collagen-treated borosilicate coverslips at sub-confluence ($7.5x10^3$ cells/cm^2) or confluence ($30x10^3$ cells/cm^2) and CD81, SR-BI or CLDN1 imaged by laser-scanning confocal microscopy (Figure 3-8). Both CLDN1 and SR-BI were predominantly localized to cellular junctions and showed no detectable immuno-staining at cell-cell contact free membrane domains, whereas CD81 localization to the plasma membrane was independent of cellular contact. Quantitative analysis of receptor expression at the plasma membrane and within the cytoplasm by pseudo-linear profiling of individual cells showed that in confluent cells, CLDN1 and SR-BI plasma membrane expression was significantly enhanced ($p<0.001$, unpaired t-test) compared to sub-confluent cells, while CD81 expression was unaltered (Figure 3-8). No significant increase in the cytoplasmic expression of the receptors was observed suggesting that cellular contact specifically modulates the expression of CLDN1 and SR-BI at the plasma membrane. These findings were supported by Western Blotting analysis of total cell lysates from sub-confluent or confluent Huh-7.5 cells, which demonstrated increased protein levels of CLDN1 and SR-BI, but not CD81, in confluent cells, whereas RNA levels were unchanged (P. Balfe,

unpublished observations), suggesting a cell contact-mediated translational regulation of CLDN1 and SR-BI expression.

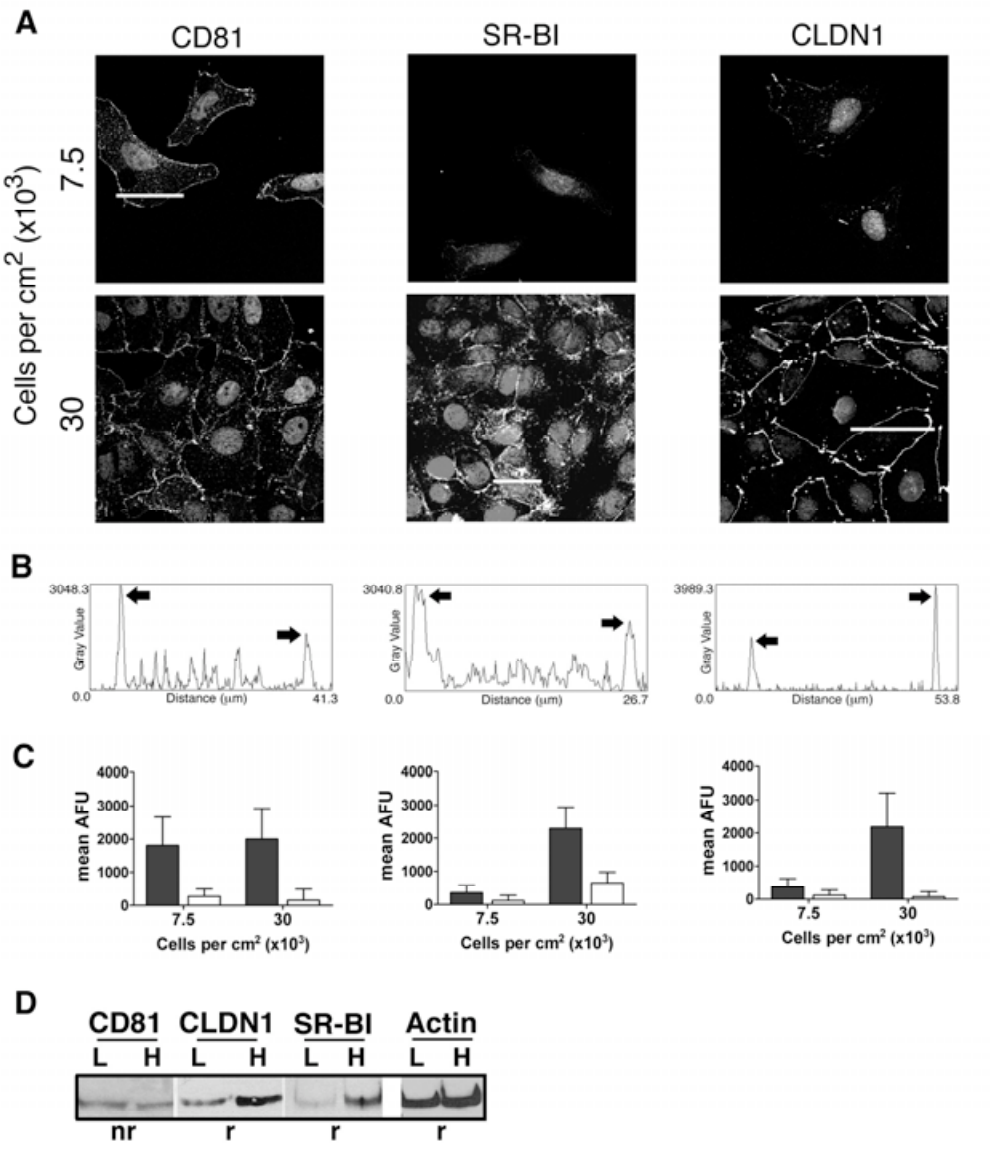

Figure 3-8 Receptor expression is modulated in confluent Huh-7.5 cells.

A. Sub-confluent and confluent cells were stained with antibodies specific for CD81 (M38), SR-BI (Cla-I), or CLDN1 (1C5-D9, Abnova). Images were taken at 63x magnification with a 1.2NA objective. **B and C.** A representative histogram of a linear profile plot for confluent cells is shown in B. Expression of plasma membrane (black bars) and cytoplasmic (white bars) receptor forms was quantified by linear profile plot analysis and is presented as arbitrary fluorescence units (AFU); arrows indicate plasma membrane staining. Background fluorescence was 20 AFU for CLDN1 and CD81, respectively, and 2,5 AFU for SR-BI. A minimum of 15 cells was analyzed per receptor at each seeding density. **D.** Western blotting analysis of protein expression in sub-confluent and confluent Huh-7.5 cells. Cells were plated at low (L) or high (H) seeding density and 5μg of total protein separated by SDS PAGE under reducing (r) or non-reducing (nr) conditions, transferred to membranes and probed for CD81, CLDN1, or SR-BI.

3.2.2 Cellular contact promotes HCV infection at the entry level

To determine the effect(s) of increased SR-BI and CLDN1 surface expression on viral entry, Huh-7.5 cells were plated at low (7.5x103 cells/cm2), standard (15x103 cells/cm2), or high seeding density (30x103 cells/cm2) (Figure 3-9) and infected with JFH-1 or J6/JFH for 1 to 6 hrs. Following a 48 hrs incubation period viral infection was determined by staining with an NS5A-specific monoclonal antibody (9E10) and enumerating the number of infected foci, which are thought to represent primary infection events (
Figure 3-10). JFH-1 and J6/JFH infection, respectively, increased linearly over time and were enhanced ~1.5-fold with each doubling in cell density. Furthermore, the infection rates (FFU/ml/h) of both virus strains were significantly enhanced in confluent cells (~800 FFU/ml/h) compared to sub-confluent cells (~400 FFU/ml/h) ($p<0.005$, comparison of slopes).

Taken together, these data suggest a relationship between cell density and HCV infectivity. To determine whether this was mediated at the viral entry level, we analyzed the infectivity of pseudoparticles (HCVpp), which display functional viral glycoproteins on retroviral core particles and carry a luciferase or GFP reporter gene, allowing measurement of HCV-glycoprotein dependent entry. In preliminary experiments designed to optimize the infection, the number of HCVpp-JFH (genotype 2a) and HCVpp-H77 (genotype 1a) infected Huh-7.5 cells increased more or less linearly over time (Figure 3-11) when cells were plated at standard seeding density, indicating that a prolonged

incubation time promotes HCV entry. Of note, HCVpp-H77 infectivity was 50% increased compared to HCVpp-JFH, therefore, the genotype 1a strain was used in subsequent experiments.

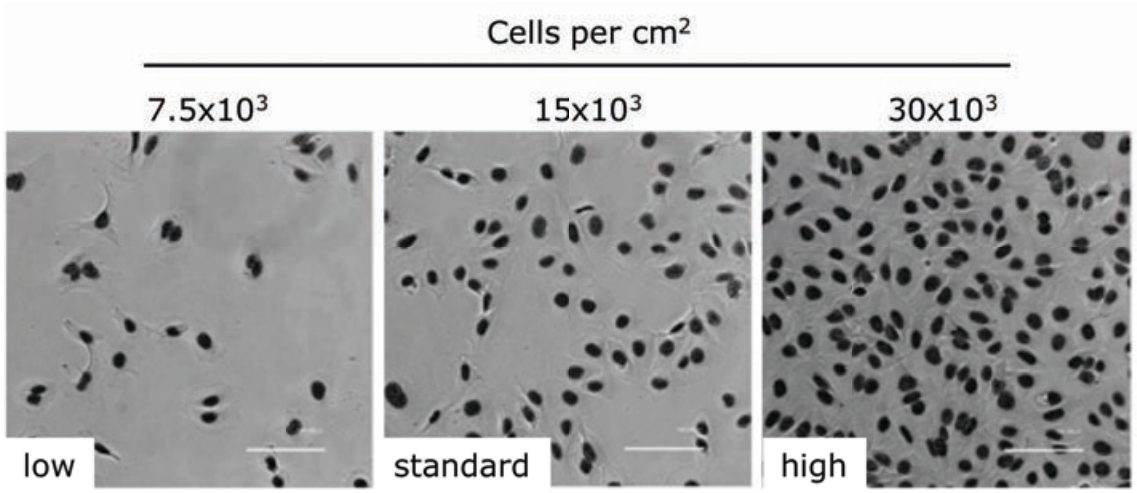

Figure 3-9 Phase images of Huh-7.5 cells plated at low, standard and high density.

Cells were plated on collagen-treated borosilicate cover slips and 26h later imaged with a Zeiss fluorescent microscope. Nuclei were counterstained with DAPI. Scale bars represent 100 μm.

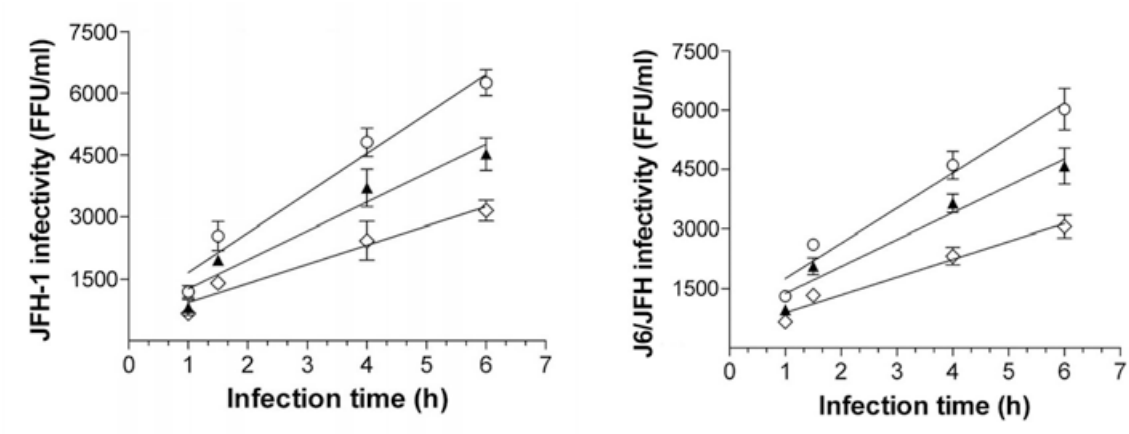

Figure 3-10 Cellular contact modulates HCVcc infectivity.

Huh-7.5 cells were plated at low (◇), standard (▲), or high (○) density and 26 hrs post plating infected with JFH-1 or J6/JFH HCVcc for 1 to 6 hrs. 48 hrs post infection, infectivity was quantified by counting NS5A-positive foci Data is presented as foci forming units (FFU)/ml. Values represent means ± standard deviation.

To define the effect of cellular contact on viral entry, Huh-7.5 cells were plated at increasing cell densities from $7.5x10^5$ to $30x10^5$ cells/cm^2 and HCVpp-H77 allowed to adsorb for 5 hrs at 37°C. Thereafter, non-internalized particles were removed by washing and luciferase activity was determined following a 72 hrs incubation period. A modest increase in HCVpp-H77 luciferase activity was observed from low to standard seeding density (Figure 3-11), whereas HCVpp-H77 infectivity was enhanced more than 2-fold at high cell density. In contrast, the effect of cell confluence on the infectivity of murine leukaemia virus pseudoparticles (MLVpp), which were used as an independent control, was negligible, indicating that the effect of cellular contact on viral infection was HCV glycoprotein-specific.

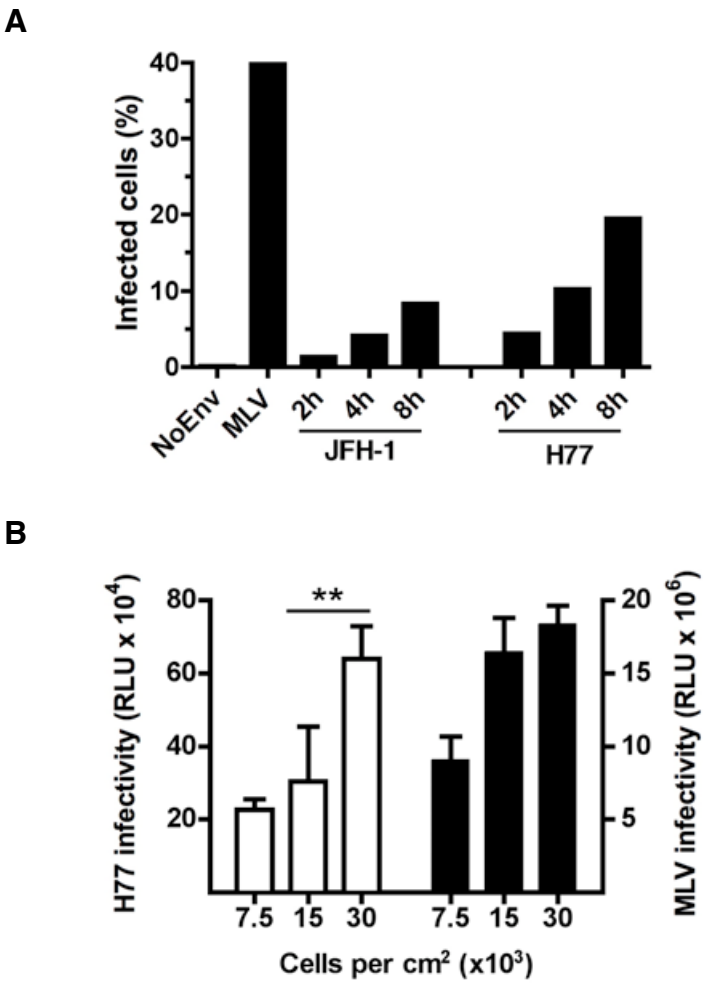

Figure 3-11 Cellular contact modulates HCV entry.

A. HCVpp infectivity is governed by incubation time. Huh-7.5 cells were plated at standard seeding density and incubated with HCVpp-JFH or HCVpp-H77 for up to 8 hrs, envelope-deficient pseudoparticles (NoEnv) and MLVpp were used as controls. Viral infectivity (per cent GFP positive cells) was determined by flow cytometry. **B. HCVpp infectivity increases with cell confluence.** Huh-7.5 cells were plated at different densities and infected with HCVpp-H77 or MLVpp for 5h. Luciferase activity (relative light units; RLU) was measured 72h post infection. Statistical analysis was performed using a paired two-tailed t-test (p=0.0046).

3.2.3 Effect of cellular contact on HCV internalization kinetics

Escape from proteinase K dependent proteolysis

Cellular contact modulates CLDN1 and SR-BI expression and distribution, and promotes HCV infection at the entry level. To determine whether a loss of cell-cell contact affected the internalization kinetics of HCV, we utilized a well-described proteolytic assay in which proteinase K (PK) is used to remove cell-bound, non-internalized virus particles from the cell surface, the hypothesis being that internalized particles become resistant to proteolysis (Figure 3-12). Receptor-mediated endocytosis is an energy-dependent process, therefore inoculation with the virus was carried out on ice to prevent uptake of bound virus particles. This also resulted in synchronized internalization of bound virus once the temperature was elevated to 37°C.

Since the PK-dependent internalization assay requires the trypsinization of cells prior to inoculation with HCVcc, we sought to ascertain, whether trypsin treatment reduced receptor expression at the cell surface. Huh-7.5 cells were treated with trypsin or an enzyme-free buffer (cell dissociation buffer; CDB) for 10 min and subsequently infected with HCVcc for 1 hr at 37°C. Thereafter, cells were washed thoroughly to remove unbound virus and re-plated at equal densities. 48 hrs post infection the percentage of NS5A positive cells was determined by flow cytometry (Figure 3-13).

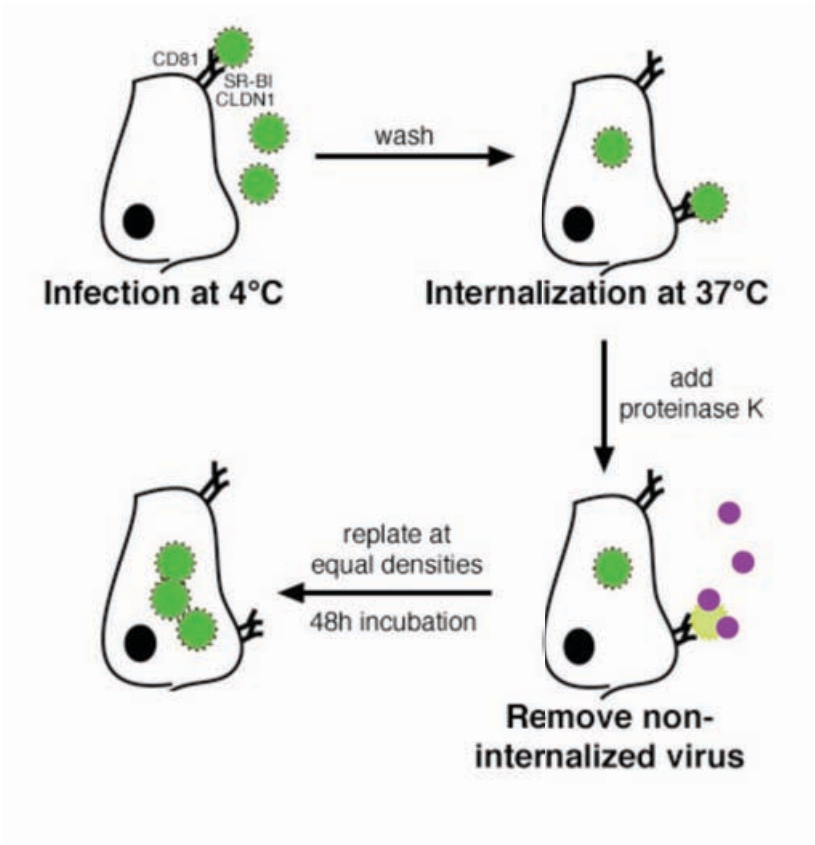

Figure 3-12 Proteinase K dependent HCV internalization assay.

Huh-7.5 cells were trypsinized, washed and the cell suspension infected with HCVcc for 1 hr on ice. Unbound particles were removed by washing and the temperature elevated to 37°C. At different time points post entry initiation, cells were incubated with proteinase K (PK) for 1 hr on ice to remove non-internalized particles, thereafter cells were re-plated. 48 hrs post infection, infectivity was determined by counting infected foci.

Viral infectivity was reduced by approximately ~30% for cells in suspension compared to adherent cells, suggesting that loss of cellular/ECM contact reduced the efficiency of virus-receptor interactions. However, trypsin-treated and CDB-treated cells were equally susceptible to infection, indicating a modest proteolytic effect of trypsin on the surface expressed HCV entry factors. Concomitantly, analysis of receptor levels by flow cytometry confirmed the presence of CD81, CLDN1, and SR-BI on trypsinized cells (Figure 3-13).

To determine the efficiency of PK at removing cell-bound infectious virus, cells in suspension were infected with HCVcc for 1 hr on ice, unbound particles removed by washing thoroughly, and the cells immediately treated with PK at 4°C. Using 50 μg/ml PK we were able to remove ~90% of cell-bound virus from the cell surface (Figure 3-14A). Furthermore, we noted that viral infectivity reached a plateau 1 hr post entry initiation (Figure 3-14B) , indicating that 100% of cell-bound virus had become resistant to PK. Due to the variability of infectivity over time, the percentage entry was calculated by comparison of the level of infection in PK treated cells to that of untreated cells.

To establish the PK-dependent escape kinetics of HCVcc, trypsinized Huh-7.5 cells were infected with JFH-1 or J6/JFH for 1 hr on ice, washed to remove unbound virus, and entry initiated by elevating the temperature to 37°C. At different time points thereafter, the cells were incubated with 50 μg/ml PK on

ice to remove non-internalized particles and re-plated in 24-well tissue culture plates. 48 hrs post infection, HCVcc infectivity was determined by enumerating NS5A-positive foci. J6/JFH internalized with a half-maximal entry rate ($t_{50\%}$) of 19 min., while JFH-1 internalization was 9 min. faster (Figure 3-15), suggesting that different HCV strains may internalize with different efficiencies. However, overall the HCVcc internalization kinetics for cells in suspension were comparable to the entry kinetics reported previously for adherent cells (278).

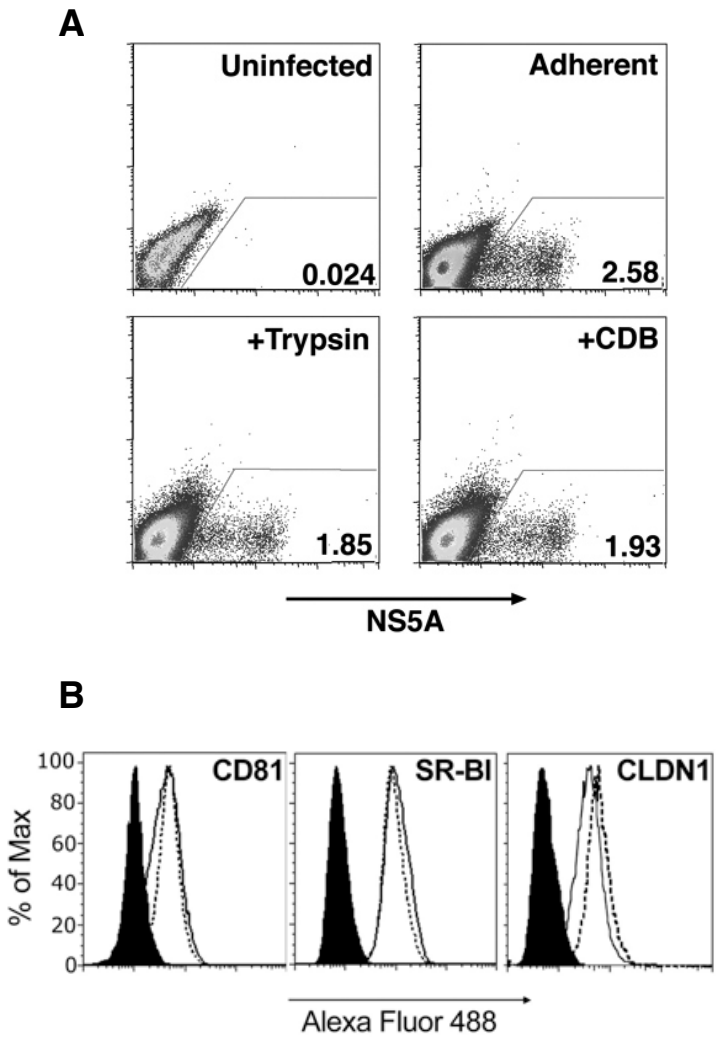

Figure 3-13 HCV infection of adherent and non-adherent Huh-7.5 cells.

A. Cells were treated with trypsin or an enzyme-free buffer (CDB) and infected with J6/JFH for 1 hr at 37°C. Cells were re-plated and viral infectivity measured by flow cytometry 48 hrs post infection. Values represent per cent infected cells of the total population. **B. Surface expression levels of CD81, SR-BI and CLDN1 in adherent (solid line) and trypsin-treated (dashed line) Huh-7.5 cells** were analyzed by flow cytometry. Species matched IgGs (black) were used as controls.

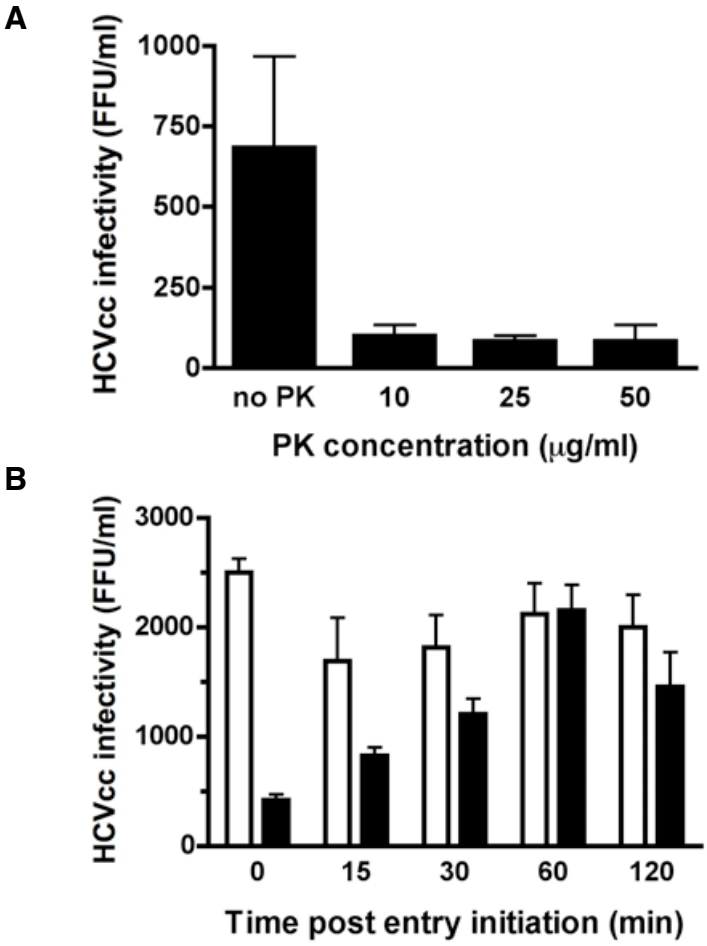

Figure 3-14 PK-mediated proteolysis of cell-bound infectious virus.

J6/JFH was pre-bound to non-adherent Huh 7.5 cells for 1 hr on ice. Thereafter, unbound particles were removed by washing. **A. Efficiency of proteolysis.** Cells were treated with 10, 25 or 50 μg/ml PK for 1 hr at 4°C to remove non-internalized particles. After which cells were re-plated and the number of infected cells determined at 48 hrs post infection. **B. PK mediated inhibition of HCV entry**. Cells were either treated with PK (black bars) on ice (0 min time point) or shifted to 37°C for 15 to 120 min, thereafter non-internalized particles were digested with PK for 1 hr on ice. Untreated cells (white bars) were used as controls.

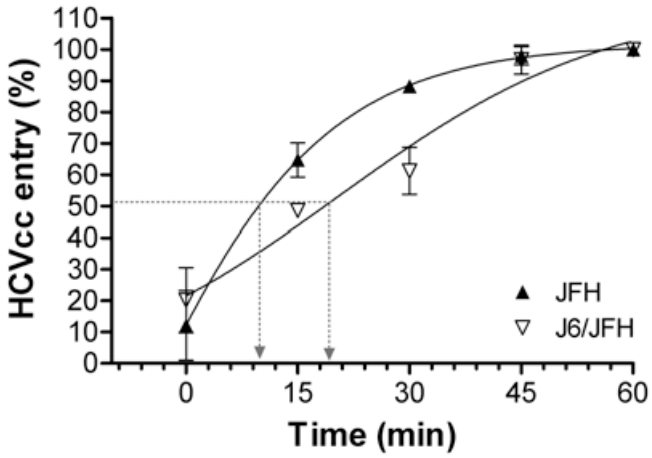

Figure 3-15 Time course of HCVcc sensitivity to proteolysis.

JFH-1 or J6/JFH was pre-bound to non-adherent Huh-7.5 cells for 1 hr on ice. Thereafter, unbound particles were removed by washing and entry initiated by shifting the temperature to 37°C. At the indicated time points, the cell suspension was treated with proteinase K for 1 hr on ice. Cells were re-plated and infected foci enumerated 48 hrs post infection. Per cent HCVcc entry were calculated relative to the 1h time point, values represent the combined data from 2 independent experiments performed in triplicate ± standard deviation; arrows indicate half maximal internalization.

Escape from neutralizing antibodies

Confluent cells support a higher level of HCV entry, concomitant with increased cell surface expression of CLDN1 and SR-BI. To elucidate whether the cell contact-mediated modulation of receptor expression promotes HCV internalization, we studied the kinetics of viral entry by monitoring the resistance of internalized virus to the neutralizing effect of antibodies (Figure 3-16). In this assay, virus is pre-bound to the cell surface at 4°C for 1 hr. Based on the assumption that internalized virus is resistant to neutralization, neutralizing antibodies (nAb) were added to the cells at different time points post entry initiation and infectivity enumerated 48 hrs post infection.

To establish a baseline, we measured the escape/internalization rate of JFH-1 and J6/JFH for Huh-7.5 cells plated at standard seeding density ($15x10^3$ cells/cm^2) from a neutralizing anti-E2 monoclonal antibody (C1). As described above, virus was adsorbed onto cells at 4°C for 1 hr, unbound particles were removed by washing thoroughly, and entry was initiated by elevating the temperature to 37°C. At different time points cell bound virus was neutralized by adding C1 and infectivity determined 48 hrs post infection. We noted that following C1 treatment, the number of infected cells reached a plateau at 2 hrs post entry initiation, indicating that 100% of bound virus was resistant to neutralization (Figure 3-17). In subsequent experiments data was expressed as per cent HCVcc entry and calculated by comparison of HCV infectivity in

nAb treated cells to the HCV infectivity measured at the 2h time point; half-maximal internalization rates were defined as 50% loss of inhibition ($t_{50\%}$).

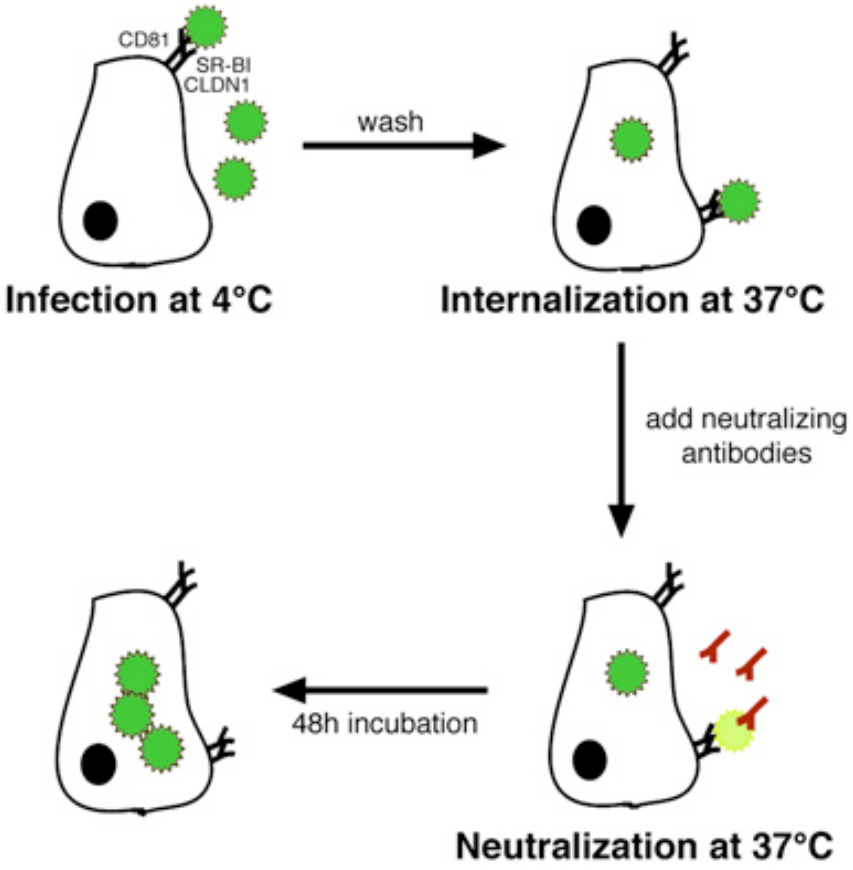

Figure 3-16 Neutralizing antibody (nAb) escape assay.

HCVcc was pre-bound to adherent Huh-7.5 cells on ice. Unbound particles were removed by washing and internalization initiated by elevating the temperature to 37°C. To block internalization, neutralizing antibodies were added at different time points post entry initiation. Infectivity was determined by counting NS5A-positive foci.

With ~23 min and ~18 min, respectively, JFH-1 and J6/JFH showed comparable half-maximal internalization rates at standard seeding density (Figure 3-18A). However, given that C1 was more efficient at neutralizing JFH-1 (~82% neutralization) than J6/JFH (~68% neutralization), JFH-1 was

used in further studies. To rule out the possibility that the observed entry kinetics were specific for the C1-mediated inhibition of E2-receptor interaction(s), we repeated the nAb escape assay using a mix of polyclonal human IgGs to neutralize cell-bound JFH-1 (Figure 3-18B). Again, the neutralizing efficacies of polyclonal IgGs (~83% neutralization) and C1 (~79% neutralization) were comparable. Similar internalization kinetics were observed after blocking infection with either antibody, with $t_{50\%}$ of ~16 min. (IgGs) and ~22 min. (C1), respectively, indicating that the observed viral entry kinetics at standard seeding density are not specific for the C1-mediated neutralization of JFH-1.

To study the effect of cellular contact on HCV internalization kinetics, the half-maximal entry times of JFH-1 were compared for sub-confluent and confluent Huh-7.5 cells. At sub-confluence, 50% of cell-bound particles became resistant to neutralization within ~30 min. post entry initiation (Figure 3-19). When cellular contact was established, the half-maximal entry time of JFH-1 was reduced to ~15 min., representing a significant acceleration of virus internalization during the early stages of the entry process ($p<0.031$; paired t-test). These data support the hypothesis that cellular contact promotes HCV internalization, presumably through the modulation of CLDN1 and/or SR-BI expression or other unidentified receptors such as occludin.

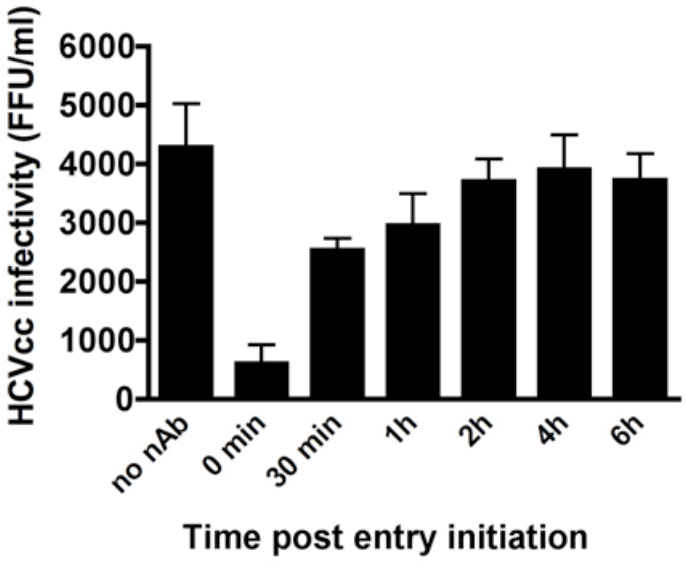

Figure 3-17 Neutralizing activity of anti-E2 nAb C1.

JFH-1 was adsorbed onto Huh-7.5 cells for 1 hr on ice, thereafter entry was initiated by elevating the temperature to 37°C. At different time points post entry initiation, virus infectivity was neutralized with an anti-E2 antibody (C1). Infectivity (foci forming units; FFU) reached a plateau approximately 2 hrs post entry initiation. Data is from a representative experiment performed in quadruplicate; error bars represent standard deviation.

A

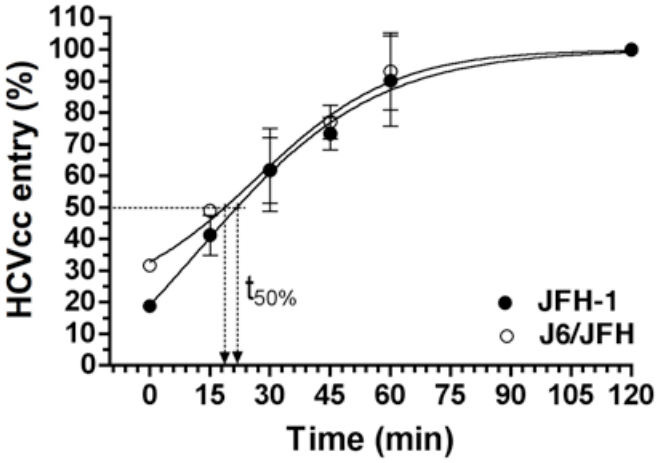

B

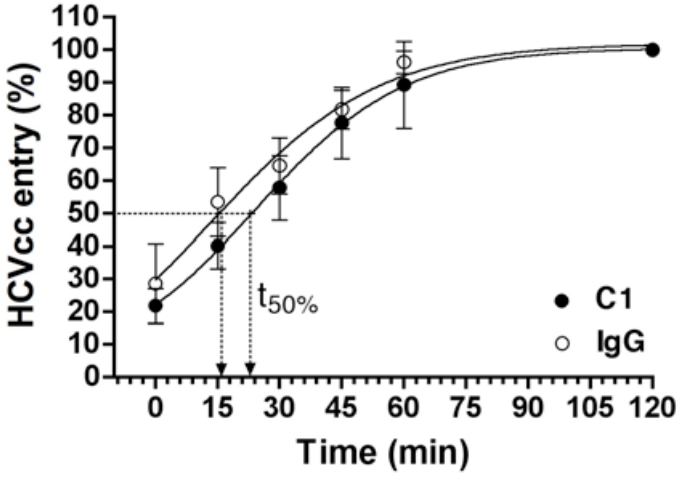

Figure 3-18 Time course of HCVcc sensitivity to antibody-mediated neutralization.

A. JFH-1 and J6/JFH internalization. Cells were infected with JFH-1 or J6/JFH for 1 hr on ice and entry initiated by elevating the temperature to 37°C. To neutralize infectivity, an anti-E2 antibody (C1) was added to the cells at the indicated time points. **B. Neutralization with anti-E2 antibody and polyclonal human IgG.** Huh-7.5 cells were infected with JFH-1 as described in (A). Viral infectivity was neutralized using an anti-E2 antibody (C1) or a mix of polyclonal human IgGs. Viral infectivity was enumerated 48 hrs post infection and per cent HCVcc entry calculated relative to the 2 hr time point (100% internalization); arrows indicate half maximal internalization ($t_{50\%}$). Values are the combined data from 3 independent experiments performed in triplicate; error bars represent standard deviation.

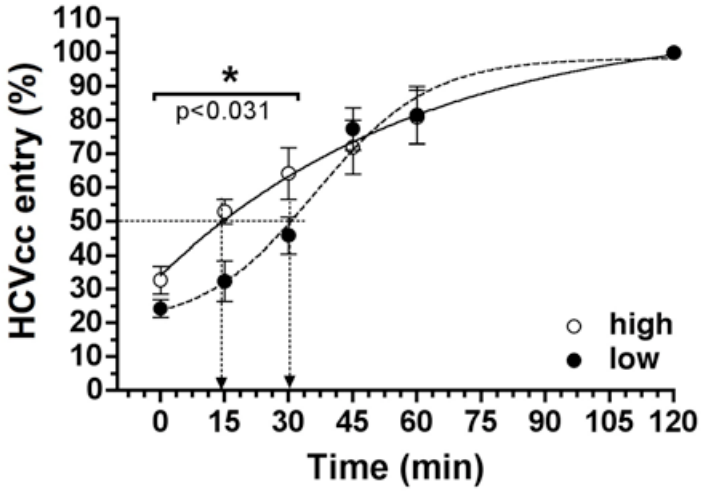

Figure 3-19 Modulation of HCVcc internalization kinetics with cell confluence.

Huh-7.5 cells were plated at low or high density and incubated with JFH-1 for 1 hr on ice. Post entry initiation, internalization was blocked with an anti-E2 antibody (C1) at the indicated time points. Infectivity was determined 48 hrs post infection, the per cent viral entry were calculated relative to the 2 hrs time point. Statistical analysis was performed as described in section 3.2.4. Values are the combined data of 2 independent experiments done in triplicate ± standard deviation.

3.2.4 Statistical analysis of internalization assays.

To ascertain whether the internalization kinetics for cells plated at low or high density were significantly different, we used a two-tailed paired t-test to compare the percentage entry at individual time points. When the mean values for all six time points (0 to 120 min) were compared, no significant difference between the two curves was detected. However, comparison of the mean values of individual time points showed a significant difference of the percentage entry at 15 and 30 min as summarized in Table 3-1.

A two-tailed paired t-test was also used to compare the internalization kinetics of parental and SR-BI and CLDN1 over-expressing cell lines.

	Two-tailed paired t-test			
Time points	**P value (two-tailed) < 0.05?**	**Correlation coefficient; r**	**P value (one-tailed)**	**Pairing significantly effective?**
0 – 120 min	0.1776	0.9194	<0.0001	Yes ***
15 – 30 min	0.031	na	Na	na

Table 3-1 Statistical analysis of HCVcc entry kinetics.

Comparison of the entry kinetics in sub-confluent and confluent cells with the two-tailed paired t-test following the guidelines in the GraphPad statistics handbook.

3.2.5 Defining the role of SR-BI and CLDN1 in HCV internalization.

The surface expression of SR-BI and CLDN1 is significantly increased at cell confluence. Likewise, HCVcc internalization is significantly accelerated in confluent cells during the early stages of the entry process when cellular

contact is established, suggesting a relationship between viral entry kinetics and the surface expression of CLDN1 and/or SR-BI. To assess the role of SR-BI and CLDN1 expression levels in HCV internalization, Huh-7.5 cells were transduced with lentiviral vectors to over-express human SR-BI or CLDN1 and viral internalisation kinetics determined by means of the nAb escape assay.

Flow cytometry confirmed 2 to 3-fold elevated CLDN1 and SR-BI surface expression levels in transduced Huh-7.5 cells (Figure 3-20). Furthermore, we did not observe any indirect effects of CLDN1 over-expression on SR-BI or CD81 levels, and *vice versa* (data not shown). Attempts to generate a Huh-7.5 cell line overexpressing CD81 failed, most likely because human hepatoma cells already express relatively high levels of CD81. LSCM analysis of receptor distribution in parental and tranduced cells demonstrated a cytoplasmic accumulation of SR-BI and CLDN1 (Figure 3-21) in the majority of over-expressing cells.

Quantification of receptor levels by linear profile plot analysis confirmed that a significant proportion of receptor molecules were retained intracellularly and receptor expression at the plasma membrane was only modestly increased. Similar observations were recently reported for HeLa and NIH3T3 cells, where ectopically expressed CLDN1 appeared to reside predominantly in intracellular vesicles (417).

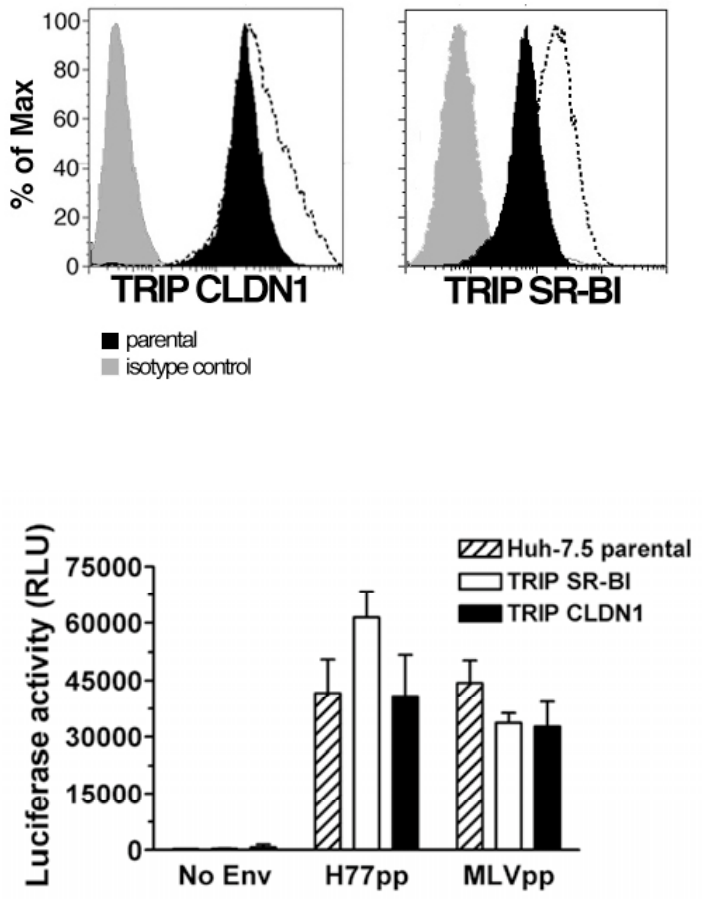

Figure 3-20 CLDN1 and SR-BI overexpression in Huh-7.5 cells.

A. Cells were transduced to overexpress human CLDN1 or SR-BI and receptor levels determined by flow cytometry. CLDN1 and SR-BI levels were up to 3-fold elevated in transduced (dashed lines) compared to parental cells (black). Species-matched irrelevant IgGs (grey) were used as controls. **B.** Transduced and parental cells were infected with HCVpp-H77, MLVpp, or envelope-defective pseudoparticles (NoEnv) for 1h and luciferase activity measured at 72h post infection.

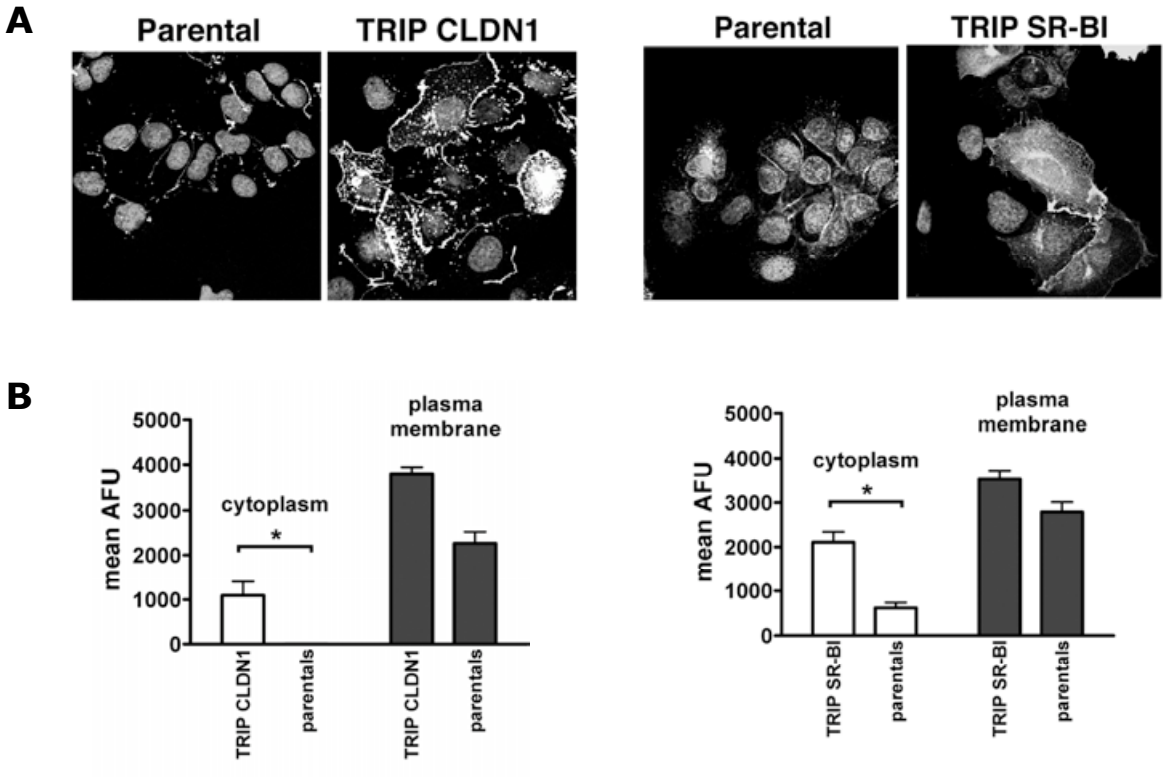

Figure 3-21 Localization of CLDN1 and SR-BI in transduced Huh-7.5 cells.

A. Parental and transduced cells were plated at standard seeding density on collagen-treated cover slips and 26 hrs post plating stained with antibodies specific for CLDN1 or SR-BI. **B.** Receptor expression levels at the plasma membrane and in the cytoplasm were determined by linear profile plot analysis, values are expressed as arbitrary fluorescence units (AFU); Background fluorescence was determined by staining with the secondary antibody only and was 36 AFU (TRIP CLDN1) and 27 AFU (TRIP SR-BI), respectively.

In accordance with published observation (159) high levels of SR-BI enhanced HCVpp infection ~ 1.5 fold, whereas high levels of CLDN1 failed to modulate HCVpp infectivity (Figure 3-20) in Huh-7.5 cells plated at standard density. Over-expression of CLDN1 or SR-BI also failed to enhance the infectivity of MLVpp, which were used as a negative control, confirming the enhancing effect of SR-BI on viral entry is HCV glycoprotein-specific.

To determine the effect(s) of CLDN1 and SR-BI over-expression on HCV internalization, transduced Huh-7.5 cells were plated at standard seeding density and the nAb escape kinetics of JFH-1 measured as described above. In support of the observation that high CLDN1 levels do not enhance HCVpp infection, CLDN1 over-expression failed to accelerate JFH-1 internalization Figure 3-22. In SR-BI overexpressing cells, on the other hand, JFH-1 internalization kinetics were significantly accelerated during the early entry stages with a half-maximal time ($t_{50\%}$) of 6 min (compared to $t_{50\%}$ = 15 min at cell confluence). Of note, the neutralizing efficacy of anti-E2 antibody C1 was markedly reduced in SR-BI overexpressing cells (~65% neutralization) compared to parental Huh-7.5 cells (~79% neutralization). In summary, these data highlight the crucial role of SR-BI in HCV entry and furthermore suggest that the receptor may be an important determinant of HCV internalization.

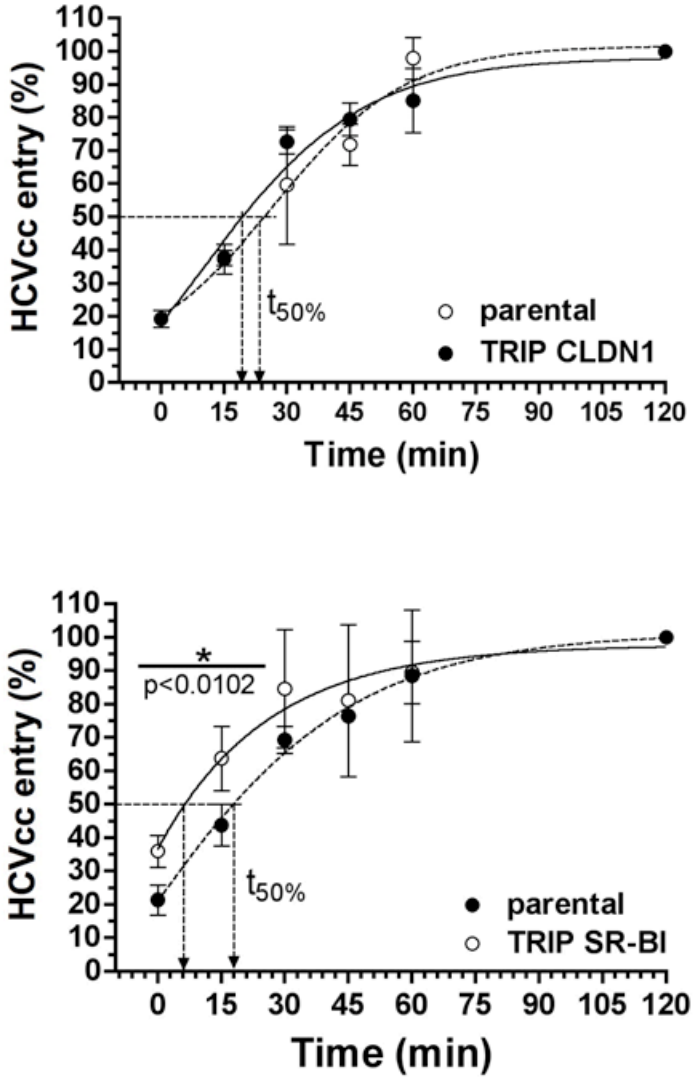

Figure 3-22 Effect of CLDN1 and SR-BI over-expression on the entry kinetics of JFH-1.

Huh-7.5 cells transduced to over-express CLDN1 or SR-BI were plated at standard seeding density and incubated with JFH-1 for 1 hr on ice. Entry was initiated by elevating the temperature to 37°C, thereafter infection was neutralized with an anti-E2 antibody (C1). NS5A-positive foci were enumerated 48 hrs post infection, and the percentage of C1-resistant particles calculated relative to the 2 hrs time point. Statistical analysis was perfomerd as described in section 3.2.4 .Values represent the means of 2 independent experiments ± standard deviation.

3.2.6 Discussion

The recent identification of CLDN1 (114) and occludin (OCLN) (326) as crucial HCV co-receptors alluded to the possible effect(s) of tight junction (TJ) formation and cell polarization on HCV entry, especially since polarized hepatocytes within the liver are thought to be the main reservoir of HCV replication. In our experience, the susceptibility of non-polarized Huh-7.5 hepatoma cells to HCVcc infection is dependent on cell seeding density. We also observed that in non-polarized hepatoma cells, the TJ proteins CLDN1, occludin and ZO-1 were enriched at cell junctions (95, 136), prompting us to investigate the role(s) of these 'TJ-like' structures in HCV entry. In this study, we demonstrate that cellular contact (i) modulates CLDN1 and SR-BI cell surface expression and distribution, (ii) promotes HCVpp and HCVcc infectivity, and (iii) enhances the rate of HCVcc internalization through an unknown mechanism(s).

CD81 and SR-BI surface expression levels are key determinants for HCV infectivity (159, 215); therefore, we sought to establish whether cellular contact affected the expression and/or localization of HCV entry receptors. Using confocal imaging and linear plot profile analysis we demonstrated that CD81 surface expression levels were comparable between sub-confluent and confluent cells and the protein was uniformly distributed in the plasma membrane with no detectable enrichment at cell-cell borders (Figure 3-8). Western blotting analysis of total cell lysates confirmed that CD81 protein

levels were unaffected by confluency status. Huh 7.5 cells express relatively high levels of CD81 and we presume that minor changes in CD81 expression may therefore be undetectable. Concomitantly, we were unable to increase CD81 surface expression using lentiviral vectors, suggesting that endogenous CD81 expression may be saturated in these cells. In contrast, we found that SR-BI and CLDN1 cell surface expression, but not intracellular forms, was significantly increased with cell confluence (Figure 3-8C). Western blotting analysis confirmed elevated SR-BI and CLDN1 protein levels in confluent cells (Figure 3-8D), whereas mRNA levels were unaffected by the confluency status (P. Balfe, unpublished observations), suggesting a post-transcriptional modulation of CLDN1 and SR-BI. A similar effect has been observed in human breast cancer cells constitutively expressing CLDN1, where protein levels at sub-confluence were low despite high CLDN1 mRNA levels (179). Likewise, the adaptor protein PDZK1, which is required for proper sorting and delivery of SR-BI to the plasma membrane (364, 365), has been shown to up-regulate hepatic SR-BI protein expression *in vivo* without affecting mRNA levels (212). These findings suggest that cellular contact induces a rapid translational regulation of CLDN1 and SR-BI mRNA, resulting in increased CLDN1 and SR-BI protein levels with possible consequences for HCV entry.

In addition to elevated CLDN1 and SR-BI surface expression levels, we observed that both receptors were enriched at cell junctions, an observation that was previously reported for CLDN1 in human, murine and canine tumour and non-tumour cell lines (136, 138, 179, 188, 223). In polarized epithelial

cells, surface expression of membrane proteins involves the sorting of proteins from the trans-Golgi network to the correct plasma membrane domains and anchoring and/or retention at the cell surface, followed by endocytosis, transcytosis or recycling (reviewed in (61). Delivery of proteins to the cell surface is mainly mediated by peripheral membrane (PDZ-domain) proteins, which interact with the C-terminal PDZ-ligand binding domains of membrane proteins including CLDN1 and SR-BI (190, 364). Potential interaction partners are the aforementioned SR-BI adaptor protein PDZK1, and the Zonula occludens (ZO) proteins -1 and -2, which localize to sites of cell-cell contact in sub-confluent cell cultures (206) where they facilitate assembly of tight junctions by directly interacting with CLDN1 and occludin (125, 190, 191, 297). The regulatory pathways involved in CLDN1 protein expression and targeting are not well understood. However, several studies suggest that mechanisms regulating membrane trafficking may be conserved between polarized and non-polarized cells and that all cells are principally equipped for polarized protein delivery (298, 403, 421).

To determine the effect of cell confluence on HCV entry, we studied the infectivity of HCVpp in Huh-7.5 cells plated at cell densities ranging from low (single cells) to high (intact monolayer) (Figure 3-9). HCVpp demonstrated a significant boost of luciferase activity at cell confluence, when cell-cell contact was established between most cells within the culture (Figure 3-11). In contrast, MLVpp infectivity was markedly enhanced at standard compared to low density, while the establishment of cellular contacts did not result in a

further increase in luciferase activity, indicating that the effect of cell density on viral entry was HCV glycoprotein-specific. The same enhancing effect was observed for HCVcc infection, with JFH-1 and J6/JFH infection increasing significantly when cellular contact was established (Figure 3-10). In our experience, prolonged inoculation promotes HCV infection (Figure 3-10 and Figure 3-11), suggesting that attachment and/or internalization are rate-limiting steps in the viral entry process. There is currently no evidence for a direct interaction between HCV particles or recombinant E1E2 glycoproteins with CLDN1 (114) and it is possible that CLDN1 may interact directly with CD81 or SR-BI, thus modulating E2-binding capacity, or the transport of virus-receptor complexes to membrane compartments permissive for virus internalization and fusion.

It is worth noting that HCV RNA replication and cell density are closely related in most human hepatoma cell lines. Within 48 hrs of reaching cell confluence, intracellular RNA levels can drop up to 20-fold in cells harbouring genomic replicons (352). Likewise, serum starvation markedly reduces RNA abundance, while cell cycle arrest reportedly has no effect on intracellular RNA levels, indicating that viral replication depends primarily on actively growing host cells (323, 352). A recent study by Nelson et al. (308) furthermore reports that confluence-mediated replicon inhibition can be reversed by supplying exogenous nucleosides, leading the authors to conclude that the diminished pools of endogenous nucleosides may be partly responsible for the decrease in HCV RNA in confluent cells.

Cellular contacts formed by CLDN1 probably promote HCV co-receptor interactions and/or the formation of specialized membrane domains amenable to the uptake of receptor-bound HCV particles (97). To determine whether cellular contact promotes the internalization of cell-bound HCVcc, we examined the ability of anti-E2 antibody to inhibit infection of sub-confluent and confluent cells when added at various times during entry. We noted that the inhibitory activity of an anti-E2 antibody was lost much earlier at cell confluence than sub-confluence (Figure 3-19), with half maximal inhibition being attained at 15 min and 30 min., respectively. Interestingly, the internalization kinetics in sub-confluent and confluent cells differed significantly during the first 30 min of the entry process and converged thereafter, suggesting that cellular contact modulates an early step in HCV entry.

It has previously been demonstrated that the inhibitory activity of anti-CD81 antibodies is lost approximately 17 min. post entry initiation (45, 114), while half-maximal HCV fusion requires 73 min. as determined by sensitivity to bafilomycin A (278) and a monoclonal anti-Flag CLDN1 antibody (114). However, in studies using antibodies against the extracellular loop of CLDN1 the viral internalization kinetics were comparable to those measured in anti-CD81 antibody escape experiments (Dr. Thomas Baumert, SA Texas HCV Meeting). In non-adherent (i.e. cell-contact deprived) Huh-7.5 cells, the inhibitory activity of proteinase K was lost approximately 19 min post entry initiation (Figure 3-15). These data were comparable to the escape kinetics

measured in 60% confluent adherent cells in the presence of an anti-E2 antibody (Figure 3-18).

To further dissect the roles of SR-BI and CLDN1 in the cell contact-mediated modulation of HCV entry, we studied HCVcc internalization kinetics in sub-confluent Huh-7.5 cells transduced to over-express SR-BI or CLDN1. Overexpression of CLDN1 failed to accelerate virus internalization (Figure 3-22). This might be due to (i) a large proportion of CLDN1 being retained in the cytoplasm in transduced cells (Figure 3-21), which may hinder the formation of functional virus-receptor complexes; (ii) efficient internalization requiring the interaction of CLDN1, CD81 and SR-BI, in which case the co-receptors would likely have to be expressed at equally high levels to exert an enhancing effect; (iii) both CLDN1 and OCLN being required for efficient internalization, which might explain why high levels of CLDN1 failed to enhance internalization in sub-confluent cells, where TJ protein levels are naturally low. Since SR-BI over-expression significantly enhances HCVpp infectivity despite the large proportion of intracellular retained molecules (Figure 3-22), we concluded that the amount of SR-BI cell surface protein was sufficient to enhance infection and that the intracellular forms of the protein may be functional.

CLDN1 on the other hand may have to be localized to the plasma membrane to promote viral entry. Two studies recently proposed that the specific localization of CLDN1 to TJ might play a crucial role in the regulation of HCV

cellular tropism (249, 417). Indeed, ectopic expression of CLDN1 in $CD81^+$/$SR\text{-}BI^+$ cell lines does not necessarily confer susceptibility to HCV infection (114), possibly because a large proportion of CLDN1 is retained in intracellular vesicles. Furthermore, the disruption of TJ-enriched CLDN1 by TNFα treatment markedly reduces the susceptibility of Huh7.5.1 cells to HCV infection (417), suggesting that the protein may have to be localized to the cell surface to allow functional virus-receptor and/or receptor-receptor interactions.

Overexpression of SR-BI accelerated the entry of cell-bound JFH-1 in a manner similar to that observed for confluent cells (Figure 3-22), suggesting a crucial role for SR-BI in HCV internalization. In addition, high levels of SR-BI, but not CLDN1, reduced the neutralizing efficacy of an anti-E2 antibody, lending support to a model of HCV entry where CD81 and SR-BI interact directly with virus particles, while CLDN1 faciliates internalization via interaction with SR-BI and other co-receptors (reviewed in (171, 290)). We presume that CLDN1 and SR-BI/CD81 have to interact to allow efficient uptake of bound particles and that high surface expression of at least SR-BI is crucial to promote internalization.

In sub-confluent cells, CLDN1 protein levels are low and plasma membrane expression virtually undetectable. Over-expression of SR-BI increases these cells' susceptibility to infection i.e. the efficiency of virus-receptor interactions as well as the efficiency of virus internalization.

CD81, SR-BI and CLDN1 co-localize in normal and HCV-infected liver and also in various liver-derived cell lines (164, 335, 417) and have to be in close proximity to allow efficient viral cell entry (164), which supports the hypothesis of a receptor-complex.

It is noteworthy that Coxsackievirus B virus utilizes TJ associated proteins to enter target cells (43) through binding to its primary receptor, decay accelerating factor (DAF), on the basolateral surface of epithelial cells. DAF binding is followed by lateral migration of the virus-receptor complex to the TJ and subsequent interaction with CAR co-receptor in a OCLN-dependent fashion (95). Similarly, HCV may interact with SR-BI, either directly or through HCV-associated lipoproteins, and subsequently with CD81, followed by lateral migration of the virus-receptor complex to the TJ and CLDN1/OCLN-mediated endocytosis and fusion (reviewed in (171).

3.3 HCV induced alterations of tight junction protein expression and localization

3.3.1 HCV infection modulates expression and localization of the tight junction protein CLDN1.

We previously observed that Claudin-1 (CLDN1) expression is increased in HCV infected liver (335), suggesting direct and/or indirect effect(s) of HCV on TJ protein expression. These findings are in line with recent studies demonstrating the modulation of TJ protein expression by RNA viruses such as HIV-1 (19, 200) and West Nile virus (405). To assess the effect of HCV infection on CLDN1 expression *in vitro*, Huh-7.5 cells were infected with high titer JFH-1 over night. Since previous studies showed (see chapter 3.2) that cellular contact modulates CLDN1 expression, infected and naïve cells were re-seeded at 60% confluence the day before harvesting to minimize cell density associated effect(s). 72h post infection, cells were harvested in RIPA buffer and defined amounts of protein separated by SDS PAGE. Immunoblotting showed markedly increased CLDN1 levels in JFH-1 infected total cell lysates, whereas CD81 levels were comparable between naïve and infected cells (Figure 3-23A).

To determine whether HCV infection modulates CLDN1 localization, JFH-1 infected and subgenomic replicon (SGR) bearing cells were stained for CLDN1 and CD81 expression and analyzed by laser scanning microscopy (LSCM) (Figure 3-23B). This allowed us to assess whether expression of only

the non-structural proteins was sufficient to modulate TJ protein localization. In naïve and SGR bearing cells, the majority of CLDN1 localized to the plasma membrane. However, in JFH-1 infected cells, which express the structural and non-structural viral proteins, CLDN1 localized to the plasma membrane and intracellular vesicular locations, whereas CD81 staining was unaltered and comparable to naïve and SGR cells. The intracellular dot-like accumulation of CLDN1 was also observed for another HCV strain, J6/JFH (data not shown). Together these findings suggest that the structural viral proteins, core-E1E2-p7, modulate CLDN1 localization in Huh-7.5 cells.

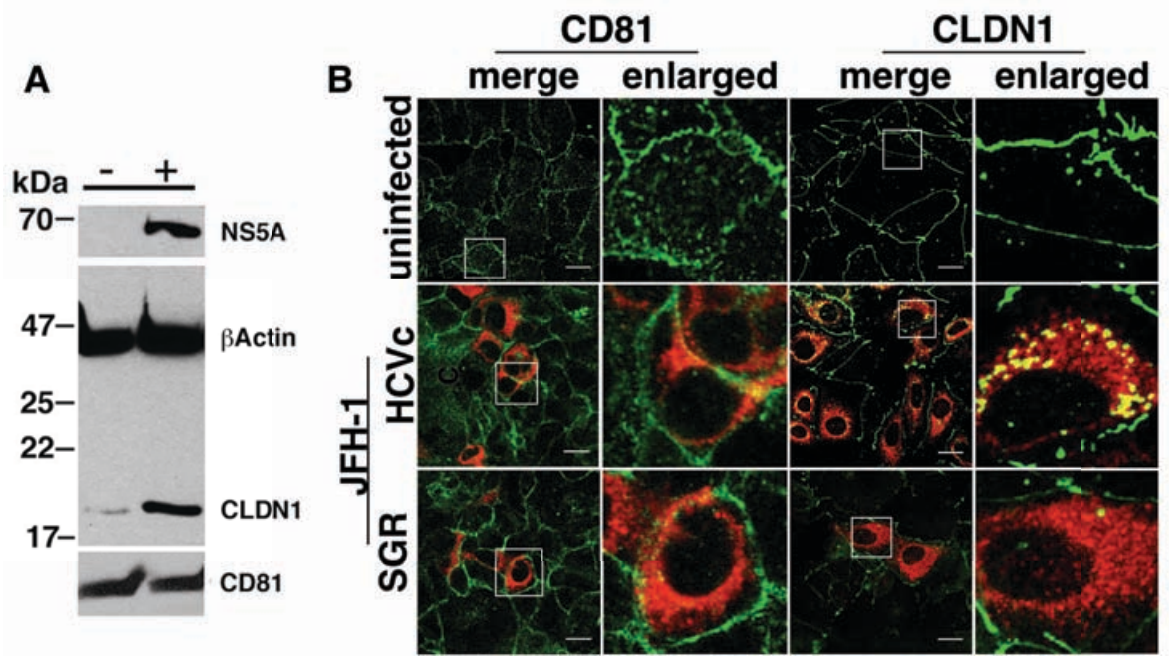

Figure 3-23 JFH-1 modulates CLDN1 expression and localization.

A. 0.5 μg of naïve and JFH-1 infected Huh-7.5 cell lysates obtained from a 95% NS5A positive culture were separated by SDS PAGE under reducing (CLDN1, NS5A) or non-reducing (CD81) conditions and probed for NS5A, CLDN1 and CD81; β–Actin was used as a loading control. **B.** CLDN1 (green) and CD81 (green) localization in naïve, JFH-1 infected, and subgenomic replicon (SGR) bearing Huh-7.5 cells. Cells were plated at equal densities on collagen-treated cover slips and fixed 24 hrs post plating. Viral protein was visualized by staining with an anti-NS5A antibody (9E10; red). LSCM images were obtained using a 63x 1.2NA objective (scale bars represent 20 μm).

3.3.2 JFH-1 infection modulates localization of OCLN and ZO-1

To assess whether HCV infection alters the localization of other tight junction proteins, we investigated the localization of occludin (OCLN) and ZO-1 in JFH-1 infected cells at 48 and 72 hrs post infection. Dual staining of infected cells for NS5A and CLDN1, OCLN and ZO-1, demonstrated a redistribution of all three TJ proteins to the cytoplasm as early as 48 hrs post infection (Figure 3-24), with ZO-1 and OCLN forming dot-like structures similar to those observed for CLDN1. As the number of infected cells within the culture increased over time this redistribution became more marked, with 70% of JFH-1 infected cells showing an intracellular accumulation of TJ proteins at 72 hrs post infection.

To determine whether the cytoplasmic forms of CLDN1, OCLN and ZO-1 localize to the same vesicular compartments, JFH-1 infected Huh-7.5 cells were co-stained for CLDN1 and OCLN or ZO-1 and analyzed by confocal microscopy. Since it was not possible to simultaneously stain cells for two TJ proteins and NS5A, the level of infection was determined separately by enumerating NS5A positive cells; the HCV infectivity obtained was 60-70% in two independent experiments. As expected, CLDN1 co-localized with OCLN and ZO-1, respectively, at cellular junctions (Figure 3-25). We observed partial co-localization of intracellular TJ protein forms. However, it is worth noting that intracellular forms of CLDN1 were present in the majority of cells within the culture, whereas OCLN and ZO-1 relocalization occurred less frequently and not necessarily in conjunction with CLDN1.

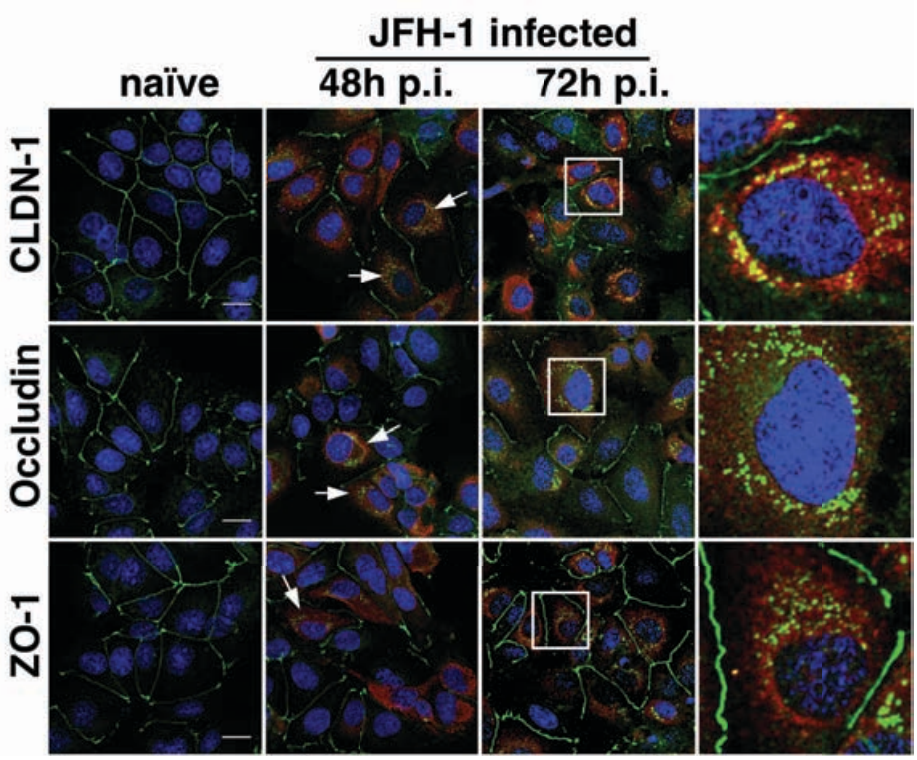

Figure 3-24 JFH-1 infection modulates CLDN1, occludin, and ZO-1 localization.

Naïve and JFH-1 infected Huh-7.5 cells were plated on collagen-treated cover slips and stained for NS5A (TRITC; red) and either CLDN1, occludin or ZO-1 (Alexa Fluor 488; green) at 48 and 72 hrs post infection. Nuclei were counterstained with DAPI (blue) and LSCM images obtained with a 63x 1.2NA objective (scale bars represent 20 μm). The boxed areas on the images obtained at 72 hrs are enlarged to show details of the intracellular staining pattern.

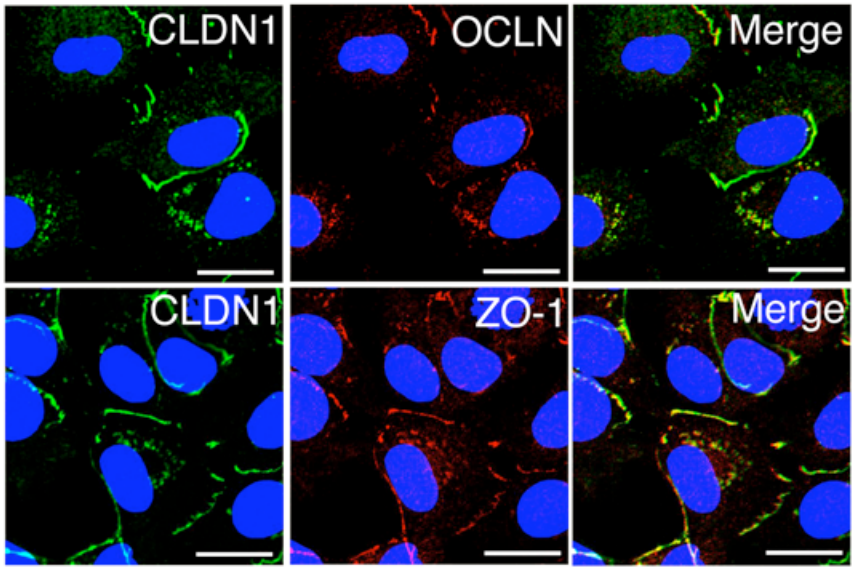

Figure 3-25 Co-localization of TJ proteins in HCV infected Huh-7.5 cells.

Cells from a 90% JFH-1 infected culture were seeded at equal density prior to analysis. TJ proteins were visualized by staining with mouse anti-CLDN1 (Abnova), and rabbit anti-OCLN and anti-ZO-1 antibodies; bound antibodies were detected with Alexa Fluor 488 (green) and Alexa Fluor 594 (red), respectively. LSCM images of single 1 μm Z sections were obtained with a 63x 1.2NA objective. Images are enlarged to show details of TJ protein localization (scale bars represent 20 μm).

3.3.3 CLDN1 localizes to an unknown intracellular compartment in HCV infected cells

The envelope proteins E1 and E2 are actively retained in the endoplasmic reticulum (ER) during replication (109, 112), where they interact with viral proteins such as core (250, 255) and NS2 (269, 353), and a number of host proteins such as calnexin and calreticulin (83). A modulation of CLDN1 localization was not observed in cells expressing subgenomic replicons (Figure 3-23), leading us to speculate that the structural viral proteins may be involved in the relocalization of CLDN1. Since the viral glycoproteins are localized to the ER, we sought to define the intracellular localization of CLDN1 in JFH-1 infected cells. CLDN1 showed no detectable colocalization with early endosomes (EEA1), late endosomes (Lamp1), the Golgi matrix protein GM130, or the Golgi-ER intermediate compartment (ERGIC53). These data suggest that intracellular CLDN1 is not retained in the ER and may localize to an unknown cytoplasmic storage compartment (192). In line with these observations, CLDN1 failed to co-localize with the HCV structural proteins E2 (C1) and core (JM122) in JFH-1 infected cells (Figure 3-27).

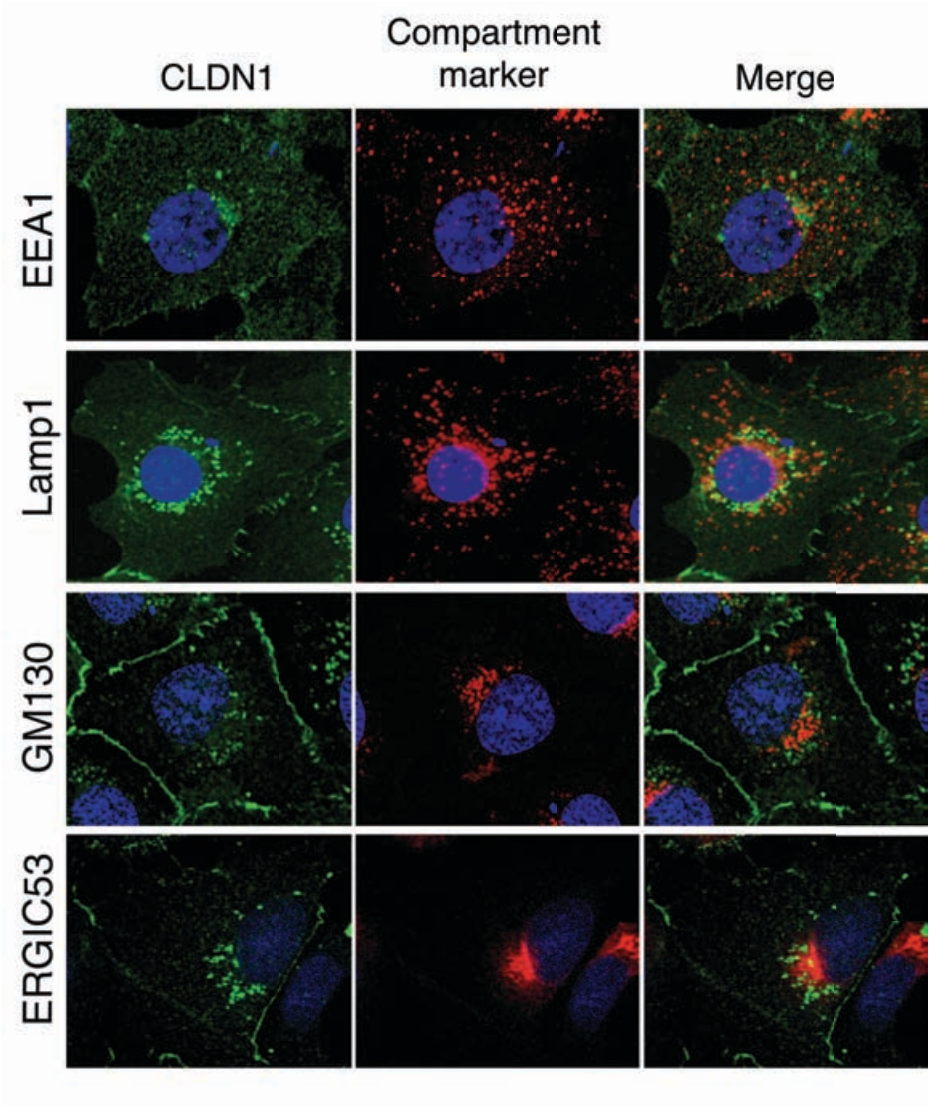

Figure 3-26 Localization of intracellular CLDN1 in HCV infected cells.

JFH-1 infected cells from a 90% NS5A positive culture were grown on collagen-treated glass cover slips and stained with antibodies specific for CLDN1, early endosomes (EEA1), late endosomes (Lamp1), Golgi matrix protein (GM130), and the Golgi-ER intermediate compartment (ERGIC53), at 72h post infection. Bound antibodies were visualized using an Alexa Fluor 488 anti-rabbit conjugate (CLDN1; green) and a TRITC anti-mouse IgG conjugate (compartment markers; red). Nuclei were counterstained with DAPI (blue) and LSCM images of single 1μm Z-sections obtained using a 63x 1.2NA objective. Representative enlarged images of single cells are shown.

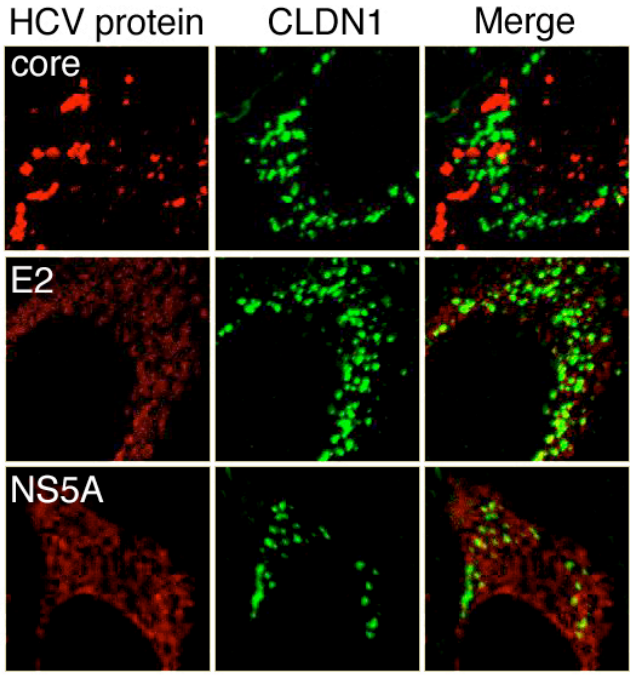

Figure 3-27 Co-localization of CLDN1 and HCV proteins.

JFH-1 infected cells were plated on collagen-treated cover slips and co-stained for CLDN1 (Alexa Fluor 488; green) and core (JM122; Alexa Fluor 594; red), E2 (C1; red) or NS5A (9E10; red). LSCM images of 1 μm Z sections were obtained at 63x magnification and enlarged for better visualization of protein localization.

3.3.4 Relocalization of TJ proteins in Huh-7.5 cells is cytokine-independent and requires infection with HCV

The disassembly and internalization of epithelial TJ is a rapid process that can be induced in response to pathophysiological stimuli such as oxidative stress (36) and pro-inflammatory cytokines (125, 163). Several studies have demonstrated that IFNγ and TNfα down-regulate the expression of TJ proteins in epithelial and endothelial cell lines (265, 422). Furthermore, IFNα has been shown to induce the internalization of TJ proteins in epithelial cells (62). Schmitt et al. recently reported that VEGF induces the disruption of hepatocellular TJ (351). Recent reports have furthermore demostrated that HCV gene expression induces VEGF expression (198, 303) and in line with these observations we found that HCV infection increases VEGF secretion in HepG2 and, to a lesser extent, in Huh-7.5 cells (Dr. Christoper Mee, manuscript in preparation).

To assess whether the intracellular accumulation of TJ proteins in HCV infected Huh-7.5 cells is mediated by cytokines, naïve Huh-7.5 cells were incubated with IFNγ, TNFα or recombinant $VEGF_{165}$ (isoform 165) for 48 hrs. Thereafter, cells were stained for CLDN1, OCLN and ZO-1 and analyzed by LSCM (Figure 3-28). Stimulation with either cytokine had no effect on TJ protein distribution, indicating that the intracellular accumulation of CLDN1, OCLN and ZO-1 is associated with HCV infection or may be mediated by unknown cellular factors.

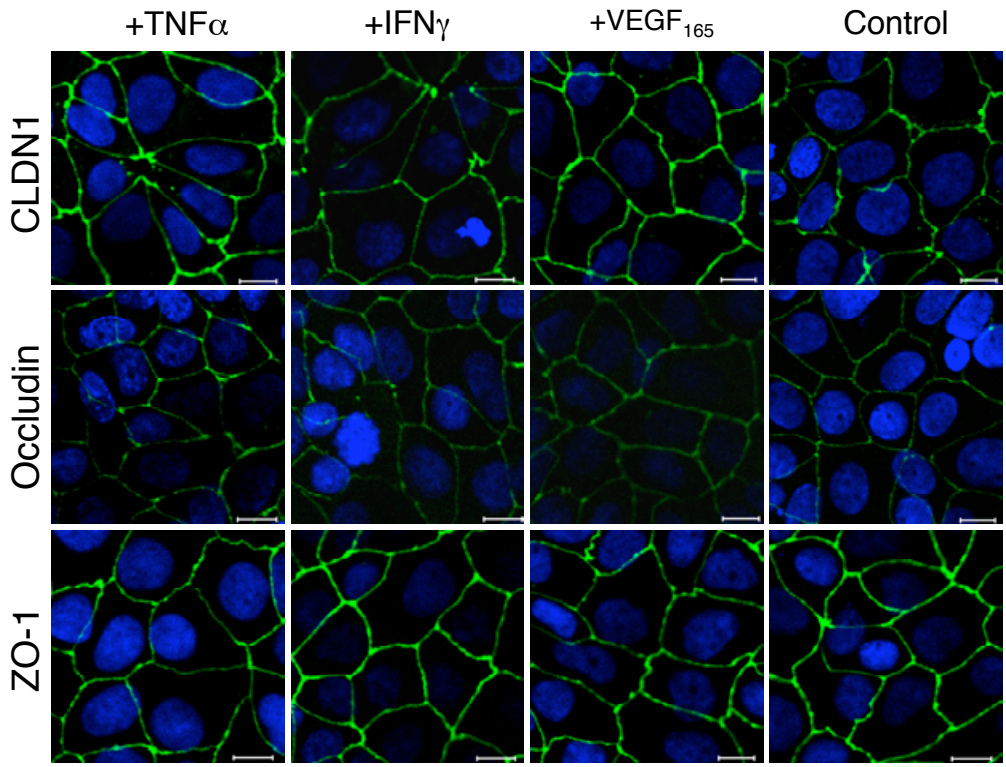

Figure 3-28 Effect of cytokines on TJ protein distribution.

Naïve Huh-7.5 cells were seeded at equal density on collagen-treated cover slips and treated with 1 ng/ml TNFα, 100 U/ml IFNγ or 500 ng/ml $VEGF_{165}$ for 48 hrs. Untreated cells were used as a control. TJ proteins (Alexa Fluor 488; green) were visualized with the respective antibodies and LSCM images taken with a x63 1.2NA objective (scale bars represent 20 μm).

Our data suggests that HCV infection induces the localization of TJ proteins to intracellular vesicles. To confirm this, Huh-7.5 cells were infected with JFH-1 and non-internalized virus particles removed 24 hrs post infection by washing thoroughly. 72 hrs post infection the conditioned culture media from these cells was collected and cleared by centrifugation to remove cell debris. Naïve Huh-7.5 cells were inoculated with the conditioned media for 72 hrs in the presence of an anti-CD81 monoclonal antibody (2s131) to block HCV infection or an anti-VEGF antibody (VG76e) to neutralize the effects of VEGF (Figure 3-29). Dual staining for CLDN1, OCLN and NS5A demonstrated intracellular TJ protein localization in the cell cultures treated with conditioned media with or without VG76e. However, neutralization of virus infectivity with anti-CD81 ablated the effect(s) on TJ protein localization. Furthermore, intracellular forms of CLDN1 were only observed in NS5A positive cells, whereas adjacent cells were unaffected. Together, these findings suggest HCV-dependent, VEGF-independent mechanism(s) of TJ protein relocalization.

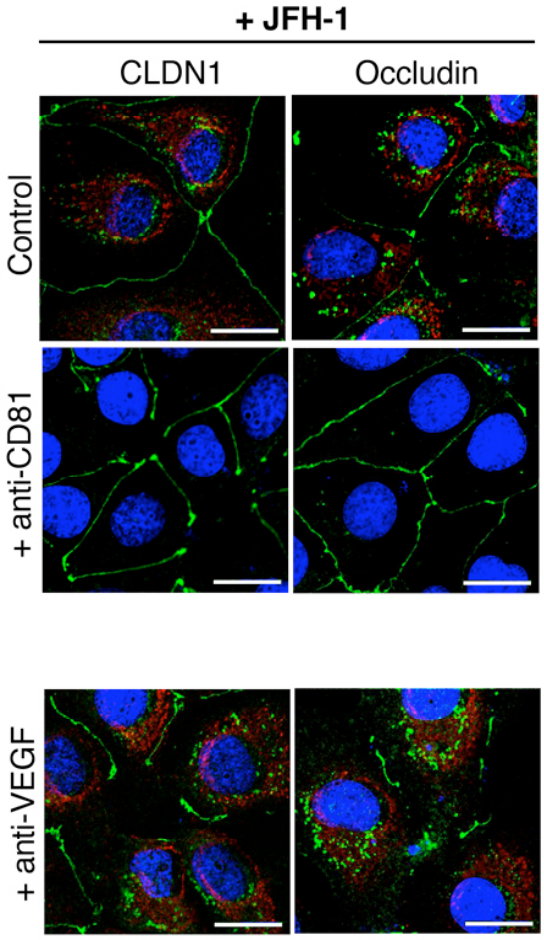

Figure 3-29 CLDN1 relocalization is associated with HCV infection.

Naïve Huh-7.5 cells were treated with conditioned media collected from a JFH-1 infected cell culture in the presence of anti-CD81 (2s131) or anti-VEGF (VG76e) antibodies. Cells incubated with conditioned media only were used as a control. Following 72 hrs incubation cells were stained for CLDN1 (Alexa Fluor 488; green) and NS5A (TRITC; red), nuclei were counterstained with DAPI (blue). LSCM images were taken with a 63x 1.2NA objective and enlarged for better visualization of CLDN1 staining (scale bars represent 20 μm).

3.3.5 HCV glycoproteins mediate CLDN1 and OCLN relocalization in infected cells

Cells supporting genomic HCV replication demonstrate a redistribution of CLDN1 to the cytoplasma, whereas hepatoma cells supporting subgenomic replicons encoding only the non-structural proteins fail to induce this relocalization (Figure 3-23). To assess the effect(s) of the viral glycoproteins on TJ protein localization we transfected Huh-7.5 cells with constructs encoding the JFH-1 (genotype 2a) structural proteins E1 and E2. Staining with a monoclonal antibody specific for E2 (C1) revealed a diffuse staining pattern of JFH-1 reminiscent of the endoplasmic reticulum (ER) (Figure 3-30). 24% and 16% JFH-1 E1E2 positive cells showed an intracellular accumulation of CLDN1 and OCLN, respectively, while no relocalization was observed for ZO-1 (data not shown). In contrast, all three TJ proteins localized exclusively to the plasma membrane of mock-transfected cells. These data suggest that the redistribution of CLDN1 and OCLN observed in infected cells may in part be mediated by the HCV encoded glycoproteins. However, ZO-1 failed to recapitulate the phenotype seen with HCVcc, suggesting that additional factor(s) may be required. Attempts to co-precipitate the viral glycoproteins and CLDN1 were repeatedly unsuccessful, as previously reported (114). However, neither CLDN1 nor OCLN co-localized with E2 (Figure 3-30), suggesting that the proteins do not associate.

Since the structural region of the HCV genome is highly variable between genotypes, we sought to confirm the effect on TJ protein localization with

glycoproteins derived from a genetically diverse strain, H77 (genotype 1a). Intracellular CLDN1 and occludin were readily observed in 30% and 61% of H77 E1E2 positive cells, respectively (Table 3-2). The frequency of cells showing CLDN1 and occludin redistribution was significantly higher in H77 than in JFH-1 E1E2 expressing Huh-7.5 cells (Fisher's exact test, $p=0.0066$), indicating that glycoprotein diversity may have functional consequences for TJ protein localization and hepatocyte polarity.

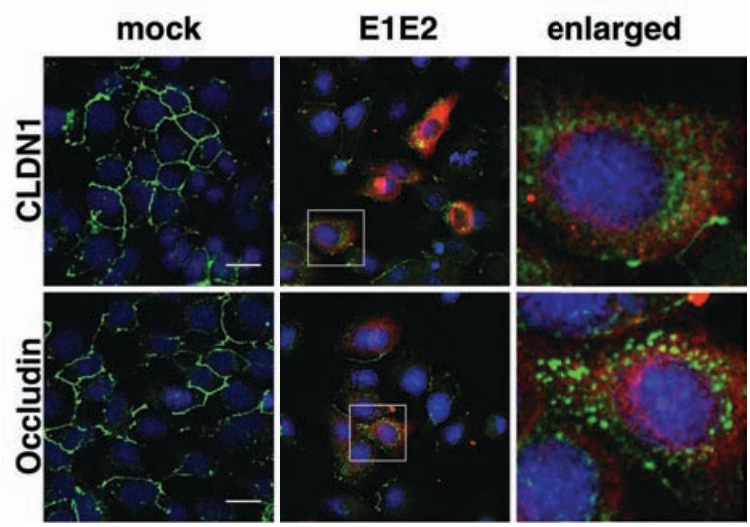

Figure 3-30 HCV glycoproteins induce CLDN1 and OCLN redistribution.

Huh-7.5 cells were transfected with constructs expressing JFH-1 glycoproteins E1E2 or an empty vector (mock) and co-stained for E2 (C1 mAb; Alexa Fluor 594; red) and either CLDN1 or occludin (Alexa Fluor 488; green); nuclei were counterstained with DAPI (blue). LSCM images of single 1mm Z-sections were obtained using a 63x 1.2NA objective (scale bars represent 20 μm). Boxed areas are enlarged to show details of E2 and TJ protein localization.

	Percent of E2 positive cells showing TJ protein redistribution	
E1E2 strain	**CLDN1**	**Occludin**
Mock	0	0
JFH-1	24	16
H77	30	61

Table 3-2 CLDN1 and OCLN relocalization frequency in E1E2 expressing cells.

Quantitative assessment of the frequency of transfected cells showing intracellular forms of CLDN1 or occludin (per 100 E1E2-positive cells).

3.3.6 CLDN1 localizes to a longer-lived storage compartment in HCV infected cells

To assess the effect(s) of HCV infection on the synthesis and degradation of CLDN1, HCV infected cells were treated with cycloheximide (CHX), which inhibits protein biosynthesis by blocking translational elongation. Naïve and JFH-1 infected cells were treated with 20 μg/ml of CHX and CLDN1 expression studied after 4, 8, and 12 hrs. There was no demonstrable change in protein expression following 8 hrs of CHX treatment. However, by 12 hrs CLDN1 expression was no longer detectable in naïve cells (Figure 3-31, left panel). Likewise, following a 12 hr treatment of JFH-1 infected cells CLDN1 expression at the plasma membrane was undetectable, however, the cytoplasmic forms were still visible, suggesting an extended half-life of the intracellular protein compared to the plasma membrane form(s) (Figure 3-31, middle panel). When naïve and JFH-1 infected Huh-7.5 cells were washed extensively following CHX treatment and new rounds of protein synthesis monitored after 1, 3, 6 and 9 hrs, newly synthesized CLDN1 was first detected after 9 hrs and localized to the plasma membrane in both naïve and infected cells (Figure 3-31, right panel). We hypothesize that in HCV infected cells CLDN1 is redistributed into a longer-lived intracellular compartment. Furthermore, our data suggests that the accumulation of CLDN1 in HCV infected cells is not the result of enhanced protein synthesis.

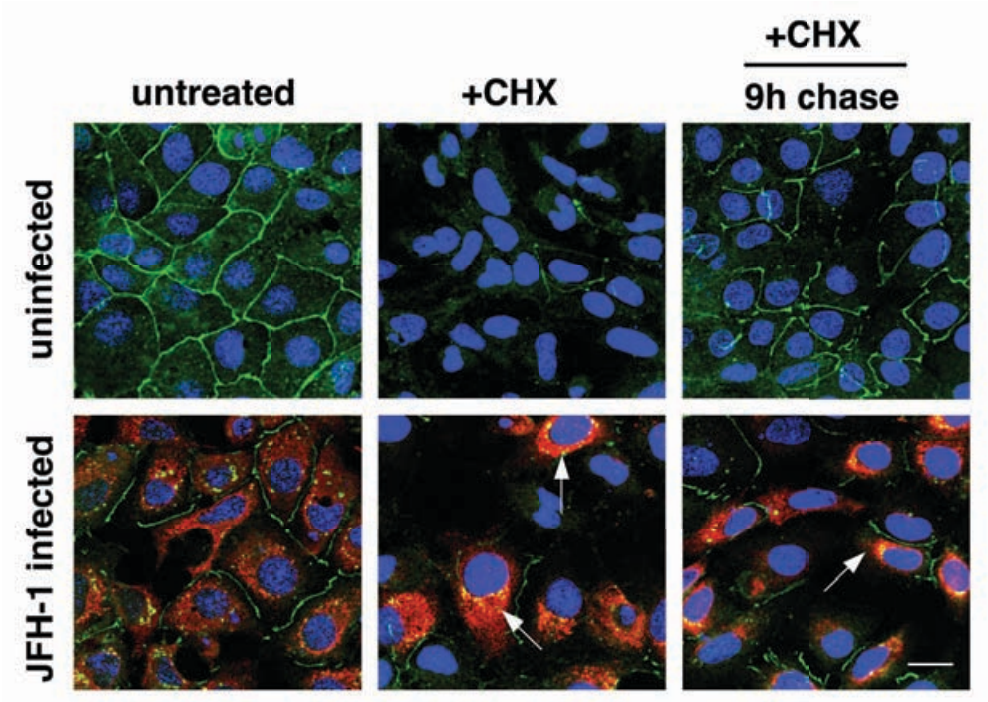

Figure 3-31 Increased half-life of intracellular CLDN1 in HCV infected cells.

72 hrs post infection JFH-1 infected cells were treated with 20 μg/ml cycloheximide (CHX) for 12 hrs. Following treatment, cells were either fixed immediately (middle panel) or washed thoroughly and incubated for a further 9h (right panel). Cells were co-stained for CLDN1 (Alexa Fluor 488; green) and NS5A (TRITC; red) Nuclei were counterstained with DAPI (blue) and LSCM images obtained using a 63x 1.2NA objective (scale bar represents 20 μm). Areas in the treated cells where intracellular CLDN1 expression persists in association with NS5A are annotated with arrows.

To assess whether intracellular forms of CLDN1 are retained in proteasomes, we treated infected cells with ALLN (Calpain inhibitor-I), a well-described proteasome inhibitor (283, 357, 409), the hypothesis being that the inhibition of proteolysis will result in the accumulation of CLDN1 if the protein indeed resides in proteasomes. Huh-7.5 cells were infected with JFH-1 and 24 hrs post infection incubated with 10 μg/ml ALLN for 24 hrs. Thereafter, cells were fixed and CLDN1 distribution in naïve and infected cells analyzed by confocal microscopy (Figure 3-32). No significant protein accumulation was observed in naïve cells, suggesting that CLDN1 degradation is proteasome-independent. Likewise, ALLN treatment had no visible effect on the level of intracellular protein in JFH-1 infected cells, lending support to the hypothesis that CLDN1 is retained in a long-lived storage compartment of unknown origin.

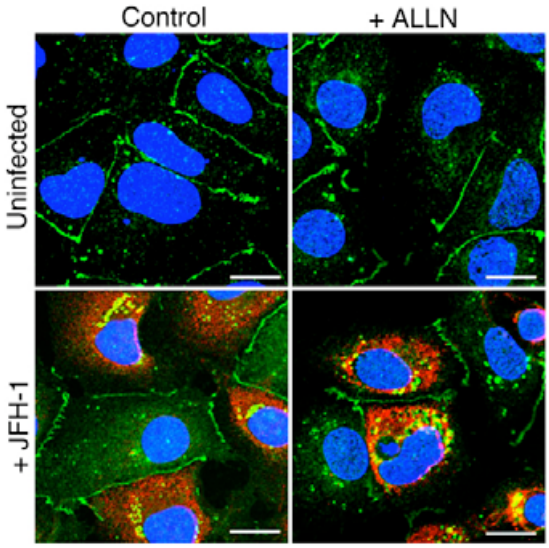

Figure 3-32 Effect of proteasome inhibition on CLDN1 protein level.

24 hrs post infection, naïve or JFH-1 infected Huh-7.5 cells were treated with 36 μM ALLN for 24 hrs. Thereafter, cells were fixed and stained for CLDN1 (Alexa Fluor 488; green) and NS5A (TRITC; red). LSCM images were taken at 63x magnification (scale bars represent 20 μM).

3.3.7 Endocytosis of intracellular forms of CLDN1 in HCV infected cells

Recent reports have illustrated the dynamic nature of proteins within the TJ, with up to 50% of proteins redistributing from the TJ area within a 10 min period (356). For some TJ proteins including Claudins -1 and -4, OCLN and ZO-1 internalization from the plasma membrane has been shown to occur via a clathrin-mediated process (192).

To ascertain whether the accumulation of intracellular CLDN1 forms in HCV infected Huh-7.5 cells is due to enhanced internalization from the plasma via clathrin-mediated endocytosis, we first attempted the pharmacological inhibition of this pathway using chlorpromazine. However, following 4 to 12 hrs incubation with 15 to 30 μM chlorpromazine we observed intracellular accumulation of CLDN1 in naïve and infected cells (data not shown), suggesting unspecific side-effects of the inhibitor. To circumvent this problem, transfection experiments were carried out using a dominant negative EPS15 construct (EPS15-GFP) to inhibit clathrin-mediated endocytosis. In these experiments, JFH-1 infected Huh-7.5 cells were transfected with EPS15-GFP expression plasmids and CLDN1 localization analyzed by LSCM 72 hrs post infection (i.e. 24 hrs post transfection) (Figure 3-33). EPS15-GFP expression was monitored by flow cytometry 24 hrs post transfection, confirming a 15-20% transfection efficiency GFP in two independent experiments. To test the ability of the EPS15 mutant to inhibit clathrin-mediated endocytosis, we monitored the internalization of fluorescently labelled transferrin from the cell

surface. We found that expression the uptake of transferring was 50% reduced in GFP positive cells (Dr. Jennifer Timpe, unpublished observations).

Due to the construct already being GFP-tagged, it was not possible to co-stain the cells for CLDN1 and NS5A, therefore, HCV infectivity was determined separately by counting NS5A positive cells. In two independent experiments, 70% infectivity and 15-20% transfection efficiency were obtained (Figure 3-33A). Also, staining of transfected cells for NS5A showed that expression of the EPS15-GFP construct did not interfere with HCV protein expression. Overall, we did not observe cytoplasmic accumulation of CLDN1 in JFH-1 infected cells expressing EPS15-GFP, whereas intracellular forms of CLDN1 were readily observed in untransfected JFH-1 infected cells (Figure 3-33B). These findings suggest that internalization events may be involved in the accumulation of the TJ proteins to vesicular compartments.

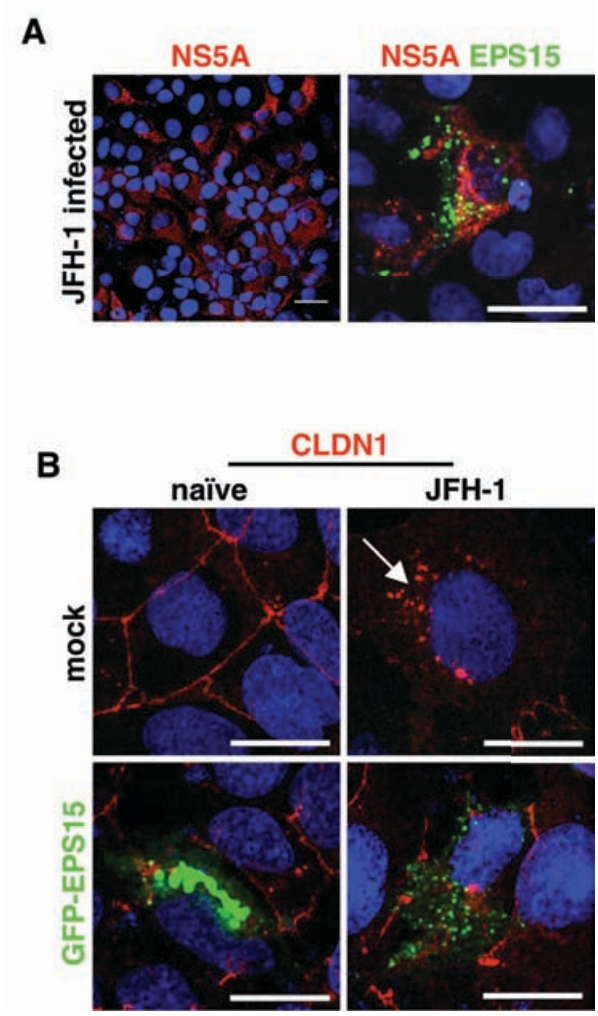

Figure 3-33 CLDN1 localization in HCV infected Huh-7.5 cells following inhibition of clathrin-mediated endocytosis.

A. JFH-1 infected Huh-7.5 cells were transfected with constructs encoding a GFP-tagged dominant negative EPS15 mutant (GFP-EPS15) 48 hrs post infection. 24 hrs post transfection, cells were stained for NS5A (Alexa Fluor 594; red) and the level of infection determined by counting NS5A positive cells. In two independent experiments, 70% infectivity was obtained (left panel). EPS15 expression (GFP; green) did not interfere with expression of viral proteins (right panel). LSCM images were taken at 40x magnification (scale bars represent 20 μm). **B.** Intracellular forms of CLDN1 (Alexa Fluor 594; red) were only observed in mock-transfected JFH-1 infected cells (upper right panel). A total of 50 cells were analyzed. LSCM images were obtained using a 63x 1.2NA objective and enlarged to show details of CLDN1 localization (scale bars represent 20 μm).

3.3.8 Discussion

In polarized cells, tight junctions limit the intra-membrane diffusion of molecules between the apical and basolateral membrane domains ('fence' function) and create a semi-permeable barrier between epithelial cells restricting diffusion of molecules through the intercellular space ('barrier' function). Hepatocyte polarity is crucial for liver functioning, with apical (canalicular) and basolateral (sinusoidal) cell surfaces performing specific tasks like the canalicular secretion of bile and the sinusoidal secretion of serum proteins, respectively. In this study we confirmed our earlier observation that CLDN1 expression is increased in HCV infected liver tissue (335). Furthermore, we demonstrate that the viral envelope glycoproteins can disrupt the localization of CLDN1 and other members of the tight junction (TJ) complex, with possible *in vivo* implications regarding the progression of liver disease in chronic hepatitis C.

In naïve Huh-7.5 cells, CLDN1 localizes predominantly to the plasma membrane with minimal intracellular staining (Figure 3-23), whereas in JFH-1 infected cells the protein shows a significant accumulation into dot-like perinuclear structures as early as 48 hours post infection (Figure 3-24). A similar intracellular staining pattern was observed for the tight junction (TJ) proteins ZO-1 and occludin (Figure 3-24). Interestingly, TJ protein redistribution was confined to $NS5A^{+}$ cells with no detectable perturbation of uninfected neighbouring cells. In line with this observation, conditioned

medium from JFH-1 infected cells failed to induce CLDN1 accumulation when HCV infection was inhibited with a monoclonal CD81-blocking antibody (Figure 3-29), implying that the effect(s) were not mediated by soluble diffusible factor(s). There was no detectable redistrubtion of CD81 from the plasma membrane as previously reported (400).

Increased epithelial permeability is characteristic for systemic and local inflammation and may be caused by bacterial and viral pathogens, respectively, or endogenous stimuli such as proinflammatory cytokines (202, 348). Interferon-γ (IFNγ) and tumor necrosis factor-α (TNFα) can cause the disruption of epithelial barriers (202, 348) (204, 346) and have been shown to increase the permeability – characterized by a decrease in transepithelial resistance (TER) and increased paracellular flux of solutes - across monolayers of various polarized cell lines (262, 266, 422). Both IFNγ and TNFα down-regulate OCLN expression in HT-29 cells (265). Likewise, IFNγ has been shown to decrease ZO-1 mRNA and protein levels in T84 cells (422) and to induce the internalization of epithelial TJ proteins into vesicular structures (62, 404). Another cytokine, vascular endothelial growth factor (VEGF), which regulates tumor angiogenesis, has been shown to down-regulate the expression of OCLN (351, 410) and ZO-1 (127) in endothelial cells, resulting in increased paracellular permeability (208). We hypothesized that the intracellular accumulation of TJ proteins in HCV infected cells may be mediated by cytokines, however, we found that CLDN1, OCLN and ZO-1

distribution was unaltered in Huh-7.5 cells treated with IFNγ, TNFα or VEGF (Figure 3-28).

Interestingly, TNFα is reportedly the central mediator of inflammation in hepatitis C (217) and elevated serum levels have been correlated with severity of fibrosis in HCV infected individuals (430). Indeed, viral NS3 protease reportedly induces TNFα production in HepG2 and Huh-7 cell lines (165), suggesting a link between HCV and the inflammatory processes in acute and chronic hepatitis C. Similarly, HCV gene expression induces stabilization of hypoxia-inducible factor 1α (HIF-1α) (303) and enhances androgen receptor-mediated transcriptional activity (198) thus stimulating the VEGF expression. Schmitt et al. recently reported that treatment of HepG2 cells with recombinant VEGF resulted in a loss of apical canalicular structures and a re-localization of OCLN, leading the authors to conclude that VEGF may promote hepatocellular metastasis within the liver (351). In accordance with these data we demonstrated that VEGF reduces TJ integrity in HepG2 cells (Dr. Christopher Mee, manuscript in preparation). Furthermore, HCV stimulated the secretion of VEGF in HepG2 and, to a lesser extent, in Huh-7.5 cells by stimulating the relocalization of OCLN (Dr. C. Mee, manuscript in preparation). In summary, these data establish a link between HCV gene expression, cytokine production and the development and progression of cirrhosis and fibrosis in hepatitis C.

Calcium-induced disassembly of adherent intracellular contacts in polarized epithelial cells involves endocytosis of TJ and AJ (adherens junction) proteins via a clathrin-mediated pathway (192). To test whether the intracellular forms of TJ proteins in HCV infected Huh-7.5 cells are trafficked from the plasma membrane, we attempted the pharmacological inhibition of clathrin-mediated endocytosis and immunofluorescence analysis of TJ protein localization. No visible effect(s) on TJ protein localization were observed when infected Huh-7.5 cells were treated with 15 μM chlorpromazine over a 4 hour-period (data not shown). The use of a higher chlorpromazine concentration resulted in cell detachment, whereas prolonged treatment time(s) led to a significant intracellular accumulation of TJ proteins and induced severe changes in cell morphology (data not shown). Moreover, the cytoplasmic accumulation of TJ proteins was observed in infected and uninfected cells, suggesting an unspecific alteration of TJ protein trafficking. To circumvent these problems, we transfected JFH-1 infected Huh-7.5 cells with dominant-negative EPS15 constructs to inhibit clathrin-mediated endocytosis and analyzed TJ protein localization in $NS5A^{+}/EPS15^{+}$ cells by immunofluorescence (Figure 3-33). Since it was not possible to co-stain EPS15-GFP expressing cells for TJ proteins and NS5A due to technical limitations, we aimed to achieve at least 90% infectivity to ensure a sufficient number of Eps15+/NS5A+ cells within the infected population. We failed to observe intracellular CLDN1 in NS5A+/ Eps15+ expressing cells, suggesting that the intracellular accumulation may be the result of internalization events. However, it is important to take into account the 70% infection rate and the 50% inhibition of clathrin-mediated

endocytosis by the EPS15 dominant negative mutant (Dr. Jennifer Timpe, unpublished observations), when interpreting these results.

Because it is known that clathrin-coated pits deliver their cargo to early endosomes (reviewed in (296)), we sought to determine whether CLDN1 localizes with markers of the endocytic pathway. CLDN1 did not co-localize with the Golgi complex (GM130) and the ER-Golgi intermediate compartment (ERGIC53), respectively. Furthermore, CLDN1 showed no co-localization with markers of the endocytic pathway, like early (EEA1) and late (Lamp1) endosomes, indicating that intracellular forms of the protein may be retained in an unknown storage compartment (Figure 3-26). Ivanov et al. demonstrated that in depolarized T84 epithelial cells, the cytoplasmic compartment containing junctional proteins did not acquire markers of any classic organelles involved in protein trafficking such as recycling and late endosomes/lysosomes, trans-Golgi network, or the ER (192). Instead, it was demonstrated that the TJ protein containing vesicles were enriched in syntaxin-4, resembling the syntaxin-4-containing storage compartment for basolateral membrane proteins found in non-polarized MDCK cells (256).

Membrane proteins that are internalized by receptor-mediated endocytosis or macropinocytosis are delivered to early endosomes for sorting (247). Interestingly, the intracellular forms of CLDN1 in infected Huh-7.5 cells failed to colocalize with the early endosomal markers EEA1 (Figure 3-26) and CD63 (data not shown), indicating that the protein was not associated with early

endosomes. Ubiquitin-mediated proteolysis plays an important role in the cellular response to stress and extracellular effectors (reviewed in (151)) and instead of following the endocytic pathway, CLDN1 may be targeted to the proteasome for degradation. Proteasome inhibition promotes rapid protein accumulation to aggresomes (proteinaceous inclusion bodies) as a result of impairments in protein removal and we speculated that an inhibition of proteasome-mediated proteolysis would lead to a visible increase in intracellular CLDN1 in HCV infected cells if the protein was destined for degradation. However, treatment with ALLN had no significant effect on the distribution of CLDN1 in naïve or NS5A positive cells (Figure 3-32), suggesting that the intracellular protein is not targeted to proteasomes in HCV infected cells.

To further investigate a possible degradation of intracellular TJ proteins, we studied CLDN1 localization in JFH-1 infected Huh-7.5 cells following treatment with cycloheximide (CHX), the hypothesis being that a block of protein synthesis will result in a decrease of intracellular CLDN1 if the protein is targeted to proteasomes or lysosomes. CHX blocking of protein biosynthesis for 12 hrs markedly reduced the expression of CLDN1 at the plasma membrane in naïve cells (Figure 3-31). In contrast, intracellular forms of CLDN1 in infected cells were still detectable, suggesting a longer half-life. Following the removal of CHX, CLDN1 was detected at the plasma membrane in naïve and infected cells, suggesting that 'trapping' of CLDN1 in infected cells occurs in a relatively long-lived intracellular compartment. Furthermore,

the inhibition of protein synthesis did not affect the level of cytosolic CLDN1, indicating that the accumulation of TJ proteins in the cytoplasma of HCV infected cells is not the result of enhanced synthesis.

In non-polarized cells, proteins are synthesized on ER-bound ribosomes followed by post-translational modification in the Golgi apparatus and sorting at the trans-Golgi network (TNG) (reviewed in (247)). Unless they contain a specific targeting signal, proteins are constitutively trafficked to the plasma membrane, where they are either retained or internalized (178, 218, 247, 398). Despite the availability of intracellular protein CLDN1 levels at the cell surface were drastically reduced following CHX treatment, indicating that the cytoplasmic forms of the protein are not recycled and transported back to the plasma membrane.

Conflicting evidence exists as to whether hepatoma cells are capable of forming functional tight junctions. Two recent studies demonstrate increased transepithelial electric resistance (TER) and dextran permeability following calcium depletion in Huh-7 cells, suggesting that these cells exhibit barrier function ((40, 417). In our experience, Huh-7 and Huh-7.5 cells from several independent sources failed to form functional tight junctions as assessed by the flow of small molecular weight dextrans, fluorescent lipids, transeptithelial resistance measurements, and the localization of multidrug resitance associated protein-2 (MRP2) and multidrug resistance protein-1 (MDRP1), which localize to the apical canalicular domain in polarized epithelial cells

(115, 391). HCV permissive HepG2-CD81 cells demonstrated decreased formation of canalicular structures following JFH-1 infection, indicating a loss of cell polarity (Dr. Christopher Mee, unpublished observations). Interestingly, both NS5A positive and naïve cells showed reduced MRP2 staining, suggesting that the depolarization of one cell within a sheet or monolayer may affect the polarity of neighbouring cells and promote virus transmission via cell-cell routes (396). Recent observations that HCV entry is significantly enhanced in calcium-depleted compared to polarized Caco-2 cells (277) led us to speculate that HCV may preferably enter hepatocytes where cell-cell contacts are damaged and tight junctions disrupted. It is worth noting that following liver transplantation, the allograft is in most cases rapidly re-infected (272). Tissue damage inflicted during the surgical procedure may facilitate this process. In addition, a low level infection with HCV in an immuno-suppressed environment may evoke a 'depolarization chain reaction', resulting in rapid viral spread within the transplanted organ.

Viruses such as HIV-1 (19, 200), human cytomegalovirus (41), and West Nile virus (405) have been shown to alter TJ protein expression and/or distribution in polarized brain endothelial cells, the disruption of the blood-brain barrier resulting in the infiltration of infected immune cells into the central nervous system. Likewise, HCV induced alterations of TJ protein localization may lead to a perturbation of hepatocyte barrier function and promote the local infiltration of leukocytes into the parenchyma (reviewed in (70)). Several reports demonstrate the infiltration of lymphocytes into the liver (reviewed in

(111). Furthermore, clinical studies suggest a link between the tissue damage characteristic for chronic hepatitis C and the sustained secretion of pro-inflammatory cytokines by intrahepatic immune cell infiltrates (reviewed in (173, 371). It is also worth noting that in hepatocytes, surrounding infiltrating lymphocytes have been shown to induce expression of the chemokine receptor ligand interferon-inducible protein (IP)-10 (358), thus promoting the infiltration of HCV non-specific natural killer (NK) cells and cytotoxic T lymphocytes (CTLs) into the liver (339). Several lines of evidence suggest that HCV is non-cytopathic (11, 60). However, by perturbing hepatocyte barrier function and promoting the local infiltration of lymphocytes into the liver, the virus may directly contribute to liver cell damage and accelerate disease progression to fibrosis and cirrhosis.

There was no observable re-organization of TJ proteins in Huh-7.5 cells supporting sub-genomic JFH-1 replication (Figure 3-23), suggesting that the structural proteins alone or in combination with the non-structural proteins mediate the changes in protein localization. Transfection of Huh-7.5 cells to express JFH-1 E1E2 induced a re-organization of CLDN1 and occludin staining in a proportion of cells (Figure 3-30). Interestingly, the genotype 1a H77 glycoproteins exerted a more profound effect on TJ protein localization than the genotype 2a JFH-1 (Table 3-2), despite comparable levels of E1E2 expression, leading us to speculate that, *in vivo*, the ability of HCV to disrupt hepatocyte barrier functions may be variable. This is consistent with clinical observations noting considerable differences in the severity of HCV-

associated defects in liver function associated with biliary cirrhosis and cholestatic liver disease (18, 104, 272, 399).

3.4 Concluding remarks.

In this study we have employed the HCVcc system to investigate the mechanisms of viral entry. We have demonstrated that the formation of cellular contacts increases CLDN1 and SR-BI expression and promotes the internalization of cell-bound virus particles in vitro. The mechanism(s) underlying this phenomenon remain to be identified, however we were able to show that in the absence of cellular contact SR-BI alone is sufficient to modulate the entry kinetics of HCVcc, demonstrating a crucial and rate-limiting role for the receptor in virus internalization. In contrast, the expression levels of CLDN1, which has been proposed to act at a late stage during viral entry (114), did not limit the rate or frequency of HCVcc internalization. Compared to other enveloped viruses HCVcc internalization is slow, which probably reflects the time required to form higher order protein complexes between CD81, SR-BI and CLDN1. Based on our findings we propose a model in which high SR-BI expression promotes receptor complex formation, resulting in the more efficient internalization of cell-bound virus particles (Figure 3-34).

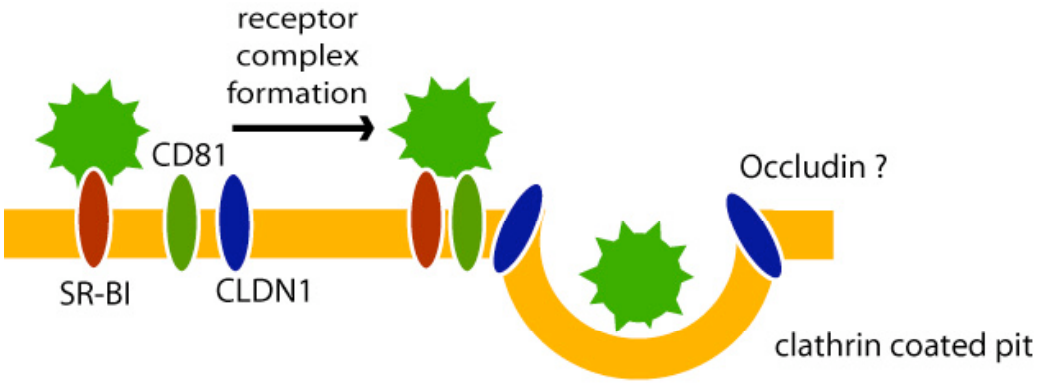

Figure 3-34 Model of HCV entry.

Within the receptor complex SR-BI acts as a primary receptor. SR-BI bound particles then interact with CD81 and CLDN1, possibly followed by TJ protein mediated endocytosis.

Chronic hepatitis C is associated with progressive liver injury, which, in many cases, leads to fibrosis and cirrhosis. The pathology of HCV infection is thought to be caused predominantly by a virus-specific cell-mediated immune response (reviewed in (307)) while the virus itself is seen as non-cytopathic (11, 60). In our study, we have demonstrated that HCV infection modulates TJ protein expression and localization and, moreover, that in Huh-7.5 cells this modulation is mediated by the viral envelope glycoproteins rather than soluble factors. Furthermore, we have demonstrated that HCV infection results in decreased cell polarity, alluding to the effect(s) the virus may have on hepatocyte functionality. In future studies we aim to define the mechanism(s) underlying the HCV-mediated disruption of TJ protein localization, which may

provide further insight into the pathogenesis of HCV infection and support the identification of alternative therapeutic targets.

Taken together, our findings highlight the importance of studying the role of TJ in HCV entry, and the effect(s) of HCV infection on TJ formation and cell polarity. It is worth noting, however, that to date the majority of *in vitro* studies facilitate Huh-7.5 cells, which, unlike human hepatocytes, do not form functional TJ. Polarized cell lines, such as Caco-2 and Hep-G2 cells, constitute a more physiological model of human hepatocytes but have the disadvantage of relatively low susceptibility to HCV infection. In this context, the recently developed uPA/SCID mouse model (279) represents a valuable tool, which will allow in depth studies of the role(s) of HCV in the progression of liver disease. After all, a detailed understanding of the pathology of HCV infection is of paramount importance for the development of effective antiviral therapeutics and the prevention of HCV-related liver injury in chronic hepatitis C.

4 Bibliography.

1. **Abe, K., G. Inchauspe, T. Shikata, and A. M. Prince.** 1992. Three different patterns of hepatitis C virus infection in chimpanzees. Hepatology **15:**690-5.
2. **Abramoff, M. D., Magelhaes, P.J., Ram, S.J.** 2004. Image Processing with ImageJ. Biophotonics International **11:**36-42.
3. **Acton, S., A. Rigotti, K. T. Landschulz, S. Xu, H. H. Hobbs, and M. Krieger.** 1996. Identification of scavenger receptor SR-BI as a high density lipoprotein receptor. Science **271:**518-20.
4. **Acton, S. L., P. E. Scherer, H. F. Lodish, and M. Krieger.** 1994. Expression cloning of SR-BI, a CD36-related class B scavenger receptor. J Biol Chem **269:**21003-9.
5. **Afdhal, N. H.** 2004. The natural history of hepatitis C. Semin Liver Dis **24 Suppl 2:**3-8.
6. **Agnello, V., G. Abel, M. Elfahal, G. B. Knight, and Q. X. Zhang.** 1999. Hepatitis C virus and other flaviviridae viruses enter cells via low density lipoprotein receptor. Proc Natl Acad Sci U S A **96:**12766-71.
7. **Ait-Goughoulte, M., C. Hourioux, R. Patient, S. Trassard, D. Brand, and P. Roingeard.** 2006. Core protein cleavage by signal peptide peptidase is required for hepatitis C virus-like particle assembly. J Gen Virol **87:**855-60.
8. **Akazawa, D., T. Date, K. Morikawa, A. Murayama, M. Miyamoto, M. Kaga, H. Barth, T. F. Baumert, J. Dubuisson, and T. Wakita.** 2007. CD81 expression is important for the permissiveness of Huh7 cell clones for heterogeneous hepatitis C virus infection. J Virol **81:**5036-45.
9. **Al, R. H., Y. Xie, Y. Wang, and C. H. Hagedorn.** 1998. Expression of recombinant hepatitis C virus non-structural protein 5B in Escherichia coli. Virus Res **53:**141-9.
10. **Alberti, A., L. Chemello, and L. Benvegnu.** 1999. Natural history of hepatitis C. J Hepatol **31 Suppl 1:**17-24.
11. **Alberti, A., G. Morsica, L. Chemello, D. Cavalletto, F. Noventa, P. Pontisso, and A. Ruol.** 1992. Hepatitis C viraemia and liver disease in symptom-free individuals with anti-HCV. Lancet **340:**697-8.
12. **Alexander, W. S.** 2002. Suppressors of cytokine signalling (SOCS) in the immune system. Nat Rev Immunol **2:**410-6.
13. **Alter, H. J., P. V. Holland, A. G. Morrow, R. H. Purcell, S. M. Feinstone, and Y. Moritsugu.** 1975. Clinical and serological analysis of transfusion-associated hepatitis. Lancet **2:**838-41.
14. **Alter, H. J., P. V. Holland, R. H. Purcell, J. J. Lander, S. M. Feinstone, A. G. Morrow, and P. J. Schmidt.** 1972. Posttransfusion hepatitis after exclusion of commercial and hepatitis-B antigen-positive donors. Ann Intern Med **77:**691-9.
15. **Alter, H. J., R. H. Purcell, P. V. Holland, and H. Popper.** 1978. Transmissible agent in non-A, non-B hepatitis. Lancet **1:**459-63.
16. **Alter, M. J.** 1997. Epidemiology of hepatitis C. Hepatology **26:**62S-65S.
17. **Alter, M. J.** 2006. Epidemiology of viral hepatitis and HIV co-infection. J Hepatol **44:**S6-9.
18. **Anderson, J. M.** 1996. Leaky junctions and cholestasis: a tight correlation. Gastroenterology **110:**1662-5.

19. **Andras, I. E., H. Pu, M. A. Deli, A. Nath, B. Hennig, and M. Toborek.** 2003. HIV-1 Tat protein alters tight junction protein expression and distribution in cultured brain endothelial cells. J Neurosci Res **74:**255-65.
20. **Andre, P., F. Komurian-Pradel, S. Deforges, M. Perret, J. L. Berland, M. Sodoyer, S. Pol, C. Brechot, G. Paranhos-Baccala, and V. Lotteau.** 2002. Characterization of low- and very-low-density hepatitis C virus RNA-containing particles. J Virol **76:**6919-28.
21. **Bain, C., A. Fatmi, F. Zoulim, J. P. Zarski, C. Trepo, and G. Inchauspe.** 2001. Impaired allostimulatory function of dendritic cells in chronic hepatitis C infection. Gastroenterology **120:**512-24.
22. **Bain, C., and G. Inchauspe.** 2001. [Dendritic cells and hepatitis C virus]. Pathol Biol (Paris) **49:**464-5.
23. **Barba, G., F. Harper, T. Harada, M. Kohara, S. Goulinet, Y. Matsuura, G. Eder, Z. Schaff, M. J. Chapman, T. Miyamura, and C. Brechot.** 1997. Hepatitis C virus core protein shows a cytoplasmic localization and associates to cellular lipid storage droplets. Proc Natl Acad Sci U S A **94:**1200-5.
24. **Bartenschlager, R., L. Ahlborn-Laake, J. Mous, and H. Jacobsen.** 1994. Kinetic and structural analyses of hepatitis C virus polyprotein processing. J Virol **68:**5045-55.
25. **Bartenschlager, R., and V. Lohmann.** 2000. Replication of hepatitis C virus. J Gen Virol **81:**1631-48.
26. **Barth, H., R. Cerino, M. Arcuri, M. Hoffmann, P. Schurmann, M. I. Adah, B. Gissler, X. Zhao, V. Ghisetti, B. Lavezzo, H. E. Blum, F. von Weizsacker, A. Vitelli, E. Scarselli, and T. F. Baumert.** 2005. Scavenger receptor class B type I and hepatitis C virus infection of primary tupaia hepatocytes. J Virol **79:**5774-85.
27. **Barth, H., C. Schafer, M. I. Adah, F. Zhang, R. J. Linhardt, H. Toyoda, A. Kinoshita-Toyoda, T. Toida, T. H. Van Kuppevelt, E. Depla, F. Von Weizsacker, H. E. Blum, and T. F. Baumert.** 2003. Cellular binding of hepatitis C virus envelope glycoprotein E2 requires cell surface heparan sulfate. J Biol Chem **278:**41003-12.
28. **Barth, H., E. K. Schnober, F. Zhang, R. J. Linhardt, E. Depla, B. Boson, F. L. Cosset, A. H. Patel, H. E. Blum, and T. F. Baumert.** 2006. Viral and cellular determinants of the hepatitis C virus envelope-heparan sulfate interaction. J Virol **80:**10579-90.
29. **Barth, H., A. Ulsenheimer, G. R. Pape, H. M. Diepolder, M. Hoffmann, C. Neumann-Haefelin, R. Thimme, P. Henneke, R. Klein, G. Paranhos-Baccala, E. Depla, T. J. Liang, H. E. Blum, and T. F. Baumert.** 2005. Uptake and presentation of hepatitis C virus-like particles by human dendritic cells. Blood **105:**3605-14.
30. **Bartosch, B., J. Dubuisson, and F. L. Cosset.** 2003. Infectious hepatitis C virus pseudo-particles containing functional E1-E2 envelope protein complexes. J Exp Med **197:**633-42.
31. **Bartosch, B., G. Verney, M. Dreux, P. Donot, Y. Morice, F. Penin, J. M. Pawlotsky, D. Lavillette, and F. L. Cosset.** 2005. An interplay between hypervariable region 1 of the hepatitis C virus E2 glycoprotein, the scavenger receptor BI, and high-density lipoprotein promotes both enhancement of infection and protection against neutralizing antibodies. J Virol **79:**8217-29.
32. **Bartosch, B., A. Vitelli, C. Granier, C. Goujon, J. Dubuisson, S. Pascale, E. Scarselli, R. Cortese, A. Nicosia, and F. L. Cosset.** 2003. Cell entry of hepatitis C virus requires a set of co-receptors that include the CD81 tetraspanin and the SR-B1 scavenger receptor. J Biol Chem **278:**41624-30.

33. **Bassett, S. E., K. M. Brasky, and R. E. Lanford.** 1998. Analysis of hepatitis C virus-inoculated chimpanzees reveals unexpected clinical profiles. J Virol **72:**2589-99.
34. **Bassett, S. E., B. Guerra, K. Brasky, E. Miskovsky, M. Houghton, G. R. Klimpel, and R. E. Lanford.** 2001. Protective immune response to hepatitis C virus in chimpanzees rechallenged following clearance of primary infection. Hepatology **33:**1479-87.
35. **Basu, A., A. Beyene, K. Meyer, and R. Ray.** 2004. The hypervariable region 1 of the E2 glycoprotein of hepatitis C virus binds to glycosaminoglycans, but this binding does not lead to infection in a pseudotype system. J Virol **78:**4478-86.
36. **Basuroy, S., P. Sheth, D. Kuppuswamy, S. Balasubramanian, R. M. Ray, and R. K. Rao.** 2003. Expression of kinase-inactive c-Src delays oxidative stress-induced disassembly and accelerates calcium-mediated reassembly of tight junctions in the Caco-2 cell monolayer. J Biol Chem **278:**11916-24.
37. **Baumert, T. F., S. Ito, D. T. Wong, and T. J. Liang.** 1998. Hepatitis C virus structural proteins assemble into viruslike particles in insect cells. J Virol **72:**3827-36.
38. **Beach, M. J., E. L. Meeks, L. T. Mimms, D. Vallari, L. DuCharme, J. Spelbring, S. Taskar, J. B. Schleicher, K. Krawczynski, and D. W. Bradley.** 1992. Temporal relationships of hepatitis C virus RNA and antibody responses following experimental infection of chimpanzees. J Med Virol **36:**226-37.
39. **Bekisz, J., H. Schmeisser, J. Hernandez, N. D. Goldman, and K. C. Zoon.** 2004. Human interferons alpha, beta and omega. Growth Factors **22:**243-51.
40. **Benedicto, I., F. Molina-Jimenez, O. Barreiro, A. Maldonado-Rodriguez, J. Prieto, R. Moreno-Otero, R. Aldabe, M. Lopez-Cabrera, and P. L. Majano.** 2008. Hepatitis C virus envelope components alter localization of hepatocyte tight junction-associated proteins and promote occludin retention in the endoplasmic reticulum. Hepatology **48:**1044-1053.
41. **Bentz, G. L., M. Jarquin-Pardo, G. Chan, M. S. Smith, C. Sinzger, and A. D. Yurochko.** 2006. Human cytomegalovirus (HCMV) infection of endothelial cells promotes naive monocyte extravasation and transfer of productive virus to enhance hematogenous dissemination of HCMV. J Virol **80:**11539-55.
42. **Berdichevsky, Y., R. Zemel, L. Bachmatov, A. Abramovich, R. Koren, P. Sathiyamoorthy, A. Golan-Goldhirsh, R. Tur-Kaspa, and I. Benhar.** 2003. A novel high throughput screening assay for HCV NS3 serine protease inhibitors. J Virol Methods **107:**245-55.
43. **Bergelson, J. M., J. A. Cunningham, G. Droguett, E. A. Kurt-Jones, A. Krithivas, J. S. Hong, M. S. Horwitz, R. L. Crowell, and R. W. Finberg.** 1997. Isolation of a common receptor for Coxsackie B viruses and adenoviruses 2 and 5. Science **275:**1320-3.
44. **Bernfield, M., M. Gotte, P. W. Park, O. Reizes, M. L. Fitzgerald, J. Lincecum, and M. Zako.** 1999. Functions of cell surface heparan sulfate proteoglycans. Annu Rev Biochem **68:**729-77.
45. **Bertaux, C., and T. Dragic.** 2006. Different domains of CD81 mediate distinct stages of hepatitis C virus pseudoparticle entry. J Virol **80:**4940-8.
46. **Beyer, B. M., R. Zhang, Z. Hong, V. Madison, and B. A. Malcolm.** 2001. Effect of naturally occurring active site mutations on hepatitis C virus NS3 protease specificity. Proteins **43:**82-8.

47. **Bigger, C. B., K. M. Brasky, and R. E. Lanford.** 2001. DNA microarray analysis of chimpanzee liver during acute resolving hepatitis C virus infection. J Virol **75:**7059-66.
48. **Bigger, C. B., B. Guerra, K. M. Brasky, G. Hubbard, M. R. Beard, B. A. Luxon, S. M. Lemon, and R. E. Lanford.** 2004. Intrahepatic gene expression during chronic hepatitis C virus infection in chimpanzees. J Virol **78:**13779-92.
49. **Blanchard, E., S. Belouzard, L. Goueslain, T. Wakita, J. Dubuisson, C. Wychowski, and Y. Rouille.** 2006. Hepatitis C virus entry depends on clathrin-mediated endocytosis. J Virol **80:**6964-72.
50. **Blight, K. J., A. A. Kolykhalov, and C. M. Rice.** 2000. Efficient initiation of HCV RNA replication in cell culture. Science **290:**1972-4.
51. **Blight, K. J., J. A. McKeating, J. Marcotrigiano, and C. M. Rice.** 2003. Efficient replication of hepatitis C virus genotype 1a RNAs in cell culture. J Virol **77:**3181-90.
52. **Blight, K. J., J. A. McKeating, and C. M. Rice.** 2002. Highly permissive cell lines for subgenomic and genomic hepatitis C virus RNA replication. J Virol **76:**13001-14.
53. **Blumberg, B. S., H. J. Alter, and S. Visnich.** 1965. A "New" Antigen in Leukemia Sera. Jama **191:**541-6.
54. **Boulant, S., M. W. Douglas, L. Moody, A. Budkowska, P. Targett-Adams, and J. McLauchlan.** 2008. Hepatitis C virus core protein induces lipid droplet redistribution in a microtubule- and dynein-dependent manner. Traffic **9:**1268-82.
55. **Boulant, S., P. Targett-Adams, and J. McLauchlan.** 2007. Disrupting the association of hepatitis C virus core protein with lipid droplets correlates with a loss in production of infectious virus. J Gen Virol **88:**2204-13.
56. **Bowen, D. G., and C. M. Walker.** 2005. Adaptive immune responses in acute and chronic hepatitis C virus infection. Nature **436:**946-52.
57. **Bowen, D. G., and C. M. Walker.** 2005. The origin of quasispecies: cause or consequence of chronic hepatitis C viral infection? J Hepatol **42:**408-17.
58. **Brass, V., D. Moradpour, and H. E. Blum.** 2006. Molecular Virology of Hepatitis C Virus (HCV): 2006 Update. Int J Med Sci **3:**29-34.
59. **Breiman, A., D. Vitour, M. Vilasco, C. Ottone, S. Molina, L. Pichard, C. Fournier, D. Delgrange, P. Charneau, G. Duverlie, C. Wychowski, P. Maurel, and E. F. Meurs.** 2006. A hepatitis C virus (HCV) NS3/4A protease-dependent strategy for the identification and purification of HCV-infected cells. J Gen Virol **87:**3587-98.
60. **Brillanti, S., M. Foli, S. Gaiani, C. Masci, M. Miglioli, and L. Barbara.** 1993. Persistent hepatitis C viraemia without liver disease. Lancet **341:**464-5.
61. **Brone, B., and J. Eggermont.** 2005. PDZ proteins retain and regulate membrane transporters in polarized epithelial cell membranes. Am J Physiol Cell Physiol **288:**C20-9.
62. **Bruewer, M., M. Utech, A. I. Ivanov, A. M. Hopkins, C. A. Parkos, and A. Nusrat.** 2005. Interferon-gamma induces internalization of epithelial tight junction proteins via a macropinocytosis-like process. FASEB J **19:**923-33.
63. **Bukh, J., T. Pietschmann, V. Lohmann, N. Krieger, K. Faulk, R. E. Engle, S. Govindarajan, M. Shapiro, M. St Claire, and R. Bartenschlager.** 2002. Mutations that permit efficient replication of hepatitis C virus RNA in Huh-7 cells prevent productive replication in chimpanzees. Proc Natl Acad Sci U S A **99:**14416-21.

64. **Bukh, J., R. H. Purcell, and R. H. Miller.** 1993. At least 12 genotypes of hepatitis C virus predicted by sequence analysis of the putative E1 gene of isolates collected worldwide. Proc Natl Acad Sci U S A **90:**8234-8.
65. **Buonocore, L., K. J. Blight, C. M. Rice, and J. K. Rose.** 2002. Characterization of vesicular stomatitis virus recombinants that express and incorporate high levels of hepatitis C virus glycoproteins. J Virol **76:**6865-72.
66. **Callens, N., Y. Ciczora, B. Bartosch, N. Vu-Dac, F. L. Cosset, J. M. Pawlotsky, F. Penin, and J. Dubuisson.** 2005. Basic residues in hypervariable region 1 of hepatitis C virus envelope glycoprotein e2 contribute to virus entry. J Virol **79:**15331-41.
67. **Calvo, D., D. Gomez-Coronado, M. A. Lasuncion, and M. A. Vega.** 1997. CLA-1 is an 85-kD plasma membrane glycoprotein that acts as a high-affinity receptor for both native (HDL, LDL, and VLDL) and modified (OxLDL and AcLDL) lipoproteins. Arterioscler Thromb Vasc Biol **17:**2341-9.
68. **Castet, V., C. Fournier, A. Soulier, R. Brillet, J. Coste, D. Larrey, D. Dhumeaux, P. Maurel, and J. M. Pawlotsky.** 2002. Alpha interferon inhibits hepatitis C virus replication in primary human hepatocytes infected in vitro. J Virol **76:**8189-99.
69. **Cella, M., M. Salio, Y. Sakakibara, H. Langen, I. Julkunen, and A. Lanzavecchia.** 1999. Maturation, activation, and protection of dendritic cells induced by double-stranded RNA. J Exp Med **189:**821-9.
70. **Cereijido, M., R. G. Contreras, L. Shoshani, D. Flores-Benitez, and I. Larre.** 2008. Tight junction and polarity interaction in the transporting epithelial phenotype. Biochim Biophys Acta **1778:**770-93.
71. **Cerny, A., and F. V. Chisari.** 1999. Pathogenesis of chronic hepatitis C: immunological features of hepatic injury and viral persistence. Hepatology **30:**595-601.
72. **Cha, T. A., E. Beall, B. Irvine, J. Kolberg, D. Chien, G. Kuo, and M. S. Urdea.** 1992. At least five related, but distinct, hepatitis C viral genotypes exist. Proc Natl Acad Sci U S A **89:**7144-8.
73. **Chang, K. S., J. Jiang, Z. Cai, and G. Luo.** 2007. Human apolipoprotein e is required for infectivity and production of hepatitis C virus in cell culture. J Virol **81:**13783-93.
74. **Charlton, M.** 2005. Recurrence of hepatitis C infection: Where are we now? Liver Transpl **11:**S57-62.
75. **Charrin, S., F. Le Naour, V. Labas, M. Billard, J. P. Le Caer, J. F. Emile, M. A. Petit, C. Boucheix, and E. Rubinstein.** 2003. EWI-2 is a new component of the tetraspanin web in hepatocytes and lymphoid cells. Biochem J **373:**409-21.
76. **Charrin, S., F. Le Naour, M. Oualid, M. Billard, G. Faure, S. M. Hanash, C. Boucheix, and E. Rubinstein.** 2001. The major CD9 and CD81 molecular partner. Identification and characterization of the complexes. J Biol Chem **276:**14329-37.
77. **Cheng, J. C., M. F. Chang, and S. C. Chang.** 1999. Specific interaction between the hepatitis C virus NS5B RNA polymerase and the 3' end of the viral RNA. J Virol **73:**7044-9.
78. **Chevaliez S., P. J.-M.** 2006. HCV Genome and Life Cycle. *In* S.-L. Tan (ed.), Hepatitis C Viruses: Genomes and Molecular Biology. Horizon Bioscience, Norfolk, UK.
79. **Chisari, F. V.** 2005. Unscrambling hepatitis C virus-host interactions. Nature **436:**930-2.

80. **Cho, Y. G., S. H. Yang, and Y. C. Sung.** 1998. In vivo assay for hepatitis C viral serine protease activity using a secreted protein. J Virol Methods **72:**109-15.
81. **Choo, Q. L., Kuo G, Weiner AJ, Overby LR, Bradley DW, and H. M.** 1989. Isolation of a cDNA clone derived from a blood-borne non-A, non-B viral hepatitis genome. Science **244:**359-62.
82. **Choo, Q. L., K. H. Richman, J. H. Han, K. Berger, C. Lee, C. Dong, C. Gallegos, D. Coit, R. Medina-Selby, P. J. Barr, and et al.** 1991. Genetic organization and diversity of the hepatitis C virus. Proc Natl Acad Sci U S A **88:**2451-5.
83. **Choukhi, A., S. Ung, C. Wychowski, and J. Dubuisson.** 1998. Involvement of endoplasmic reticulum chaperones in the folding of hepatitis C virus glycoproteins. J Virol **72:**3851-8.
84. **Clark, K. L., Z. Zeng, A. L. Langford, S. M. Bowen, and S. C. Todd.** 2001. PGRL is a major CD81-associated protein on lymphocytes and distinguishes a new family of cell surface proteins. J Immunol **167:**5115-21.
85. **Clontech.** 2003. Proteasome Sensor Vector. Clontechniques **XVIII**.
86. **Coccia, E. M., M. Severa, E. Giacomini, D. Monneron, M. E. Remoli, I. Julkunen, M. Cella, R. Lande, and G. Uze.** 2004. Viral infection and Toll-like receptor agonists induce a differential expression of type I and lambda interferons in human plasmacytoid and monocyte-derived dendritic cells. Eur J Immunol **34:**796-805.
87. **Cocquerel, L., C. Voisset, and J. Dubuisson.** 2006. Hepatitis C virus entry: potential receptors and their biological functions. J Gen Virol **87:**1075-84.
88. **Codran, A., C. Royer, D. Jaeck, M. Bastien-Valle, T. F. Baumert, M. P. Kieny, C. A. Pereira, and J. P. Martin.** 2006. Entry of hepatitis C virus pseudotypes into primary human hepatocytes by clathrin-dependent endocytosis. J Gen Virol **87:**2583-93.
89. **Collier, J., and J. Heathcote.** 1998. Hepatitis C viral infection in the immunosuppressed patient. Hepatology **27:**2-6.
90. **Colombo, M.** 1999. Natural history and pathogenesis of hepatitis C virus related hepatocellular carcinoma. J Hepatol **31 Suppl 1:**25-30.
91. **Cooper, S., A. L. Erickson, E. J. Adams, J. Kansopon, A. J. Weiner, D. Y. Chien, M. Houghton, P. Parham, and C. M. Walker.** 1999. Analysis of a successful immune response against hepatitis C virus. Immunity **10:**439-49.
92. **Cormier, E. G., R. J. Durso, F. Tsamis, L. Boussemart, C. Manix, W. C. Olson, J. P. Gardner, and T. Dragic.** 2004. L-SIGN (CD209L) and DC-SIGN (CD209) mediate transinfection of liver cells by hepatitis C virus. Proc Natl Acad Sci U S A **101:**14067-72.
93. **Cormier, E. G., F. Tsamis, F. Kajumo, R. J. Durso, J. P. Gardner, and T. Dragic.** 2004. CD81 is an entry coreceptor for hepatitis C virus. Proc Natl Acad Sci U S A **101:**7270-4.
94. **Couto LB, K. A.** 2006. Animal Models for HCV Study. *In* S.-L. Tan (ed.), Hepatitis C Viruses: Genomes and Molecular Biology. Horizon Bioscience, Norfolk, UK.
95. **Coyne, C. B., and J. M. Bergelson.** 2006. Virus-induced Abl and Fyn kinase signals permit coxsackievirus entry through epithelial tight junctions. Cell **124:**119-31.
96. **Cristofari, G., R. Ivanyi-Nagy, C. Gabus, S. Boulant, J. P. Lavergne, F. Penin, and J. L. Darlix.** 2004. The hepatitis C virus Core protein is a potent nucleic acid chaperone that directs dimerization of the viral (+) strand RNA in vitro. Nucleic Acids Res **32:**2623-31.

97. **Cukierman, L., L. Meertens, C. Bertaux, F. Kajumo, and T. Dragic.** 2009. Residues in a highly conserved claudin-1 motif are required for hepatitis C virus entry and mediate the formation of cell-cell contacts. J Virol **83:**5477-84.
98. **Culp, T. D., C. M. Spatz, C. A. Reed, and N. D. Christensen.** 2007. Binding and neutralization efficiencies of monoclonal antibodies, Fab fragments, and scFv specific for L1 epitopes on the capsid of infectious HPV particles. Virology **361:**435-46.
99. **Dandri, M., M. R. Burda, E. Torok, J. M. Pollok, A. Iwanska, G. Sommer, X. Rogiers, C. E. Rogler, S. Gupta, H. Will, H. Greten, and J. Petersen.** 2001. Repopulation of mouse liver with human hepatocytes and in vivo infection with hepatitis B virus. Hepatology **33:**981-8.
100. **De Francesco, R., and G. Migliaccio.** 2005. Challenges and successes in developing new therapies for hepatitis C. Nature **436:**953-60.
101. **Di Bisceglie, A. M.** 1997. Hepatitis C and hepatocellular carcinoma. Hepatology **26:**34S-38S.
102. **Dienstag, J. L., and J. G. McHutchison.** 2006. American Gastroenterological Association technical review on the management of hepatitis C. Gastroenterology **130:**231-64; quiz 214-7.
103. **Dolganiuc, A., S. Oak, K. Kodys, D. T. Golenbock, R. W. Finberg, E. Kurt-Jones, and G. Szabo.** 2004. Hepatitis C core and nonstructural 3 proteins trigger toll-like receptor 2-mediated pathways and inflammatory activation. Gastroenterology **127:**1513-24.
104. **Doughty, A. L., J. D. Spencer, Y. E. Cossart, and G. W. McCaughan.** 1998. Cholestatic hepatitis after liver transplantation is associated with persistently high serum hepatitis C virus RNA levels. Liver Transpl Surg **4:**15-21.
105. **Dreux, M., V. L. Dao Thi, J. Fresquet, M. Guerin, Z. Julia, G. Verney, D. Durantel, F. Zoulim, D. Lavillette, F. L. Cosset, and B. Bartosch.** 2009. Receptor complementation and mutagenesis reveal SR-BI as an essential HCV entry factor and functionally imply its intra- and extra-cellular domains. PLoS Pathog **5:**e1000310.
106. **Drummer, H. E., A. Maerz, and P. Poumbourios.** 2003. Cell surface expression of functional hepatitis C virus E1 and E2 glycoproteins. FEBS Lett **546:**385-90.
107. **Drummer, H. E., K. A. Wilson, and P. Poumbourios.** 2005. Determinants of CD81 dimerization and interaction with hepatitis C virus glycoprotein E2. Biochem Biophys Res Commun **328:**251-7.
108. **Dubuisson, J.** 2000. Folding, assembly and subcellular localization of hepatitis C virus glycoproteins. Curr Top Microbiol Immunol **242:**135-48.
109. **Dubuisson, J., H. H. Hsu, R. C. Cheung, H. B. Greenberg, D. G. Russell, and C. M. Rice.** 1994. Formation and intracellular localization of hepatitis C virus envelope glycoprotein complexes expressed by recombinant vaccinia and Sindbis viruses. J Virol **68:**6147-60.
110. **Dusheiko, G., H. Schmilovitz-Weiss, D. Brown, F. McOmish, P. L. Yap, S. Sherlock, N. McIntyre, and P. Simmonds.** 1994. Hepatitis C virus genotypes: an investigation of type-specific differences in geographic origin and disease. Hepatology **19:**13-8.
111. **Dustin, L. B., and C. M. Rice.** 2007. Flying under the radar: the immunobiology of hepatitis C. Annu Rev Immunol **25:**71-99.
112. **Duvet, S., L. Cocquerel, A. Pillez, R. Cacan, A. Verbert, D. Moradpour, C. Wychowski, and J. Dubuisson.** 1998. Hepatitis C virus glycoprotein

complex localization in the endoplasmic reticulum involves a determinant for retention and not retrieval. J Biol Chem **273:**32088-95.

113. **Engel, P., and T. F. Tedder.** 1994. New CD from the B cell section of the Fifth International Workshop on Human Leukocyte Differentiation Antigens. Leuk Lymphoma **13 Suppl 1:**61-4.
114. **Evans, M. J., T. von Hahn, D. M. Tscherne, A. J. Syder, M. Panis, B. Wolk, T. Hatziioannou, J. A. McKeating, P. D. Bieniasz, and C. M. Rice.** 2007. Claudin-1 is a hepatitis C virus co-receptor required for a late step in entry. Nature.
115. **Evers, R., G. J. Zaman, L. van Deemter, H. Jansen, J. Calafat, L. C. Oomen, R. P. Oude Elferink, P. Borst, and A. H. Schinkel.** 1996. Basolateral localization and export activity of the human multidrug resistance-associated protein in polarized pig kidney cells. J Clin Invest **97:**1211-8.
116. **Fan, F. S., C. H. Tzeng, K. I. Hsiao, S. T. Hu, W. T. Liu, and P. M. Chen.** 1991. Withdrawal of immunosuppressive therapy in allogeneic bone marrow transplantation reactivates chronic viral hepatitis C. Bone Marrow Transplant **8:**417-20.
117. **Fan, Z., Q. R. Yang, J. S. Twu, and A. H. Sherker.** 1999. Specific in vitro association between the hepatitis C viral genome and core protein. J Med Virol **59:**131-4.
118. **Farci, P., H. J. Alter, A. Shimoda, S. Govindarajan, L. C. Cheung, J. C. Melpolder, R. A. Sacher, J. W. Shih, and R. H. Purcell.** 1996. Hepatitis C virus-associated fulminant hepatic failure. N Engl J Med **335:**631-4.
119. **Farci, P., A. Shimoda, A. Coiana, G. Diaz, G. Peddis, J. C. Melpolder, A. Strazzera, D. Y. Chien, S. J. Munoz, A. Balestrieri, R. H. Purcell, and H. J. Alter.** 2000. The outcome of acute hepatitis C predicted by the evolution of the viral quasispecies. Science **288:**339-44.
120. **Farci, P., R. Strazzera, H. J. Alter, S. Farci, D. Degioannis, A. Coiana, G. Peddis, F. Usai, G. Serra, L. Chessa, G. Diaz, A. Balestrieri, and R. H. Purcell.** 2002. Early changes in hepatitis C viral quasispecies during interferon therapy predict the therapeutic outcome. Proc Natl Acad Sci U S A **99:**3081-6.
121. **Farquhar, M. G., and G. E. Palade.** 1963. Junctional complexes in various epithelia. J Cell Biol **17:**375-412.
122. **Feinstone, S. M., A. Z. Kapikian, R. H. Purcell, H. J. Alter, and P. V. Holland.** 1975. Transfusion-associated hepatitis not due to viral hepatitis type A or B. N Engl J Med **292:**767-70.
123. **Feinstone, S. M., K. B. Mihalik, T. Kamimura, H. J. Alter, W. T. London, and R. H. Purcell.** 1983. Inactivation of hepatitis B virus and non-A, non-B hepatitis by chloroform. Infect Immun **41:**816-21.
124. **Feld, J. J., and J. H. Hoofnagle.** 2005. Mechanism of action of interferon and ribavirin in treatment of hepatitis C. Nature **436:**967-72.
125. **Feldman, G. J., J. M. Mullin, and M. P. Ryan.** 2005. Occludin: structure, function and regulation. Adv Drug Deliv Rev **57:**883-917.
126. **Ferrari, E., J. Wright-Minogue, J. W. Fang, B. M. Baroudy, J. Y. Lau, and Z. Hong.** 1999. Characterization of soluble hepatitis C virus RNA-dependent RNA polymerase expressed in Escherichia coli. J Virol **73:**1649-54.
127. **Fischer, S., M. Wobben, H. H. Marti, D. Renz, and W. Schaper.** 2002. Hypoxia-induced hyperpermeability in brain microvessel endothelial cells involves VEGF-mediated changes in the expression of zonula occludens-1. Microvasc Res **63:**70-80.

128. **Flint, M., C. Maidens, L. D. Loomis-Price, C. Shotton, J. Dubuisson, P. Monk, A. Higginbottom, S. Levy, and J. A. McKeating.** 1999. Characterization of hepatitis C virus E2 glycoprotein interaction with a putative cellular receptor, CD81. J Virol **73:**6235-44.
129. **Foy, E., K. Li, R. Sumpter, Jr., Y. M. Loo, C. L. Johnson, C. Wang, P. M. Fish, M. Yoneyama, T. Fujita, S. M. Lemon, and M. Gale, Jr.** 2005. Control of antiviral defenses through hepatitis C virus disruption of retinoic acid-inducible gene-I signaling. Proc Natl Acad Sci U S A **102:**2986-91.
130. **Frese, M., T. Pietschmann, D. Moradpour, O. Haller, and R. Bartenschlager.** 2001. Interferon-alpha inhibits hepatitis C virus subgenomic RNA replication by an MxA-independent pathway. J Gen Virol **82:**723-33.
131. **Friedman, S. L.** 1996. Hepatic stellate cells. Prog Liver Dis **14:**101-30.
132. **Friedman, S. L.** 2000. Molecular regulation of hepatic fibrosis, an integrated cellular response to tissue injury. J Biol Chem **275:**2247-50.
133. **Fuertes, G., J. J. Martin De Llano, A. Villarroya, A. J. Rivett, and E. Knecht.** 2003. Changes in the proteolytic activities of proteasomes and lysosomes in human fibroblasts produced by serum withdrawal, amino-acid deprivation and confluent conditions. Biochem J **375:**75-86.
134. **Fuertes, G., A. Villarroya, and E. Knecht.** 2003. Role of proteasomes in the degradation of short-lived proteins in human fibroblasts under various growth conditions. Int J Biochem Cell Biol **35:**651-64.
135. **Fukumoto, T., T. Berg, Y. Ku, W. O. Bechstein, M. Knoop, H. P. Lemmens, H. Lobeck, U. Hopf, and P. Neuhaus.** 1996. Viral dynamics of hepatitis C early after orthotopic liver transplantation: evidence for rapid turnover of serum virions. Hepatology **24:**1351-4.
136. **Furuse, M., K. Fujita, T. Hiiragi, K. Fujimoto, and S. Tsukita.** 1998. Claudin-1 and -2: novel integral membrane proteins localizing at tight junctions with no sequence similarity to occludin. J Cell Biol **141:**1539-50.
137. **Furuse, M., M. Hata, K. Furuse, Y. Yoshida, A. Haratake, Y. Sugitani, T. Noda, A. Kubo, and S. Tsukita.** 2002. Claudin-based tight junctions are crucial for the mammalian epidermal barrier: a lesson from claudin-1-deficient mice. J Cell Biol **156:**1099-111.
138. **Furuse, M., H. Sasaki, and S. Tsukita.** 1999. Manner of interaction of heterogeneous claudin species within and between tight junction strands. J Cell Biol **147:**891-903.
139. **Gale, M., Jr.** 2003. Effector genes of interferon action against hepatitis C virus. Hepatology **37:**975-8.
140. **Gale, M., Jr., C. M. Blakely, B. Kwieciszewski, S. L. Tan, M. Dossett, N. M. Tang, M. J. Korth, S. J. Polyak, D. R. Gretch, and M. G. Katze.** 1998. Control of PKR protein kinase by hepatitis C virus nonstructural 5A protein: molecular mechanisms of kinase regulation. Mol Cell Biol **18:**5208-18.
141. **Gale, M., Jr., and E. M. Foy.** 2005. Evasion of intracellular host defence by hepatitis C virus. Nature **436:**939-45.
142. **Gallagher JT, M. L.** 2000. Molecular structure of Heparan Sulfate and interactions with growth factors and morphogens, p. 27-59. *In* M. Iozzo (ed.), Proteoglycans: structure, biology and molecular interactions. Marcel Dekker Inc., New York.
143. **Gane, E. J., N. V. Naoumov, K. P. Qian, M. U. Mondelli, G. Maertens, B. C. Portmann, J. Y. Lau, and R. Williams.** 1996. A longitudinal analysis of hepatitis C virus replication following liver transplantation. Gastroenterology **110:**167-77.

144. **Garcia-Retortillo, M., X. Forns, A. Feliu, E. Moitinho, J. Costa, M. Navasa, A. Rimola, and J. Rodes.** 2002. Hepatitis C virus kinetics during and immediately after liver transplantation. Hepatology **35:**680-7.
145. **Gardner, J. P., R. J. Durso, R. R. Arrigale, G. P. Donovan, P. J. Maddon, T. Dragic, and W. C. Olson.** 2003. L-SIGN (CD 209L) is a liver-specific capture receptor for hepatitis C virus. Proc Natl Acad Sci U S A **100:**4498-503.
146. **Gastaminza, P., G. Cheng, S. Wieland, J. Zhong, W. Liao, and F. V. Chisari.** 2008. Cellular determinants of hepatitis C virus assembly, maturation, degradation, and secretion. J Virol **82:**2120-9.
147. **Gastaminza, P., S. B. Kapadia, and F. V. Chisari.** 2006. Differential biophysical properties of infectious intracellular and secreted hepatitis C virus particles. J Virol **80:**11074-81.
148. **Germi, R., J. M. Crance, D. Garin, J. Guimet, H. Lortat-Jacob, R. W. Ruigrok, J. P. Zarski, and E. Drouet.** 2002. Heparan sulfate-mediated binding of infectious dengue virus type 2 and yellow fever virus. Virology **292:**162-8.
149. **Ghosh, A. K., M. Majumder, R. Steele, P. Yaciuk, J. Chrivia, R. Ray, and R. B. Ray.** 2000. Hepatitis C virus NS5A protein modulates transcription through a novel cellular transcription factor SRCAP. J Biol Chem **275:**7184-8.
150. **Giannini, C., and C. Brechot.** 2003. Hepatitis C virus biology. Cell Death Differ **10 Suppl 1:**S27-38.
151. **Glickman, M. H., and A. Ciechanover.** 2002. The ubiquitin-proteasome proteolytic pathway: destruction for the sake of construction. Physiol Rev **82:**373-428.
152. **Gocke, D. J., H. B. Greenberg, and N. B. Kavey.** 1970. Correlation of Australia antigen with posttransfusion hepatitis. JAMA **212:**877-9.
153. **Gong, G., G. Waris, R. Tanveer, and A. Siddiqui.** 2001. Human hepatitis C virus NS5A protein alters intracellular calcium levels, induces oxidative stress, and activates STAT-3 and NF-kappa B. Proc Natl Acad Sci U S A **98:**9599-604.
154. **Gonzalez-Amaro, R., C. Garcia-Monzon, L. Garcia-Buey, R. Moreno-Otero, J. L. Alonso, E. Yague, J. P. Pivel, M. Lopez-Cabrera, E. Fernandez-Ruiz, and F. Sanchez-Madrid.** 1994. Induction of tumor necrosis factor alpha production by human hepatocytes in chronic viral hepatitis. J Exp Med **179:**841-8.
155. **Gonzalez-Mariscal, L., A. Betanzos, P. Nava, and B. E. Jaramillo.** 2003. Tight junction proteins. Prog Biophys Mol Biol **81:**1-44.
156. **Gottwein, J. M., T. K. Scheel, T. B. Jensen, J. B. Lademann, J. C. Prentoe, M. L. Knudsen, A. M. Hoegh, and J. Bukh.** 2009. Development and characterization of hepatitis C virus genotype 1-7 cell culture systems: role of CD81 and scavenger receptor class B type I and effect of antiviral drugs. Hepatology **49:**364-77.
157. **Grakoui, A., C. Wychowski, C. Lin, S. M. Feinstone, and C. M. Rice.** 1993. Expression and identification of hepatitis C virus polyprotein cleavage products. J Virol **67:**1385-95.
158. **Griffin, S. D., L. P. Beales, D. S. Clarke, O. Worsfold, S. D. Evans, J. Jaeger, M. P. Harris, and D. J. Rowlands.** 2003. The p7 protein of hepatitis C virus forms an ion channel that is blocked by the antiviral drug, Amantadine. FEBS Lett **535:**34-8.
159. **Grove, J., T. Huby, Z. Stamataki, T. Vanwolleghem, P. Meuleman, M. Farquhar, A. Schwarz, M. Moreau, J. S. Owen, G. Leroux-Roels, P. Balfe,**

and J. A. McKeating. 2007. Scavenger receptor BI and BII expression levels modulate hepatitis C virus infectivity. J Virol **81:**3162-9.

160. **Gruber, A., L. G. Lundberg, and M. Bjorkholm.** 1993. Reactivation of chronic hepatitis C after withdrawal of immunosuppressive therapy. J Intern Med **234:**223-5.
161. **Grummer, B., S. Grotha, and I. Greiser-Wilke.** 2004. Bovine viral diarrhoea virus is internalized by clathrin-dependent receptor-mediated endocytosis. J Vet Med B Infect Dis Vet Public Health **51:**427-32.
162. **Gunji, T., N. Kato, M. Hijikata, K. Hayashi, S. Saitoh, and K. Shimotohno.** 1994. Specific detection of positive and negative stranded hepatitis C viral RNA using chemical RNA modification. Arch Virol **134:**293-302.
163. **Han, X., M. P. Fink, and R. L. Delude.** 2003. Proinflammatory cytokines cause NO*-dependent and -independent changes in expression and localization of tight junction proteins in intestinal epithelial cells. Shock **19:**229-37.
164. **Harris, H. J., M. J. Farquhar, C. J. Mee, C. Davis, G. M. Reynolds, A. Jennings, K. Hu, F. Yuan, H. Deng, S. G. Hubscher, J. H. Han, P. Balfe, and J. A. McKeating.** 2008. CD81 and claudin 1 coreceptor association: role in hepatitis C virus entry. J Virol **82:**5007-20.
165. **Hassan, M., D. Selimovic, H. Ghozlan, and O. Abdel-Kader.** 2007. Induction of high-molecular-weight (HMW) tumor necrosis factor(TNF) alpha by hepatitis C virus (HCV) non-structural protein 3 (NS3) in liver cells is AP-1 and NF-kappaB-dependent activation. Cell Signal **19:**301-11.
166. **Havens, W. P., Jr.** 1956. Viral hepatitis: multiple attacks in a narcotic addict. Ann Intern Med **44:**199-203.
167. **Havens, W. P., R. Ward, V. Drill, and J. Paul.** 1944. Experimental production of hepatitis by feeding icterogenic materials. Proceedings of the Society of Experimental Biology and Medicine **57**.
168. **He, L. F., D. Alling, T. Popkin, M. Shapiro, H. J. Alter, and R. H. Purcell.** 1987. Determining the size of non-A, non-B hepatitis virus by filtration. J Infect Dis **156:**636-40.
169. **Heathcote, J., and J. Main.** 2005. Treatment of hepatitis C. J Viral Hepat **12:**223-35.
170. **Heinz, F. X., and S. L. Allison.** 2000. Structures and mechanisms in flavivirus fusion. Adv Virus Res **55:**231-69.
171. **Helle, F., and J. Dubuisson.** 2008. Hepatitis C virus entry into host cells. Cell Mol Life Sci **65:**100-12.
172. **Hertzog, P. J., L. A. O'Neill, and J. A. Hamilton.** 2003. The interferon in TLR signaling: more than just antiviral. Trends Immunol **24:**534-9.
173. **Heydtmann, M., and D. H. Adams.** 2009. Chemokines in the immunopathogenesis of hepatitis C infection. Hepatology **49:**676-88.
174. **Higginbottom, A., E. R. Quinn, C. C. Kuo, M. Flint, L. H. Wilson, E. Bianchi, A. Nicosia, P. N. Monk, J. A. McKeating, and S. Levy.** 2000. Identification of amino acid residues in CD81 critical for interaction with hepatitis C virus envelope glycoprotein E2. J Virol **74:**3642-9.
175. **Hijikata, M., H. Mizushima, T. Akagi, S. Mori, N. Kakiuchi, N. Kato, T. Tanaka, K. Kimura, and K. Shimotohno.** 1993. Two distinct proteinase activities required for the processing of a putative nonstructural precursor protein of hepatitis C virus. J Virol **67:**4665-75.
176. **Hiramatsu, N., N. Hayashi, K. Katayama, K. Mochizuki, Y. Kawanishi, A. Kasahara, H. Fusamoto, and T. Kamada.** 1994. Immunohistochemical

detection of Fas antigen in liver tissue of patients with chronic hepatitis C. Hepatology **19:**1354-9.

177. **Hirowatari, Y., M. Hijikata, and K. Shimotohno.** 1995. A novel method for analysis of viral proteinase activity encoded by hepatitis C virus in cultured cells. Anal Biochem **225:**113-20.
178. **Hirschberg, K., C. M. Miller, J. Ellenberg, J. F. Presley, E. D. Siggia, R. D. Phair, and J. Lippincott-Schwartz.** 1998. Kinetic analysis of secretory protein traffic and characterization of golgi to plasma membrane transport intermediates in living cells. J Cell Biol **143:**1485-503.
179. **Hoevel, T., R. Macek, O. Mundigl, K. Swisshelm, and M. Kubbies.** 2002. Expression and targeting of the tight junction protein CLDN1 in CLDN1-negative human breast tumor cells. J Cell Physiol **191:**60-8.
180. **Honda, M., S. Kaneko, T. Shimazaki, E. Matsushita, K. Kobayashi, L. H. Ping, H. C. Zhang, and S. M. Lemon.** 2000. Hepatitis C virus core protein induces apoptosis and impairs cell-cycle regulation in stably transformed Chinese hamster ovary cells. Hepatology **31:**1351-9.
181. **Hou, J., D. L. Paul, and D. A. Goodenough.** 2005. Paracellin-1 and the modulation of ion selectivity of tight junctions. J Cell Sci **118:**5109-18.
182. **Hsu, E. C., B. Hsi, M. Hirota-Tsuchihara, J. Ruland, C. Iorio, F. Sarangi, J. Diao, G. Migliaccio, D. L. Tyrrell, N. Kneteman, and C. D. Richardson.** 2003. Modified apoptotic molecule (BID) reduces hepatitis C virus infection in mice with chimeric human livers. Nat Biotechnol **21:**519-25.
183. **Hsu, M., J. Zhang, M. Flint, C. Logvinoff, C. Cheng-Mayer, C. M. Rice, and J. A. McKeating.** 2003. Hepatitis C virus glycoproteins mediate pH-dependent cell entry of pseudotyped retroviral particles. Proc Natl Acad Sci U S A **100:**7271-6.
184. **Huang, H., F. Sun, D. M. Owen, W. Li, Y. Chen, M. Gale, Jr., and J. Ye.** 2007. Hepatitis C virus production by human hepatocytes dependent on assembly and secretion of very low-density lipoproteins. Proc Natl Acad Sci U S A **104:**5848-53.
185. **Iacovacci, S., A. Manzin, S. Barca, M. Sargiacomo, A. Serafino, M. B. Valli, G. Macioce, H. J. Hassan, A. Ponzetto, M. Clementi, C. Peschle, and G. Carloni.** 1997. Molecular characterization and dynamics of hepatitis C virus replication in human fetal hepatocytes infected in vitro. Hepatology **26:**1328-37.
186. **Iacovacci, S., M. Sargiacomo, I. Parolini, A. Ponzetto, C. Peschle, and G. Carloni.** 1993. Replication and multiplication of hepatitis C virus genome in human foetal liver cells. Res Virol **144:**275-9.
187. **Ikeda, M., M. Yi, K. Li, and S. M. Lemon.** 2002. Selectable subgenomic and genome-length dicistronic RNAs derived from an infectious molecular clone of the HCV-N strain of hepatitis C virus replicate efficiently in cultured Huh7 cells. J Virol **76:**2997-3006.
188. **Inai, T., J. Kobayashi, and Y. Shibata.** 1999. Claudin-1 contributes to the epithelial barrier function in MDCK cells. Eur J Cell Biol **78:**849-55.
189. **Ishii, N., K. Watashi, T. Hishiki, K. Goto, D. Inoue, M. Hijikata, T. Wakita, N. Kato, and K. Shimotohno.** 2006. Diverse effects of cyclosporine on hepatitis C virus strain replication. J Virol **80:**4510-20.
190. **Itoh, M., M. Furuse, K. Morita, K. Kubota, M. Saitou, and S. Tsukita.** 1999. Direct binding of three tight junction-associated MAGUKs, ZO-1, ZO-2, and ZO-3, with the COOH termini of claudins. J Cell Biol **147:**1351-63.

191. **Itoh, M., K. Morita, and S. Tsukita.** 1999. Characterization of ZO-2 as a MAGUK family member associated with tight as well as adherens junctions with a binding affinity to occludin and alpha catenin. J Biol Chem **274:**5981-6.
192. **Ivanov, A. I., A. Nusrat, and C. A. Parkos.** 2004. Endocytosis of epithelial apical junctional proteins by a clathrin-mediated pathway into a unique storage compartment. Mol Biol Cell **15:**176-88.
193. **Iwasaki, A., and R. Medzhitov.** 2004. Toll-like receptor control of the adaptive immune responses. Nat Immunol **5:**987-95.
194. **Jarrossay, D., G. Napolitani, M. Colonna, F. Sallusto, and A. Lanzavecchia.** 2001. Specialization and complementarity in microbial molecule recognition by human myeloid and plasmacytoid dendritic cells. Eur J Immunol **31:**3388-93.
195. **Ji, Y., B. Jian, N. Wang, Y. Sun, M. L. Moya, M. C. Phillips, G. H. Rothblat, J. B. Swaney, and A. R. Tall.** 1997. Scavenger receptor BI promotes high density lipoprotein-mediated cellular cholesterol efflux. J Biol Chem **272:**20982-5.
196. **Jian, B., M. de la Llera-Moya, Y. Ji, N. Wang, M. C. Phillips, J. B. Swaney, A. R. Tall, and G. H. Rothblat.** 1998. Scavenger receptor class B type I as a mediator of cellular cholesterol efflux to lipoproteins and phospholipid acceptors. J Biol Chem **273:**5599-606.
197. **Kabir, A., S. M. Alavian, and H. Keyvani.** 2006. Distribution of hepatitis C virus genotypes in patients infected by different sources and its correlation with clinical and virological parameters: a preliminary study. Comp Hepatol **5:**4.
198. **Kanda, T., R. Steele, R. Ray, and R. B. Ray.** 2008. Hepatitis C virus core protein augments androgen receptor-mediated signaling. J Virol **82:**11066-72.
199. **Kaneko, T., Y. Tanji, S. Satoh, M. Hijikata, S. Asabe, K. Kimura, and K. Shimotohno.** 1994. Production of two phosphoproteins from the NS5A region of the hepatitis C viral genome. Biochem Biophys Res Commun **205:**320-6.
200. **Kanmogne, G. D., K. Schall, J. Leibhart, B. Knipe, H. E. Gendelman, and Y. Persidsky.** 2007. HIV-1 gp120 compromises blood-brain barrier integrity and enhances monocyte migration across blood-brain barrier: implication for viral neuropathogenesis. J Cereb Blood Flow Metab **27:**123-34.
201. **Kao, C. C., A. M. Del Vecchio, and W. Zhong.** 1999. De novo initiation of RNA synthesis by a recombinant flaviviridae RNA-dependent RNA polymerase. Virology **253:**1-7.
202. **Karlinger, K., T. Gyorke, E. Mako, A. Mester, and Z. Tarjan.** 2000. The epidemiology and the pathogenesis of inflammatory bowel disease. Eur J Radiol **35:**154-67.
203. **Kato, N., K. Sugiyama, K. Namba, H. Dansako, T. Nakamura, M. Takami, K. Naka, A. Nozaki, and K. Shimotohno.** 2003. Establishment of a hepatitis C virus subgenomic replicon derived from human hepatocytes infected in vitro. Biochem Biophys Res Commun **306:**756-66.
204. **Katz, K. D., D. Hollander, C. M. Vadheim, C. McElree, T. Delahunty, V. D. Dadufalza, P. Krugliak, and J. I. Rotter.** 1989. Intestinal permeability in patients with Crohn's disease and their healthy relatives. Gastroenterology **97:**927-31.
205. **Katze, M. G., Y. He, and M. Gale, Jr.** 2002. Viruses and interferon: a fight for supremacy. Nat Rev Immunol **2:**675-87.
206. **Kausalya, P. J., D. C. Phua, and W. Hunziker.** 2004. Association of ARVCF with zonula occludens (ZO)-1 and ZO-2: binding to PDZ-domain proteins and

cell-cell adhesion regulate plasma membrane and nuclear localization of ARVCF. Mol Biol Cell **15:**5503-15.

207. **Kawai, T., and S. Akira.** 2006. Innate immune recognition of viral infection. Nat Immunol **7:**131-7.
208. **Kevil, C. G., D. K. Payne, E. Mire, and J. S. Alexander.** 1998. Vascular permeability factor/vascular endothelial cell growth factor-mediated permeability occurs through disorganization of endothelial junctional proteins. J Biol Chem **273:**15099-103.
209. **Kielian, M.** 2006. Class II virus membrane fusion proteins. Virology **344:**38-47.
210. **Kielian, M., and F. A. Rey.** 2006. Virus membrane-fusion proteins: more than one way to make a hairpin. Nat Rev Microbiol **4:**67-76.
211. **Knust, E., and O. Bossinger.** 2002. Composition and formation of intercellular junctions in epithelial cells. Science **298:**1955-9.
212. **Kocher, O., A. Yesilaltay, C. Cirovic, R. Pal, A. Rigotti, and M. Krieger.** 2003. Targeted disruption of the PDZK1 gene in mice causes tissue-specific depletion of the high density lipoprotein receptor scavenger receptor class B type I and altered lipoprotein metabolism. J Biol Chem **278:**52820-5.
213. **Kolykhalov, A. A., E. V. Agapov, K. J. Blight, K. Mihalik, S. M. Feinstone, and C. M. Rice.** 1997. Transmission of hepatitis C by intrahepatic inoculation with transcribed RNA. Science **277:**570-4.
214. **Kolykhalov, A. A., E. V. Agapov, and C. M. Rice.** 1994. Specificity of the hepatitis C virus NS3 serine protease: effects of substitutions at the 3/4A, 4A/4B, 4B/5A, and 5A/5B cleavage sites on polyprotein processing. J Virol **68:**7525-33.
215. **Koutsoudakis, G., E. Herrmann, S. Kallis, R. Bartenschlager, and T. Pietschmann.** 2007. The level of CD81 cell surface expression is a key determinant for productive entry of hepatitis C virus into host cells. J Virol **81:**588-98.
216. **Koutsoudakis, G., A. Kaul, E. Steinmann, S. Kallis, V. Lohmann, T. Pietschmann, and R. Bartenschlager.** 2006. Characterization of the early steps of hepatitis C virus infection by using luciferase reporter viruses. J Virol **80:**5308-20.
217. **Kowdley, K. V.** 1999. TNF-alpha in chronic hepatitis C: the smoking gun? Am J Gastroenterol **94:**1132-5.
218. **Kreitzer, G., A. Marmorstein, P. Okamoto, R. Vallee, and E. Rodriguez-Boulan.** 2000. Kinesin and dynamin are required for post-Golgi transport of a plasma-membrane protein. Nat Cell Biol **2:**125-7.
219. **Krieger, N., V. Lohmann, and R. Bartenschlager.** 2001. Enhancement of hepatitis C virus RNA replication by cell culture-adaptive mutations. J Virol **75:**4614-24.
220. **Krugman, S.** 1964. Studies on the Natural History and Prevention of Infectious Hepatitis. Tijdschr Gastroenterol **36:**236.
221. **Krugman, S., and J. P. Giles.** 1970. Viral hepatitis. New light on an old disease. JAMA **212:**1019-29.
222. **Krugman, S., R. Ward, and J. P. Giles.** 1962. The natural history of infectious hepatitis. Am J Med **32:**717-28.
223. **Kubota, K., M. Furuse, H. Sasaki, N. Sonoda, K. Fujita, A. Nagafuchi, and S. Tsukita.** 1999. Ca(2+)-independent cell-adhesion activity of claudins, a family of integral membrane proteins localized at tight junctions. Curr Biol **9:**1035-8.

224. **Lamas, E., P. Baccarini, C. Housset, D. Kremsdorf, and C. Brechot.** 1992. Detection of hepatitis C virus (HCV) RNA sequences in liver tissue by in situ hybridization. J Hepatol **16:**219-23.
225. **Lanford, R. E., C. Sureau, J. R. Jacob, R. White, and T. R. Fuerst.** 1994. Demonstration of in vitro infection of chimpanzee hepatocytes with hepatitis C virus using strand-specific RT/PCR. Virology **202:**606-14.
226. **Laskus, T., M. Radkowski, A. Piasek, M. Nowicki, A. Horban, J. Cianciara, and J. Rakela.** 2000. Hepatitis C virus in lymphoid cells of patients coinfected with human immunodeficiency virus type 1: evidence of active replication in monocytes/macrophages and lymphocytes. J Infect Dis **181:**442-8.
227. **Laskus, T., M. Radkowski, L. F. Wang, M. Nowicki, and J. Rakela.** 2000. Uneven distribution of hepatitis C virus quasispecies in tissues from subjects with end-stage liver disease: confounding effect of viral adsorption and mounting evidence for the presence of low-level extrahepatic replication. J Virol **74:**1014-7.
228. **Lau, G. K., G. L. Davis, S. P. Wu, R. G. Gish, L. A. Balart, and J. Y. Lau.** 1996. Hepatic expression of hepatitis C virus RNA in chronic hepatitis C: a study by in situ reverse-transcription polymerase chain reaction. Hepatology **23:**1318-23.
229. **Lavillette, D., A. W. Tarr, C. Voisset, P. Donot, B. Bartosch, C. Bain, A. H. Patel, J. Dubuisson, J. K. Ball, and F. L. Cosset.** 2005. Characterization of host-range and cell entry properties of the major genotypes and subtypes of hepatitis C virus. Hepatology **41:**265-74.
230. **Law, M., T. Maruyama, J. Lewis, E. Giang, A. W. Tarr, Z. Stamataki, P. Gastaminza, F. V. Chisari, I. M. Jones, R. I. Fox, J. K. Ball, J. A. McKeating, N. M. Kneteman, and D. R. Burton.** 2008. Broadly neutralizing antibodies protect against hepatitis C virus quasispecies challenge. Nat Med **14:**25-7.
231. **Layden, T. J., N. P. Lam, and T. E. Wiley.** 1999. Hepatitis C viral dynamics. Clin Liver Dis **3:**793-810.
232. **Le Bon, A., G. Schiavoni, G. D'Agostino, I. Gresser, F. Belardelli, and D. F. Tough.** 2001. Type i interferons potently enhance humoral immunity and can promote isotype switching by stimulating dendritic cells in vivo. Immunity **14:**461-70.
233. **Lechner, F., D. K. Wong, P. R. Dunbar, R. Chapman, R. T. Chung, P. Dohrenwend, G. Robbins, R. Phillips, P. Klenerman, and B. D. Walker.** 2000. Analysis of successful immune responses in persons infected with hepatitis C virus. J Exp Med **191:**1499-512.
234. **Lee, J. C., C. F. Chang, Y. H. Chi, D. R. Hwang, and J. T. Hsu.** 2004. A reporter-based assay for identifying hepatitis C virus inhibitors based on subgenomic replicon cells. J Virol Methods **116:**27-33.
235. **Lee, J. C., Y. F. Shih, S. P. Hsu, T. Y. Chang, L. H. Chen, and J. T. Hsu.** 2003. Development of a cell-based assay for monitoring specific hepatitis C virus NS3/4A protease activity in mammalian cells. Anal Biochem **316:**162-70.
236. **Lerat, H., S. Rumin, F. Habersetzer, F. Berby, M. A. Trabaud, C. Trepo, and G. Inchauspe.** 1998. In vivo tropism of hepatitis C virus genomic sequences in hematopoietic cells: influence of viral load, viral genotype, and cell phenotype. Blood **91:**3841-9.
237. **Leroux-Roels, G.** 2005. Development of prophylactic and therapeutic vaccines against hepatitis C virus. Expert Rev Vaccines **4:**351-71.

238. **Levine, R. A., and M. A. Payne.** 1960. Homologous serum hepatitis in youthful heroin users. Ann Intern Med **53:**164-78.
239. **Levy, S., V. Q. Nguyen, M. L. Andria, and S. Takahashi.** 1991. Structure and membrane topology of TAPA-1. J Biol Chem **266:**14597-602.
240. **Levy, S., and T. Shoham.** 2005. The tetraspanin web modulates immune-signalling complexes. Nat Rev Immunol **5:**136-48.
241. **Levy, S., S. C. Todd, and H. T. Maecker.** 1998. CD81 (TAPA-1): a molecule involved in signal transduction and cell adhesion in the immune system. Annu Rev Immunol **16:**89-109.
242. **Li, K., E. Foy, J. C. Ferreon, M. Nakamura, A. C. Ferreon, M. Ikeda, S. C. Ray, M. Gale, Jr., and S. M. Lemon.** 2005. Immune evasion by hepatitis C virus NS3/4A protease-mediated cleavage of the Toll-like receptor 3 adaptor protein TRIF. Proc Natl Acad Sci U S A **102:**2992-7.
243. **Li, X. D., L. Sun, R. B. Seth, G. Pineda, and Z. J. Chen.** 2005. Hepatitis C virus protease NS3/4A cleaves mitochondrial antiviral signaling protein off the mitochondria to evade innate immunity. Proc Natl Acad Sci U S A **102:**17717-22.
244. **Lindenbach, B. D., M. J. Evans, A. J. Syder, B. Wolk, T. L. Tellinghuisen, C. C. Liu, T. Maruyama, R. O. Hynes, D. R. Burton, J. A. McKeating, and C. M. Rice.** 2005. Complete replication of hepatitis C virus in cell culture. Science **309:**623-6.
245. **Lindenbach, B. D., P. Meuleman, A. Ploss, T. Vanwolleghem, A. J. Syder, J. A. McKeating, R. E. Lanford, S. M. Feinstone, M. E. Major, G. Leroux-Roels, and C. M. Rice.** 2006. Cell culture-grown hepatitis C virus is infectious in vivo and can be recultured in vitro. Proc Natl Acad Sci U S A **103:**3805-9.
246. **Lindenbach, B. D., and C. M. Rice.** 2005. Unravelling hepatitis C virus replication from genome to function. Nature **436:**933-8.
247. **Lippincott-Schwartz, J., T. H. Roberts, and K. Hirschberg.** 2000. Secretory protein trafficking and organelle dynamics in living cells. Annu Rev Cell Dev Biol **16:**557-89.
248. **Liu, Q., C. Tackney, R. A. Bhat, A. M. Prince, and P. Zhang.** 1997. Regulated processing of hepatitis C virus core protein is linked to subcellular localization. J Virol **71:**657-62.
249. **Liu, S., W. Yang, L. Shen, J. R. Turner, C. B. Coyne, and T. Wang.** 2009. Tight junction proteins claudin-1 and occludin control hepatitis C virus entry and are downregulated during infection to prevent superinfection. J Virol **83:**2011-4.
250. **Lo, S. Y., M. J. Selby, and J. H. Ou.** 1996. Interaction between hepatitis C virus core protein and E1 envelope protein. J Virol **70:**5177-82.
251. **Logvinoff, C., M. E. Major, D. Oldach, S. Heyward, A. Talal, P. Balfe, S. M. Feinstone, H. Alter, C. M. Rice, and J. A. McKeating.** 2004. Neutralizing antibody response during acute and chronic hepatitis C virus infection. Proc Natl Acad Sci U S A **101:**10149-54.
252. **Lohmann, V., S. Hoffmann, U. Herian, F. Penin, and R. Bartenschlager.** 2003. Viral and cellular determinants of hepatitis C virus RNA replication in cell culture. J Virol **77:**3007-19.
253. **Lohmann, V., F. Korner, A. Dobierzewska, and R. Bartenschlager.** 2001. Mutations in hepatitis C virus RNAs conferring cell culture adaptation. J Virol **75:**1437-49.

254. **Lohmann, V., F. Korner, J. Koch, U. Herian, L. Theilmann, and R. Bartenschlager.** 1999. Replication of subgenomic hepatitis C virus RNAs in a hepatoma cell line. Science **285:**110-3.
255. **Lorenz, I. C., J. A. McKeating, and C. M. Rice.** 2005. Assembly and Entry of Hepatitis C Virus
.
256. **Low, S. H., M. Miura, P. A. Roche, A. C. Valdez, K. E. Mostov, and T. Weimbs.** 2000. Intracellular redirection of plasma membrane trafficking after loss of epithelial cell polarity. Mol Biol Cell **11:**3045-60.
257. **Lozach, P. Y., A. Amara, B. Bartosch, J. L. Virelizier, F. Arenzana-Seisdedos, F. L. Cosset, and R. Altmeyer.** 2004. C-type lectins L-SIGN and DC-SIGN capture and transmit infectious hepatitis C virus pseudotype particles. J Biol Chem **279:**32035-45.
258. **Lozach, P. Y., H. Lortat-Jacob, A. de Lacroix de Lavalette, I. Staropoli, S. Foung, A. Amara, C. Houles, F. Fieschi, O. Schwartz, J. L. Virelizier, F. Arenzana-Seisdedos, and R. Altmeyer.** 2003. DC-SIGN and L-SIGN are high affinity binding receptors for hepatitis C virus glycoprotein E2. J Biol Chem **278:**20358-66.
259. **Ma, Y., J. Yates, Y. Liang, S. M. Lemon, and M. Yi.** 2008. NS3 helicase domains involved in infectious intracellular hepatitis C virus particle assembly. J Virol **82:**7624-39.
260. **MacCallum, F., and W. Bradley.** 1944. Transmission of hepatitis to human volunteers. Lancet **2**.
261. **Machida, K., K. T. Cheng, V. M. Sung, A. M. Levine, S. Foung, and M. M. Lai.** 2006. Hepatitis C virus induces toll-like receptor 4 expression, leading to enhanced production of beta interferon and interleukin-6. J Virol **80:**866-74.
262. **Madara, J. L., and J. Stafford.** 1989. Interferon-gamma directly affects barrier function of cultured intestinal epithelial monolayers. J Clin Invest **83:**724-7.
263. **Maillard, P., T. Huby, U. Andreo, M. Moreau, J. Chapman, and A. Budkowska.** 2006. The interaction of natural hepatitis C virus with human scavenger receptor SR-BI/Cla1 is mediated by ApoB-containing lipoproteins. FASEB J **20:**735-7.
264. **Majeau, N., V. Gagne, A. Boivin, M. Bolduc, J. A. Majeau, D. Ouellet, and D. Leclerc.** 2004. The N-terminal half of the core protein of hepatitis C virus is sufficient for nucleocapsid formation. J Gen Virol **85:**971-81.
265. **Mankertz, J., S. Tavalali, H. Schmitz, A. Mankertz, E. O. Riecken, M. Fromm, and J. D. Schulzke.** 2000. Expression from the human occludin promoter is affected by tumor necrosis factor alpha and interferon gamma. J Cell Sci **113 (Pt 11):**2085-90.
266. **Marano, C. W., S. A. Lewis, L. A. Garulacan, A. P. Soler, and J. M. Mullin.** 1998. Tumor necrosis factor-alpha increases sodium and chloride conductance across the tight junction of CACO-2 BBE, a human intestinal epithelial cell line. J Membr Biol **161:**263-74.
267. **Marsh, M., and A. Helenius.** 2006. Virus entry: open sesame. Cell **124:**729-40.
268. **Marsh, M., and A. Pelchen-Matthews.** 2000. Endocytosis in viral replication. Traffic **1:**525-32.
269. **Matsumoto, M., S. B. Hwang, K. S. Jeng, N. Zhu, and M. M. Lai.** 1996. Homotypic interaction and multimerization of hepatitis C virus core protein. Virology **218:**43-51.

270. **Mazzeo, C., F. Azzaroli, S. Giovanelli, A. Dormi, D. Festi, A. Colecchia, A. Miracolo, P. Natale, G. Nigro, A. Alberti, E. Roda, and G. Mazzella.** 2003. Ten year incidence of HCV infection in northern Italy and frequency of spontaneous viral clearance. Gut **52:**1030-4.
271. **McCarthy, K. M., S. A. Francis, J. M. McCormack, J. Lai, R. A. Rogers, I. B. Skare, R. D. Lynch, and E. E. Schneeberger.** 2000. Inducible expression of claudin-1-myc but not occludin-VSV-G results in aberrant tight junction strand formation in MDCK cells. J Cell Sci **113 Pt 19:**3387-98.
272. **McCaughan, G. W., and A. Zekry.** 2004. Mechanisms of HCV reinfection and allograft damage after liver transplantation. J Hepatol **40:**368-74.
273. **McKeating, J. A., L. Q. Zhang, C. Logvinoff, M. Flint, J. Zhang, J. Yu, D. Butera, D. D. Ho, L. B. Dustin, C. M. Rice, and P. Balfe.** 2004. Diverse hepatitis C virus glycoproteins mediate viral infection in a CD81-dependent manner. J Virol **78:**8496-505.
274. **McKenna, K., A. S. Beignon, and N. Bhardwaj.** 2005. Plasmacytoid dendritic cells: linking innate and adaptive immunity. J Virol **79:**17-27.
275. **McLauchlan, J., M. K. Lemberg, G. Hope, and B. Martoglio.** 2002. Intramembrane proteolysis promotes trafficking of hepatitis C virus core protein to lipid droplets. Embo J **21:**3980-8.
276. **McOmish, F., P. L. Yap, B. C. Dow, E. A. Follett, C. Seed, A. J. Keller, T. J. Cobain, T. Krusius, E. Kolho, R. Naukkarinen, and et al.** 1994. Geographical distribution of hepatitis C virus genotypes in blood donors: an international collaborative survey. J Clin Microbiol **32:**884-92.
277. **Mee, C. J., J. Grove, H. J. Harris, K. Hu, P. Balfe, and J. A. McKeating.** 2008. Effect of cell polarization on hepatitis C virus entry. J Virol **82:**461-70.
278. **Meertens, L., C. Bertaux, and T. Dragic.** 2006. Hepatitis C virus entry requires a critical postinternalization step and delivery to early endosomes via clathrin-coated vesicles. J Virol **80:**11571-8.
279. **Mercer, D. F., D. E. Schiller, J. F. Elliott, D. N. Douglas, C. Hao, A. Rinfret, W. R. Addison, K. P. Fischer, T. A. Churchill, J. R. Lakey, D. L. Tyrrell, and N. M. Kneteman.** 2001. Hepatitis C virus replication in mice with chimeric human livers. Nat Med **7:**927-33.
280. **Meuleman, P., J. Hesselgesser, M. Paulson, T. Vanwolleghem, I. Desombere, H. Reiser, and G. Leroux-Roels.** 2008. Anti-CD81 antibodies can prevent a hepatitis C virus infection in vivo. Hepatology **48:**1761-8.
281. **Meuleman, P., L. Libbrecht, R. De Vos, B. de Hemptinne, K. Gevaert, J. Vandekerckhove, T. Roskams, and G. Leroux-Roels.** 2005. Morphological and biochemical characterization of a human liver in a uPA-SCID mouse chimera. Hepatology **41:**847-56.
282. **Meunier, J. C., R. E. Engle, K. Faulk, M. Zhao, B. Bartosch, H. Alter, S. U. Emerson, F. L. Cosset, R. H. Purcell, and J. Bukh.** 2005. Evidence for cross-genotype neutralization of hepatitis C virus pseudo-particles and enhancement of infectivity by apolipoprotein C1. Proc Natl Acad Sci U S A **102:**4560-5.
283. **Milligan, S. A., M. W. Owens, and M. B. Grisham.** 1996. Inhibition of IkappaB-alpha and IkappaB-beta proteolysis by calpain inhibitor I blocks nitric oxide synthesis. Arch Biochem Biophys **335:**388-95.
284. **Missale, G., R. Bertoni, V. Lamonaca, A. Valli, M. Massari, C. Mori, M. G. Rumi, M. Houghton, F. Fiaccadori, and C. Ferrari.** 1996. Different clinical behaviors of acute hepatitis C virus infection are associated with different vigor of the anti-viral cell-mediated immune response. J Clin Invest **98:**706-14.

285. **Miyanari, Y., K. Atsuzawa, N. Usuda, K. Watashi, T. Hishiki, M. Zayas, R. Bartenschlager, T. Wakita, M. Hijikata, and K. Shimotohno.** 2007. The lipid droplet is an important organelle for hepatitis C virus production. Nat Cell Biol **9:**1089-97.
286. **Miyanari, Y., M. Hijikata, M. Yamaji, M. Hosaka, H. Takahashi, and K. Shimotohno.** 2003. Hepatitis C virus non-structural proteins in the probable membranous compartment function in viral genome replication. J Biol Chem **278:**50301-8.
287. **Molina, S., V. Castet, C. Fournier-Wirth, L. Pichard-Garcia, R. Avner, D. Harats, J. Roitelman, R. Barbaras, P. Graber, P. Ghersa, M. Smolarsky, A. Funaro, F. Malavasi, D. Larrey, J. Coste, J. M. Fabre, A. Sa-Cunha, and P. Maurel.** 2007. The low-density lipoprotein receptor plays a role in the infection of primary human hepatocytes by hepatitis C virus. J Hepatol **46:**411-9.
288. **Monazahian, M., I. Bohme, S. Bonk, A. Koch, C. Scholz, S. Grethe, and R. Thomssen.** 1999. Low density lipoprotein receptor as a candidate receptor for hepatitis C virus. J Med Virol **57:**223-9.
289. **Moradpour, D., R. Gosert, D. Egger, F. Penin, H. E. Blum, and K. Bienz.** 2003. Membrane association of hepatitis C virus nonstructural proteins and identification of the membrane alteration that harbors the viral replication complex. Antiviral Res **60:**103-9.
290. **Moradpour, D., F. Penin, and C. M. Rice.** 2007. Replication of hepatitis C virus. Nat Rev Microbiol **5:**453-63.
291. **Morita, K., M. Furuse, K. Fujimoto, and S. Tsukita.** 1999. Claudin multigene family encoding four-transmembrane domain protein components of tight junction strands. Proc Natl Acad Sci U S A **96:**511-6.
292. **Moriya, K., H. Fujie, Y. Shintani, H. Yotsuyanagi, T. Tsutsumi, K. Ishibashi, Y. Matsuura, S. Kimura, T. Miyamura, and K. Koike.** 1998. The core protein of hepatitis C virus induces hepatocellular carcinoma in transgenic mice. Nat Med **4:**1065-7.
293. **Moriya, K., H. Fujie, H. Yotsuyanagi, Y. Shintani, T. Tsutsumi, Y. Matsuura, T. Miyamura, S. Kimura, and K. Koike.** 1997. Subcellular localization of hepatitis C virus structural proteins in the liver of transgenic mice. Jpn J Med Sci Biol **50:**169-77.
294. **Mosley, J. W.** 1975. The epidemiology of viral hepatitis: an overview. Am J Med Sci **270:**253-70.
295. **Mousavi, S. A., L. Malerod, T. Berg, and R. Kjeken.** 2004. Clathrin-dependent endocytosis. Biochem J **377:**1-16.
296. **Mukherjee, S., R. N. Ghosh, and F. R. Maxfield.** 1997. Endocytosis. Physiol Rev **77:**759-803.
297. **Muller, S. L., M. Portwich, A. Schmidt, D. I. Utepbergenov, O. Huber, I. E. Blasig, and G. Krause.** 2005. The tight junction protein occludin and the adherens junction protein alpha-catenin share a common interaction mechanism with ZO-1. J Biol Chem **280:**3747-56.
298. **Musch, A., H. Xu, D. Shields, and E. Rodriguez-Boulan.** 1996. Transport of vesicular stomatitis virus G protein to the cell surface is signal mediated in polarized and nonpolarized cells. J Cell Biol **133:**543-58.
299. **Nahmias, Y., J. Goldwasser, M. Casali, D. van Poll, T. Wakita, R. T. Chung, and M. L. Yarmush.** 2008. Apolipoprotein B-dependent hepatitis C virus secretion is inhibited by the grapefruit flavonoid naringenin. Hepatology **47:**1437-45.

300. **Nakagawa, M., N. Sakamoto, Y. Tanabe, T. Koyama, Y. Itsui, Y. Takeda, C. H. Chen, S. Kakinuma, S. Oooka, S. Maekawa, N. Enomoto, and M. Watanabe.** 2005. Suppression of hepatitis C virus replication by cyclosporin a is mediated by blockade of cyclophilins. Gastroenterology **129:**1031-41.
301. **Napoli, J., G. A. Bishop, P. H. McGuinness, D. M. Painter, and G. W. McCaughan.** 1996. Progressive liver injury in chronic hepatitis C infection correlates with increased intrahepatic expression of Th1-associated cytokines. Hepatology **24:**759-65.
302. **Nascimbeni, M., E. Mizukoshi, M. Bosmann, M. E. Major, K. Mihalik, C. M. Rice, S. M. Feinstone, and B. Rehermann.** 2003. Kinetics of CD4+ and CD8+ memory T-cell responses during hepatitis C virus rechallenge of previously recovered chimpanzees. J Virol **77:**4781-93.
303. **Nasimuzzaman, M., G. Waris, D. Mikolon, D. G. Stupack, and A. Siddiqui.** 2007. Hepatitis C virus stabilizes hypoxia-inducible factor 1alpha and stimulates the synthesis of vascular endothelial growth factor. J Virol **81:**10249-57.
304. **Nattermann, J., G. Feldmann, G. Ahlenstiel, B. Langhans, T. Sauerbruch, and U. Spengler.** 2006. Surface expression and cytolytic function of natural killer cell receptors is altered in chronic hepatitis C. Gut **55:**869-77.
305. **Navas, S., J. Martin, J. A. Quiroga, I. Castillo, and V. Carreno.** 1998. Genetic diversity and tissue compartmentalization of the hepatitis C virus genome in blood mononuclear cells, liver, and serum from chronic hepatitis C patients. J Virol **72:**1640-6.
306. **Neefe, J. R., J. Stokes, and J. G. Reinhold.** 1945. Oral administration to volunteers of feces from patients with homologous serum hepatitis and infectious (epidemic) hepatitis. American Journal of Medical Science **210**.
307. **Nelson, D. R.** 2001. The immunopathogenesis of hepatitis C virus infection. Clin Liver Dis **5:**931-53.
308. **Nelson, H. B., and H. Tang.** 2006. Effect of cell growth on hepatitis C virus (HCV) replication and a mechanism of cell confluence-based inhibition of HCV RNA and protein expression. J Virol **80:**1181-90.
309. **Nielsen, S. U., M. F. Bassendine, A. D. Burt, C. Martin, W. Pumeechockchai, and G. L. Toms.** 2006. Association between hepatitis C virus and very-low-density lipoprotein (VLDL)/LDL analyzed in iodixanol density gradients. J Virol **80:**2418-28.
310. **O'Neill, L. A.** 2004. Immunology. After the toll rush. Science **303:**1481-2.
311. **Okazaki, M., K. Hino, K. Fujii, N. Kobayashi, and K. Okita.** 1996. Hepatic Fas antigen expression before and after interferon therapy in patients with chronic hepatitis C. Dig Dis Sci **41:**2453-8.
312. **Pachiadakis, I., G. Pollara, B. M. Chain, and N. V. Naoumov.** 2005. Is hepatitis C virus infection of dendritic cells a mechanism facilitating viral persistence? Lancet Infect Dis **5:**296-304.
313. **Pacini, L., L. Bartholomew, A. Vitelli, and G. Migliaccio.** 2004. Reporter substrates for assessing the activity of the hepatitis C virus NS3-4A serine protease in living cells. Anal Biochem **331:**46-59.
314. **Pasquinelli, C., J. M. Shoenberger, J. Chung, K. M. Chang, L. G. Guidotti, M. Selby, K. Berger, R. Lesniewski, M. Houghton, and F. V. Chisari.** 1997. Hepatitis C virus core and E2 protein expression in transgenic mice. Hepatology **25:**719-27.
315. **Patzwahl, R., V. Meier, G. Ramadori, and S. Mihm.** 2001. Enhanced expression of interferon-regulated genes in the liver of patients with chronic

hepatitis C virus infection: detection by suppression-subtractive hybridization. J Virol **75:**1332-8.

316. **Paul, J., W. P. Havens, and A. Sabin.** 1945. Transmission experiments in serum jaundice and infectious hepatitis. Journal of the American Medical Association **128**.
317. **Pawlotsky, J. M.** 1999. Diagnostic tests for hepatitis C. J Hepatol **31 Suppl 1:**71-9.
318. **Penin, F., J. Dubuisson, F. A. Rey, D. Moradpour, and J. M. Pawlotsky.** 2004. Structural biology of hepatitis C virus. Hepatology **39:**5-19.
319. **Pestka, J. M., M. B. Zeisel, E. Blaser, P. Schurmann, B. Bartosch, F. L. Cosset, A. H. Patel, H. Meisel, J. Baumert, S. Viazov, K. Rispeter, H. E. Blum, M. Roggendorf, and T. F. Baumert.** 2007. Rapid induction of virus-neutralizing antibodies and viral clearance in a single-source outbreak of hepatitis C. Proc Natl Acad Sci U S A **104:**6025-30.
320. **Petracca, R., F. Falugi, G. Galli, N. Norais, D. Rosa, S. Campagnoli, V. Burgio, E. Di Stasio, B. Giardina, M. Houghton, S. Abrignani, and G. Grandi.** 2000. Structure-function analysis of hepatitis C virus envelope-CD81 binding. J Virol **74:**4824-30.
321. **Pianko, S., S. Patella, G. Ostapowicz, P. Desmond, and W. Sievert.** 2001. Fas-mediated hepatocyte apoptosis is increased by hepatitis C virus infection and alcohol consumption, and may be associated with hepatic fibrosis: mechanisms of liver cell injury in chronic hepatitis C virus infection. J Viral Hepat **8:**406-13.
322. **Pietschmann, T., V. Lohmann, A. Kaul, N. Krieger, G. Rinck, G. Rutter, D. Strand, and R. Bartenschlager.** 2002. Persistent and transient replication of full-length hepatitis C virus genomes in cell culture. J Virol **76:**4008-21.
323. **Pietschmann, T., V. Lohmann, G. Rutter, K. Kurpanek, and R. Bartenschlager.** 2001. Characterization of cell lines carrying self-replicating hepatitis C virus RNAs. J Virol **75:**1252-64.
324. **Pileri, P., Y. Uematsu, S. Campagnoli, G. Galli, F. Falugi, R. Petracca, A. J. Weiner, M. Houghton, D. Rosa, G. Grandi, and S. Abrignani.** 1998. Binding of hepatitis C virus to CD81. Science **282:**938-41.
325. **Pinzani, M., and F. Marra.** 2001. Cytokine receptors and signaling in hepatic stellate cells. Semin Liver Dis **21:**397-416.
326. **Ploss, A., M. J. Evans, V. A. Gaysinskaya, M. Panis, H. You, Y. P. de Jong, and C. M. Rice.** 2009. Human occludin is a hepatitis C virus entry factor required for infection of mouse cells. Nature **457:**882-6.
327. **Pohlmann, S., J. Zhang, F. Baribaud, Z. Chen, G. J. Leslie, G. Lin, A. Granelli-Piperno, R. W. Doms, C. M. Rice, and J. A. McKeating.** 2003. Hepatitis C virus glycoproteins interact with DC-SIGN and DC-SIGNR. J Virol **77:**4070-80.
328. **Polyak, S. J., K. S. Khabar, D. M. Paschal, H. J. Ezelle, G. Duverlie, G. N. Barber, D. E. Levy, N. Mukaida, and D. R. Gretch.** 2001. Hepatitis C virus nonstructural 5A protein induces interleukin-8, leading to partial inhibition of the interferon-induced antiviral response. J Virol **75:**6095-106.
329. **Polyak, S. J., K. S. Khabar, M. Rezeiq, and D. R. Gretch.** 2001. Elevated levels of interleukin-8 in serum are associated with hepatitis C virus infection and resistance to interferon therapy. J Virol **75:**6209-11.
330. **Prince, A. M., B. Brotman, G. F. Grady, W. J. Kuhns, C. Hazzi, R. W. Levine, and S. J. Millian.** 1974. Long-incubation post-transfusion hepatitis without serological evidence of exposure to hepatitis-B virus. Lancet **2:**241-6.

331. **Prince, A. M., B. Brotman, T. Huima, D. Pascual, M. Jaffery, and G. Inchauspe.** 1992. Immunity in hepatitis C infection. J Infect Dis **165:**438-43.
332. **Reed, K. E., J. Xu, and C. M. Rice.** 1997. Phosphorylation of the hepatitis C virus NS5A protein in vitro and in vivo: properties of the NS5A-associated kinase. J Virol **71:**7187-97.
333. **Rehermann, B., and M. Nascimbeni.** 2005. Immunology of hepatitis B virus and hepatitis C virus infection. Nat Rev Immunol **5:**215-29.
334. **Resti, M., P. Jara, L. Hierro, C. Azzari, R. Giacchino, G. Zuin, L. Zancan, S. Pedditzi, and F. Bortolotti.** 2003. Clinical features and progression of perinatally acquired hepatitis C virus infection. J Med Virol **70:**373-7.
335. **Reynolds, G. M., H. J. Harris, A. Jennings, K. Hu, J. Grove, P. F. Lalor, D. H. Adams, P. Balfe, S. G. Hubscher, and J. A. McKeating.** 2008. Hepatitis C virus receptor expression in normal and diseased liver tissue. Hepatology **47:**418-27.
336. **Rhainds, D., and L. Brissette.** 2004. The role of scavenger receptor class B type I (SR-BI) in lipid trafficking. defining the rules for lipid traders. Int J Biochem Cell Biol **36:**39-77.
337. **Rocha-Perugini, V., C. Montpellier, D. Delgrange, C. Wychowski, F. Helle, A. Pillez, H. Drobecq, F. Le Naour, S. Charrin, S. Levy, E. Rubinstein, J. Dubuisson, and L. Cocquerel.** 2008. The CD81 partner EWI-2wint inhibits hepatitis C virus entry. PLoS ONE **3:**e1866.
338. **Rodrigueza, W. V., S. T. Thuahnai, R. E. Temel, S. Lund-Katz, M. C. Phillips, and D. L. Williams.** 1999. Mechanism of scavenger receptor class B type I-mediated selective uptake of cholesteryl esters from high density lipoprotein to adrenal cells. J Biol Chem **274:**20344-50.
339. **Romagnani, P., F. Annunziato, E. Lazzeri, L. Cosmi, C. Beltrame, L. Lasagni, G. Galli, M. Francalanci, R. Manetti, F. Marra, V. Vanini, E. Maggi, and S. Romagnani.** 2001. Interferon-inducible protein 10, monokine induced by interferon gamma, and interferon-inducible T-cell alpha chemoattractant are produced by thymic epithelial cells and attract T-cell receptor (TCR) alphabeta+ CD8+ single-positive T cells, TCRgammadelta+ T cells, and natural killer-type cells in human thymus. Blood **97:**601-7.
340. **Rosenstein, B. J.** 1967. Viral hepatitis in narcotics users. An outbreak in Rhode Island. JAMA **199:**698-700.
341. **Rost F., O. R.** 2000. Fluoescence Miroscopy: Photography with a Microscope, 2 ed. Cambridge University Press, Cambridge, UK.
342. **Rubbia-Brandt, L., P. Fabris, S. Paganin, G. Leandro, P. J. Male, E. Giostra, A. Carlotto, L. Bozzola, A. Smedile, and F. Negro.** 2004. Steatosis affects chronic hepatitis C progression in a genotype specific way. Gut **53:**406-12.
343. **Rubbia-Brandt, L., R. Quadri, K. Abid, E. Giostra, P. J. Male, G. Mentha, L. Spahr, J. P. Zarski, B. Borisch, A. Hadengue, and F. Negro.** 2000. Hepatocyte steatosis is a cytopathic effect of hepatitis C virus genotype 3. J Hepatol **33:**106-15.
344. **Rubinstein, E., F. Le Naour, C. Lagaudriere-Gesbert, M. Billard, H. Conjeaud, and C. Boucheix.** 1996. CD9, CD63, CD81, and CD82 are components of a surface tetraspan network connected to HLA-DR and VLA integrins. Eur J Immunol **26:**2657-65.
345. **Sala-Valdes, M., A. Ursa, S. Charrin, E. Rubinstein, M. E. Hemler, F. Sanchez-Madrid, and M. Yanez-Mo.** 2006. EWI-2 and EWI-F link the tetraspanin web to the actin cytoskeleton through their direct association with ezrin-radixin-moesin proteins. J Biol Chem **281:**19665-75.

346. **Sandle, G. I., N. Higgs, P. Crowe, M. N. Marsh, S. Venkatesan, and T. J. Peters.** 1990. Cellular basis for defective electrolyte transport in inflamed human colon. Gastroenterology **99:**97-105.
347. **Sangar, D. V., and A. R. Carroll.** 1998. A tale of two strands: reverse-transcriptase polymerase chain reaction detection of hepatitis C virus replication. Hepatology **28:**1173-6.
348. **Sartor, R. B.** 2003. Targeting enteric bacteria in treatment of inflammatory bowel diseases: why, how, and when. Curr Opin Gastroenterol **19:**358-65.
349. **Scarselli, E., H. Ansuini, R. Cerino, R. M. Roccasecca, S. Acali, G. Filocamo, C. Traboni, A. Nicosia, R. Cortese, and A. Vitelli.** 2002. The human scavenger receptor class B type I is a novel candidate receptor for the hepatitis C virus. Embo J **21:**5017-25.
350. **Schmidt-Mende, J., E. Bieck, T. Hugle, F. Penin, C. M. Rice, H. E. Blum, and D. Moradpour.** 2001. Determinants for membrane association of the hepatitis C virus RNA-dependent RNA polymerase. J Biol Chem **276:**44052-63.
351. **Schmitt, M., A. Horbach, R. Kubitz, A. Frilling, and D. Haussinger.** 2004. Disruption of hepatocellular tight junctions by vascular endothelial growth factor (VEGF): a novel mechanism for tumor invasion. J Hepatol **41:**274-83.
352. **Scholle, F., K. Li, F. Bodola, M. Ikeda, B. A. Luxon, and S. M. Lemon.** 2004. Virus-host cell interactions during hepatitis C virus RNA replication: impact of polyprotein expression on the cellular transcriptome and cell cycle association with viral RNA synthesis. J Virol **78:**1513-24.
353. **Selby, M. J., E. Glazer, F. Masiarz, and M. Houghton.** 1994. Complex processing and protein:protein interactions in the E2:NS2 region of HCV. Virology **204:**114-22.
354. **Sen, G. C.** 2001. Viruses and interferons. Annu Rev Microbiol **55:**255-81.
355. **Shavinskaya, A., S. Boulant, F. Penin, J. McLauchlan, and R. Bartenschlager.** 2007. The lipid droplet binding domain of hepatitis C virus core protein is a major determinant for efficient virus assembly. J Biol Chem **282:**37158-69.
356. **Shen, L., C. R. Weber, and J. R. Turner.** 2008. The tight junction protein complex undergoes rapid and continuous molecular remodeling at steady state. J Cell Biol **181:**683-95.
357. **Sherwood, S. W., A. L. Kung, J. Roitelman, R. D. Simoni, and R. T. Schimke.** 1993. In vivo inhibition of cyclin B degradation and induction of cell-cycle arrest in mammalian cells by the neutral cysteine protease inhibitor N-acetylleucylleucylnorleucinal. Proc Natl Acad Sci U S A **90:**3353-7.
358. **Shields, P. L., C. M. Morland, M. Salmon, S. Qin, S. G. Hubscher, and D. H. Adams.** 1999. Chemokine and chemokine receptor interactions provide a mechanism for selective T cell recruitment to specific liver compartments within hepatitis C-infected liver. J Immunol **163:**6236-43.
359. **Shimoike, T., S. Mimori, H. Tani, Y. Matsuura, and T. Miyamura.** 1999. Interaction of hepatitis C virus core protein with viral sense RNA and suppression of its translation. J Virol **73:**9718-25.
360. **Shin, K., V. C. Fogg, and B. Margolis.** 2006. Tight junctions and cell polarity. Annu Rev Cell Dev Biol **22:**207-35.
361. **Shirota, Y., H. Luo, W. Qin, S. Kaneko, T. Yamashita, K. Kobayashi, and S. Murakami.** 2002. Hepatitis C virus (HCV) NS5A binds RNA-dependent RNA polymerase (RdRP) NS5B and modulates RNA-dependent RNA polymerase activity. J Biol Chem **277:**11149-55.

362. **Shoukry, N. H., A. G. Cawthon, and C. M. Walker.** 2004. Cell-mediated immunity and the outcome of hepatitis C virus infection. Annu Rev Microbiol **58:**391-424.
363. **Shoukry, N. H., A. Grakoui, M. Houghton, D. Y. Chien, J. Ghrayeb, K. A. Reimann, and C. M. Walker.** 2003. Memory CD8+ T cells are required for protection from persistent hepatitis C virus infection. J Exp Med **197:**1645-55.
364. **Silver, D. L.** 2002. A carboxyl-terminal PDZ-interacting domain of scavenger receptor B, type I is essential for cell surface expression in liver. J Biol Chem **277:**34042-7.
365. **Silver, D. L., and A. R. Tall.** 2001. The cellular biology of scavenger receptor class B type I. Curr Opin Lipidol **12:**497-504.
366. **Simmonds, P.** 2004. Genetic diversity and evolution of hepatitis C virus--15 years on. J Gen Virol **85:**3173-88.
367. **Simmonds, P., E. C. Holmes, T. A. Cha, S. W. Chan, F. McOmish, B. Irvine, E. Beall, P. L. Yap, J. Kolberg, and M. S. Urdea.** 1993. Classification of hepatitis C virus into six major genotypes and a series of subtypes by phylogenetic analysis of the NS-5 region. J Gen Virol **74 (Pt 11):**2391-9.
368. **Simon, D. B., Y. Lu, K. A. Choate, H. Velazquez, E. Al-Sabban, M. Praga, G. Casari, A. Bettinelli, G. Colussi, J. Rodriguez-Soriano, D. McCredie, D. Milford, S. Sanjad, and R. P. Lifton.** 1999. Paracellin-1, a renal tight junction protein required for paracellular Mg2+ resorption. Science **285:**103-6.
369. **Smith, A. E., and A. Helenius.** 2004. How viruses enter animal cells. Science **304:**237-42.
370. **Song, O. K. C., O.H.; Hahm, B.S.; Jang, S.K.** 1996. Development of an in vivo assay system suitable for screening inhibitors of hepatitis C viral protease Molecules and Cells (Korean Republic) **6:**183-189.
371. **Spengler, U., and J. Nattermann.** 2007. Immunopathogenesis in hepatitis C virus cirrhosis. Clin Sci (Lond) **112:**141-55.
372. **Stamataki, Z., J. Grove, P. Balfe, and J. A. McKeating.** 2008. Hepatitis C virus entry and neutralization. Clin Liver Dis **12:**693-712, x.
373. **Stamataki, Z., C. Shannon-Lowe, J. Shaw, D. Mutimer, A. B. Rickinson, J. Gordon, D. H. Adams, P. Balfe, and J. A. McKeating.** 2009. Hepatitis C virus association with peripheral blood B lymphocytes potentiates viral infection of liver-derived hepatoma cells. Blood **113:**585-93.
374. **Stangl, H., M. Hyatt, and H. H. Hobbs.** 1999. Transport of lipids from high and low density lipoproteins via scavenger receptor-BI. J Biol Chem **274:**32692-8.
375. **Steen, H. B.** 1990. Characteristics of Flow Cytometers. *In* L. T. Melamed M.R., Mendelsohn M. (ed.), Flow Cytometry and Sorting, 2nd ed. Wiley-Liss., New York.
376. **Stipp, C. S., T. V. Kolesnikova, and M. E. Hemler.** 2001. EWI-2 is a major CD9 and CD81 partner and member of a novel Ig protein subfamily. J Biol Chem **276:**40545-54.
377. **Stipp, C. S., D. Orlicky, and M. E. Hemler.** 2001. FPRP, a major, highly stoichiometric, highly specific CD81- and CD9-associated protein. J Biol Chem **276:**4853-62.
378. **Su, A. I., J. P. Pezacki, L. Wodicka, A. D. Brideau, L. Supekova, R. Thimme, S. Wieland, J. Bukh, R. H. Purcell, P. G. Schultz, and F. V. Chisari.** 2002. Genomic analysis of the host response to hepatitis C virus infection. Proc Natl Acad Sci U S A **99:**15669-74.
379. **Sudo, K., H. Inoue, Y. Shimizu, K. Yamaji, K. Konno, S. Shigeta, T. Kaneko, T. Yokota, and K. Shimotohno.** 1996. Establishment of an in vitro

assay system for screening hepatitis C virus protease inhibitors using high performance liquid chromatography. Antiviral Res **32:**9-18.

380. **Sumpter, R., Jr., Y. M. Loo, E. Foy, K. Li, M. Yoneyama, T. Fujita, S. M. Lemon, and M. Gale, Jr.** 2005. Regulating intracellular antiviral defense and permissiveness to hepatitis C virus RNA replication through a cellular RNA helicase, RIG-I. J Virol **79:**2689-99.
381. **Tabor, E., R. J. Gerety, J. A. Drucker, L. B. Seeff, J. H. Hoofnagle, D. R. Jackson, M. April, L. F. Barker, and G. Pineda-Tamondong.** 1978. Transmission of non-A, non-B hepatitis from man to chimpanzee. Lancet **1:**463-6.
382. **Takada, N., S. Takase, A. Takada, and T. Date.** 1992. HCV genotypes in different countries. Lancet **339:**808.
383. **Takeshita, N., N. Kakiuchi, T. Kanazawa, Y. Komoda, M. Nishizawa, T. Tani, and K. Shimotohno.** 1997. An enzyme-linked immunosorbent assay for detecting proteolytic activity of hepatitis C virus proteinase. Anal Biochem **247:**242-6.
384. **Takyar, S. T., D. Li, Y. Wang, R. Trowbridge, and E. J. Gowans.** 2000. Specific detection of minus-strand hepatitis C virus RNA by reverse-transcription polymerase chain reaction on PolyA(+)-purified RNA. Hepatology **32:**382-7.
385. **Taliani, M., E. Bianchi, F. Narjes, M. Fossatelli, A. Urbani, C. Steinkuhler, R. De Francesco, and A. Pessi.** 1996. A continuous assay of hepatitis C virus protease based on resonance energy transfer depsipeptide substrates. Anal Biochem **240:**60-7.
386. **Targett-Adams, P., S. Boulant, and J. McLauchlan.** 2008. Visualization of double-stranded RNA in cells supporting hepatitis C virus RNA replication. J Virol **82:**2182-95.
387. **Taylor, D. R., S. T. Shi, and M. M. Lai.** 2000. Hepatitis C virus and interferon resistance. Microbes Infect **2:**1743-56.
388. **Taylor, D. R., S. T. Shi, P. R. Romano, G. N. Barber, and M. M. Lai.** 1999. Inhibition of the interferon-inducible protein kinase PKR by HCV E2 protein. Science **285:**107-10.
389. **Tellinghuisen, T. L., K. L. Foss, and J. Treadaway.** 2008. Regulation of hepatitis C virion production via phosphorylation of the NS5A protein. PLoS Pathog **4:**e1000032.
390. **Tellinghuisen, T. L., M. S. Paulson, and C. M. Rice.** 2006. The NS5A protein of bovine viral diarrhea virus contains an essential zinc-binding site similar to that of the hepatitis C virus NS5A protein. J Virol **80:**7450-8.
391. **Thiebaut, F., T. Tsuruo, H. Hamada, M. M. Gottesman, I. Pastan, and M. C. Willingham.** 1987. Cellular localization of the multidrug-resistance gene product P-glycoprotein in normal human tissues. Proc Natl Acad Sci U S A **84:**7735-8.
392. **Thimme, R., J. Bukh, H. C. Spangenberg, S. Wieland, J. Pemberton, C. Steiger, S. Govindarajan, R. H. Purcell, and F. V. Chisari.** 2002. Viral and immunological determinants of hepatitis C virus clearance, persistence, and disease. Proc Natl Acad Sci U S A **99:**15661-8.
393. **Thimme, R., D. Oldach, K. M. Chang, C. Steiger, S. C. Ray, and F. V. Chisari.** 2001. Determinants of viral clearance and persistence during acute hepatitis C virus infection. J Exp Med **194:**1395-406.
394. **Thomssen, R., S. Bonk, and A. Thiele.** 1993. Density heterogeneities of hepatitis C virus in human sera due to the binding of beta-lipoproteins and immunoglobulins. Med Microbiol Immunol **182:**329-34.

395. **Tilg, H.** 1997. New insights into the mechanisms of interferon alfa: an immunoregulatory and anti-inflammatory cytokine. Gastroenterology **112:**1017-21.
396. **Timpe, J. M., Z. Stamataki, A. Jennings, K. Hu, M. J. Farquhar, H. J. Harris, A. Schwarz, I. Desombere, G. L. Roels, P. Balfe, and J. A. McKeating.** 2008. Hepatitis C virus cell-cell transmission in hepatoma cells in the presence of neutralizing antibodies. Hepatology **47:**17-24.
397. **Tokushige, K., N. Yamaguchi, I. Ikeda, E. Hashimoto, K. Yamauchi, and N. Hayashi.** 2000. Significance of soluble TNF receptor-I in acute-type fulminant hepatitis. Am J Gastroenterol **95:**2040-6.
398. **Toomre, D., P. Keller, J. White, J. C. Olivo, and K. Simons.** 1999. Dual-color visualization of trans-Golgi network to plasma membrane traffic along microtubules in living cells. J Cell Sci **112 (Pt 1):**21-33.
399. **Trauner, M., M. Wagner, P. Fickert, and G. Zollner.** 2005. Molecular regulation of hepatobiliary transport systems: clinical implications for understanding and treating cholestasis. J Clin Gastroenterol **39:**S111-24.
400. **Tscherne, D. M., M. J. Evans, T. von Hahn, C. T. Jones, Z. Stamataki, J. A. McKeating, B. D. Lindenbach, and C. M. Rice.** 2007. Superinfection exclusion in cells infected with hepatitis C virus. J Virol **81:**3693-703.
401. **Tscherne, D. M., T. J. Jones, M. J. Evans, B. D. Lindenbach, A. McKeating J, and M. Rice C.** 2005. Hepatitis C virus is resistant to acidic pH but undergoes pH-dependent entry, Journal of Virology (submitted).
402. **Tu, H., L. Gao, S. T. Shi, D. R. Taylor, T. Yang, A. K. Mircheff, Y. Wen, A. E. Gorbalenya, S. B. Hwang, and M. M. Lai.** 1999. Hepatitis C virus RNA polymerase and NS5A complex with a SNARE-like protein. Virology **263:**30-41.
403. **Tuma, P. L., C. M. Finnegan, J. H. Yi, and A. L. Hubbard.** 1999. Evidence for apical endocytosis in polarized hepatic cells: phosphoinositide 3-kinase inhibitors lead to the lysosomal accumulation of resident apical plasma membrane proteins. J Cell Biol **145:**1089-102.
404. **Utech, M., A. I. Ivanov, S. N. Samarin, M. Bruewer, J. R. Turner, R. J. Mrsny, C. A. Parkos, and A. Nusrat.** 2005. Mechanism of IFN-gamma-induced endocytosis of tight junction proteins: myosin II-dependent vacuolarization of the apical plasma membrane. Mol Biol Cell **16:**5040-52.
405. **Verma, S., Y. Lo, M. Chapagain, S. Lum, M. Kumar, U. Gurjav, H. Luo, A. Nakatsuka, and V. R. Nerurkar.** 2009. West Nile virus infection modulates human brain microvascular endothelial cells tight junction proteins and cell adhesion molecules: Transmigration across the in vitro blood-brain barrier. Virology.
406. **Vinken, M., P. Papeleu, S. Snykers, E. De Rop, T. Henkens, J. K. Chipman, V. Rogiers, and T. Vanhaecke.** 2006. Involvement of cell junctions in hepatocyte culture functionality. Crit Rev Toxicol **36:**299-318.
407. **Voisset, C., N. Callens, E. Blanchard, A. Op De Beeck, J. Dubuisson, and N. Vu-Dac.** 2005. High density lipoproteins facilitate hepatitis C virus entry through the scavenger receptor class B type I. J Biol Chem **280:**7793-9.
408. **Wakita, T., T. Pietschmann, T. Kato, T. Date, M. Miyamoto, Z. Zhao, K. Murthy, A. Habermann, H. G. Krausslich, M. Mizokami, R. Bartenschlager, and T. J. Liang.** 2005. Production of infectious hepatitis C virus in tissue culture from a cloned viral genome. Nat Med **11:**791-6.
409. **Wang, K. K., and P. W. Yuen.** 1994. Calpain inhibition: an overview of its therapeutic potential. Trends Pharmacol Sci **15:**412-9.

410. **Wang, W., W. L. Dentler, and R. T. Borchardt.** 2001. VEGF increases BMEC monolayer permeability by affecting occludin expression and tight junction assembly. Am J Physiol Heart Circ Physiol **280:**H434-40.
411. **Watashi, K., M. Hijikata, M. Hosaka, M. Yamaji, and K. Shimotohno.** 2003. Cyclosporin A suppresses replication of hepatitis C virus genome in cultured hepatocytes. Hepatology **38:**1282-8.
412. **Watashi, K., N. Ishii, M. Hijikata, D. Inoue, T. Murata, Y. Miyanari, and K. Shimotohno.** 2005. Cyclophilin B is a functional regulator of hepatitis C virus RNA polymerase. Mol Cell **19:**111-22.
413. **Weiner, A. J., X. Paliard, M. J. Selby, A. Medina-Selby, D. Coit, S. Nguyen, J. Kansopon, C. L. Arian, P. Ng, J. Tucker, C. T. Lee, N. K. Polakos, J. Han, S. Wong, H. H. Lu, S. Rosenberg, K. M. Brasky, D. Chien, G. Kuo, and M. Houghton.** 2001. Intrahepatic genetic inoculation of hepatitis C virus RNA confers cross-protective immunity. J Virol **75:**7142-8.
414. **Wolk, B., D. Sansonno, H. G. Krausslich, F. Dammacco, C. M. Rice, H. E. Blum, and D. Moradpour.** 2000. Subcellular localization, stability, and trans-cleavage competence of the hepatitis C virus NS3-NS4A complex expressed in tetracycline-regulated cell lines. J Virol **74:**2293-304.
415. **Wu, L., N. P. Gerard, R. Wyatt, H. Choe, C. Parolin, N. Ruffing, A. Borsetti, A. A. Cardoso, E. Desjardin, W. Newman, C. Gerard, and J. Sodroski.** 1996. CD4-induced interaction of primary HIV-1 gp120 glycoproteins with the chemokine receptor CCR-5. Nature **384:**179-83.
416. **Yanagi, M., M. St Claire, M. Shapiro, S. U. Emerson, R. H. Purcell, and J. Bukh.** 1998. Transcripts of a chimeric cDNA clone of hepatitis C virus genotype 1b are infectious in vivo. Virology **244:**161-72.
417. **Yang, W., C. Qiu, N. Biswas, J. Jin, S. C. Watkins, R. C. Montelaro, C. B. Coyne, and T. Wang.** 2008. Correlation of the tight junction-like distribution of Claudin-1 to the cellular tropism of hepatitis C virus. J Biol Chem **283:**8643-53.
418. **Yasui, K., T. Wakita, K. Tsukiyama-Kohara, S. I. Funahashi, M. Ichikawa, T. Kajita, D. Moradpour, J. R. Wands, and M. Kohara.** 1998. The native form and maturation process of hepatitis C virus core protein. J Virol **72:**6048-55.
419. **Yi, M., R. A. Villanueva, D. L. Thomas, T. Wakita, and S. M. Lemon.** 2006. Production of infectious genotype 1a hepatitis C virus (Hutchinson strain) in cultured human hepatoma cells. Proc Natl Acad Sci U S A **103:**2310-5.
420. **Yin, W., P. Xiang, and Q. Li.** 2005. Investigations of the effect of DNA size in transient transfection assay using dual luciferase system. Anal Biochem **346:**289-94.
421. **Yoshimori, T., P. Keller, M. G. Roth, and K. Simons.** 1996. Different biosynthetic transport routes to the plasma membrane in BHK and CHO cells. J Cell Biol **133:**247-56.
422. **Youakim, A., and M. Ahdieh.** 1999. Interferon-gamma decreases barrier function in T84 cells by reducing ZO-1 levels and disrupting apical actin. Am J Physiol **276:**G1279-88.
423. **Zahn, A., and J. P. Allain.** 2005. Hepatitis C virus and hepatitis B virus bind to heparin: purification of largely IgG-free virions from infected plasma by heparin chromatography. J Gen Virol **86:**677-85.
424. **Zein, N. N.** 2000. Clinical significance of hepatitis C virus genotypes. Clin Microbiol Rev **13:**223-35.

425. **Zennou, V., C. Serguera, C. Sarkis, P. Colin, E. Perret, J. Mallet, and P. Charneau.** 2001. The HIV-1 DNA flap stimulates HIV vector-mediated cell transduction in the brain. Nat Biotechnol **19:**446-50.
426. **Zeuzem, S.** 2004. Heterogeneous virologic response rates to interferon-based therapy in patients with chronic hepatitis C: who responds less well? Ann Intern Med **140:**370-81.
427. **Zhang, J., G. Randall, A. Higginbottom, P. Monk, C. M. Rice, and J. A. McKeating.** 2004. CD81 is required for hepatitis C virus glycoprotein-mediated viral infection. J Virol **78:**1448-55.
428. **Zheng, A., F. Yuan, Y. Li, F. Zhu, P. Hou, J. Li, X. Song, M. Ding, and H. Deng.** 2007. Claudin-6 and claudin-9 function as additional coreceptors for hepatitis C virus. J Virol **81:**12465-71.
429. **Zhong, J., P. Gastaminza, G. Cheng, S. Kapadia, T. Kato, D. R. Burton, S. F. Wieland, S. L. Uprichard, T. Wakita, and F. V. Chisari.** 2005. Robust hepatitis C virus infection in vitro. Proc Natl Acad Sci U S A **102:**9294-9.
430. **Zylberberg, H., A. C. Rimaniol, S. Pol, A. Masson, D. De Groote, P. Berthelot, J. F. Bach, C. Brechot, and F. Zavala.** 1999. Soluble tumor necrosis factor receptors in chronic hepatitis C: a correlation with histological fibrosis and activity. J Hepatol **30:**185-91.